4-1-1981

Real-Time Water Quality Model of the Elizabeth River System

Carl F. Cerco
Virginia Institute of Marine Science

Albert Y. Kuo
Virginia Institute of Marine Science

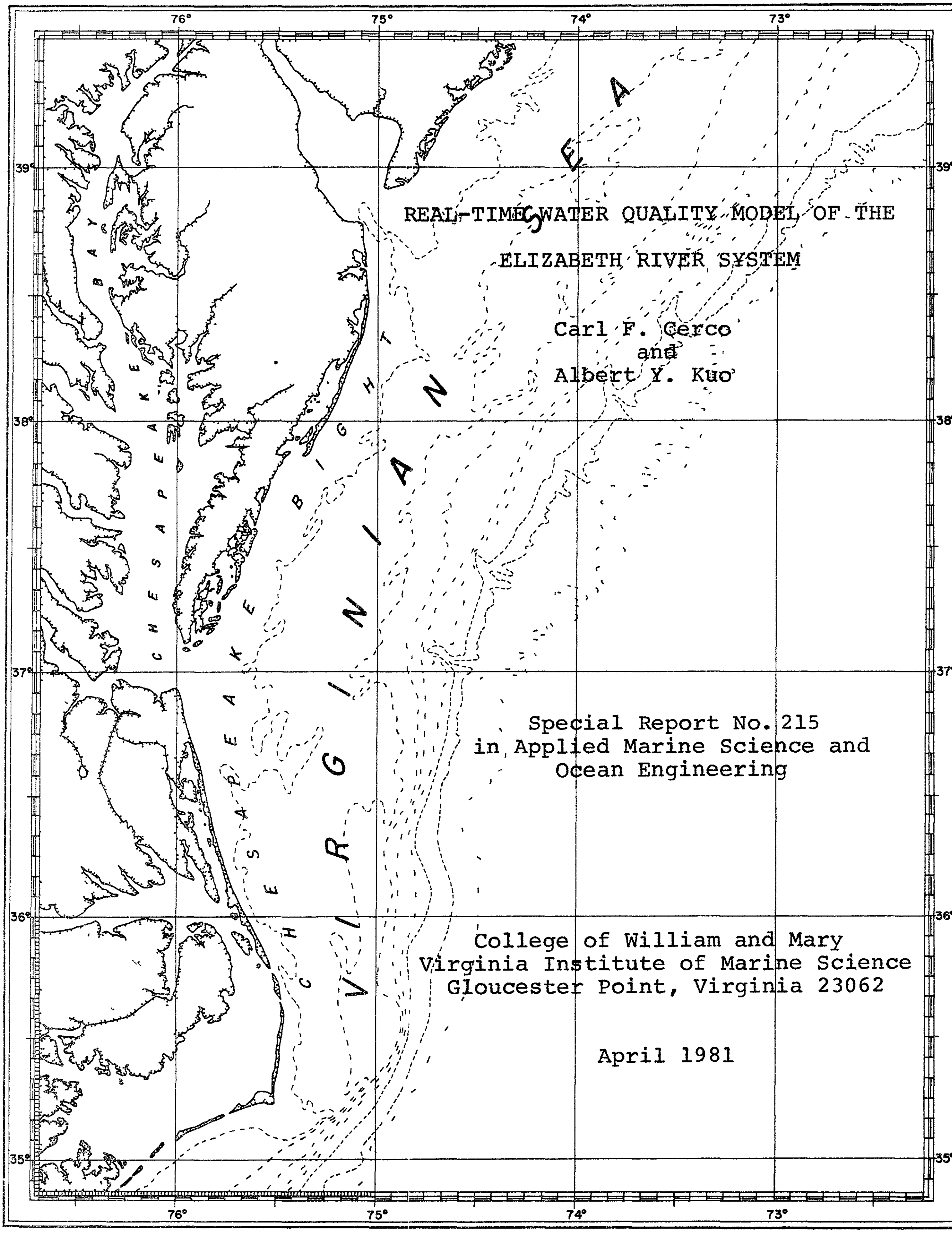

REAL-TIME WATER QUALITY MODEL OF THE ELIZABETH RIVER SYSTEM

Carl F. Cerco
and
Albert Y. Kuo

Special Report No. 215
in Applied Marine Science and
Ocean Engineering

College of William and Mary
Virginia Institute of Marine Science
Gloucester Point, Virginia 23062

April 1981

REAL-TIME WATER QUALITY MODEL OF THE ELIZABETH RIVER SYSTEM

Carl F. Cerco
and
Albert Y. Kuo

PREPARED UNDER

THE COOPERATIVE STATE AGENCIES PROGRAM

OF

THE VIRGINIA STATE WATER CONTROL BOARD
AND THE VIRGINIA INSTITUTE OF MARINE SCIENCE

Project Officers

Dale Jones
Raymond Bowles

Virginia State Water Control Board

Special Report No. 215
in Applied Marine Science and
Ocean Engineering

College of William and Mary
Virginia Institute of Marine Science
Gloucester Point, Virginia 23062

April 1981

TABLE OF CONTENTS

		Page
List of Figures		iii
List of Tables		vii
Acknowledgements		viii
Introduction		1
I.	Summary and Conclusions	4
	A. Water Quality Surveys	4
	B. Model Application	6
	C. Model Sensitivity	8
II.	The Mathematical Model	10
	A. Basic Equations	10
	B. Evaluation of Parameters and Rate Constants	17
	C. Solution to the Governing Equation	24
III.	Model Parameter Evaluation	26
	A. Physical Parameters	26
	B. Calibration Parameters	28
	C. Input Parameters	39
IV.	Model Calibration and Verification	48
	A. Model Calibration	49
	B. Model Verification	53
V.	Sensitivity Analysis	88
	A. Sensitivity to CBOD Decay Rate	89
	B. Sensitivity to Point Source Inputs	91
	C. Non-Point Source Inputs	91
	D. Benthic Oxygen Demand	95
	E. Photosynthetic Production	95
	F. Effect of Hydrolysis and Nitrification Parameters	98
	G. Sensitivity to the Reaeration Parameter	102
References		104

LIST OF FIGURES

Page

1. The Elizabeth River basin.......................... 2
2. Schematic diagram of interaction of Ecosystem Model.. 12
3. Segmentation of the Elizabeth River into finite sections.. 27
4. Benthic sampling stations.......................... 44
5. Plan view of intensive sampling stations........... 50
6. Location of intensive sampling stations............ 51
7. Results of salinity calibration for Southern and Main Branches...................................... 54
8. Results of ammonia calibration for Southern and Main Branches...................................... 55
9. Results of nitrate calibration for Southern and Main Branches...................................... 56
10. Results of organic nitrogen calibration for Southern and Main Branches......................... 56
11. Results of inorganic phosphorous calibration for Southern and Main Branches......................... 57
12. Results of organic phosphorous calibration for Southern and Main Branches......................... 57
13. Results of CBOD calibration for Southern and Main Branches.. 58
14. Results of dissolved oxygen calibration for Southern and Main Branches......................... 58
15. Results of chlorophyll 'a' calibration for Southern and Main Branches......................... 59
16. Results of fecal coliform calibration for Southern and Main Branches............................. 60
17. Results of salinity calibration for Eastern Branch. 61
18. Results of ammonia calibration for Eastern Branch.. 61
19. Results of nitrate calibration for Eastern Branch.. 62

List of Figures (Cont'd)

Page

20. Results of organic nitrogen calibration for Eastern Branch.. 62

21. Results of inorganic phosphorous calibration for Eastern Branch.. 63

22. Results of organic phosphorous calibration for Eastern Branch.. 63

23. Results of CBOD calibration for Eastern Branch..... 64

24. Results of dissolved oxygen calibration for Eastern Branch.. 64

25. Results of chlorophyll 'a' calibration for Eastern Branch.. 65

26. Results of fecal coliform calibration for Eastern Branch.. 65

27. Results of salinity calibration for Western Branch. 66

28. Results of ammonia calibration for Western Branch.. 66

29. Results of nitrate calibration for Western Branch.. 67

30. Results of organic nitrogen calibration for Western Branch.. 67

31. Results of inorganic phosphorous calibration for Western Branch.. 68

32. Results of organic phosphorous calibration for Western Branch.. 68

33. Results of CBOD calibration for Western Branch..... 69

34. Results of dissolved oxygen calibration for Western Branch.. 69

35. Results of chlorophyll 'a' calibration for Western Branch.. 70

36. Results of fecal coliform calibration for Western Branch.. 70

37. Results and salinity calibration for Lafayette River.. 71

38. Results of ammonia calibration for Lafayette River. 71

List of Figures (Cont'd)

Page

39. Results of nitrate calibration for Lafayette River. 72

40. Results of organic nitrogen calibration for Lafayette River.................................. 72

41. Results of inorganic phosphorous calibration for Lafayette River.................................. 73

42. Results of organic phosphorous calibration for Lafayette River.................................. 73

43. Results of CBOD calibration for Lafayette River.... 74

44. Results of dissolved oxygen calibration for Lafayette River.................................. 74

45. Results of chlorophyll 'a' calibration for Lafayette River.................................. 75

46. Results of fecal coliform calibration for Lafayette River.................................. 75

47. Results of salinity verification for Southern and Main Branches...................................... 77

48. Results of ammonia verification for Southern and Main Branches...................................... 78

49. Results of nitrate verification for Southern and Main Branches...................................... 79

50. Results of organic nitrogen verification for Southern and Main Branches........................ 79

51. Results of total phosphorous verification for Southern and Main Branches........................ 80

52. Results of CBOD verification for Southern and Main Branches...................................... 81

53. Results of dissolved oxygen verification for Southern and Main Branches........................ 81

54. Results of chlorophyll 'a' verification for Southern and Main Branches........................ 82

55. Results of fecal coliform verification for Southern and Main Branches.................................. 83

56. Elizabeth River stratification following rainstorm. 84

Page

57. Elizabeth River salinity, low slack water, Aug. 7-9, 1976 87

58. Elizabeth River salinity, low slack water, Aug. 23, 1976 87

59. Sensitivity of CBOD concentration to decay rate.... 90

60. Sensitivity of dissolved oxygen to CBOD decay rate. 90

61. Sensitivity of CBOD concentration to point sources. 92

62. Sensitivity of dissolved oxygen concentration to point sources 92

63. Sensitivity of CBOD concentration to non-point source inputs 94

64. Sensitivity of dissolved oxygen concentration to non-point source inputs 94

65. Sensitivity of dissolved oxygen concentration to benthal oxygen demand 96

66. Sensitivity of dissolved oxygen to photosynthetic production 97

67. Sensitivity of organic nitrogen to rate parameters. 99

68. Sensitivity of ammonia concentration to rate parameters 100

69. Sensitivity of dissolved oxygen concentration to nitrification rate parameters 101

70. Sensitivity of dissolved oxygen concentration to reaeration correction 103

LIST OF TABLES

Page

1. Physical Characteristics of Finite Sections English and Metric Units.......................... 29

2. Tidal Velocities.................................. 33

3. The Reaeration Parameter.......................... 35

4. Biochemical Rate Parameters....................... 36

5. Phytoplankton Related Parameters.................. 38

6. Extinction Coefficient........................... 38

7. Point Source Discharges to Southern Branch and Main Stem.. 40

8. Non-point Source Inputs During Calibration Period, June - July, 1976......................... 42

9. Percentages of Total Runoff Allocated to Model Segments... 43

10. Benthic Demand.................................. 45

11. Downstream Boundary Concentrations............... 47

ACKNOWLEDGEMENTS

Funding of this project is jointly supported by Virginia State Water Control Board and Virginia Institute of Marine Science through the Cooperative State Agencies program.

We thank the technical staff of the Department of Physical Oceanography and Hydraulics of the Virginia Institute of Marine Science for their participation in the field study, and Mrs. Shirley Crossley for her patient typing of this report.

INTRODUCTION

In the management of water resources, it is often necessary to predict the environmental effect of changes in the configuration, use and waste loading of a water body. The predictive mathematical model is a widely used tool in these management efforts since, once calibrated and verified, it can provide consistent, rational water quality forecasts before irrevocable changes are made and it can do so without excessive economic commitments.

This report details the formulation and application of a mathematical ecosystem model to the Elizabeth River System of southeastern Virginia. The Elizabeth River System, shown in Figure 1, is a tidal basin comprised of four branches, the Western, Southern and Eastern Branches and the Lafayette River, which converge to form a main stem which empties into Hampton Roads. In its Southern Branch, the system is connected, via the Dismal Swamp Canal, to the Intercoastal Waterway leading to Albermarle Sound and, via the Virginia Cut, to the Intercoastal Waterway leading to Pamlico Sound. The drainage area of the Elizabeth is approximately 300 square miles (777 km^2). The basin is highly urbanized in nature, including portions of the cities of Norfolk, Portsmouth, Chesapeake and Virginia Beach. Since the drainage basin is not large and there is very little topographic relief, freshwater input to the system is small, composed mainly of stormwater runoff and drainage from the Dismal Swamp which

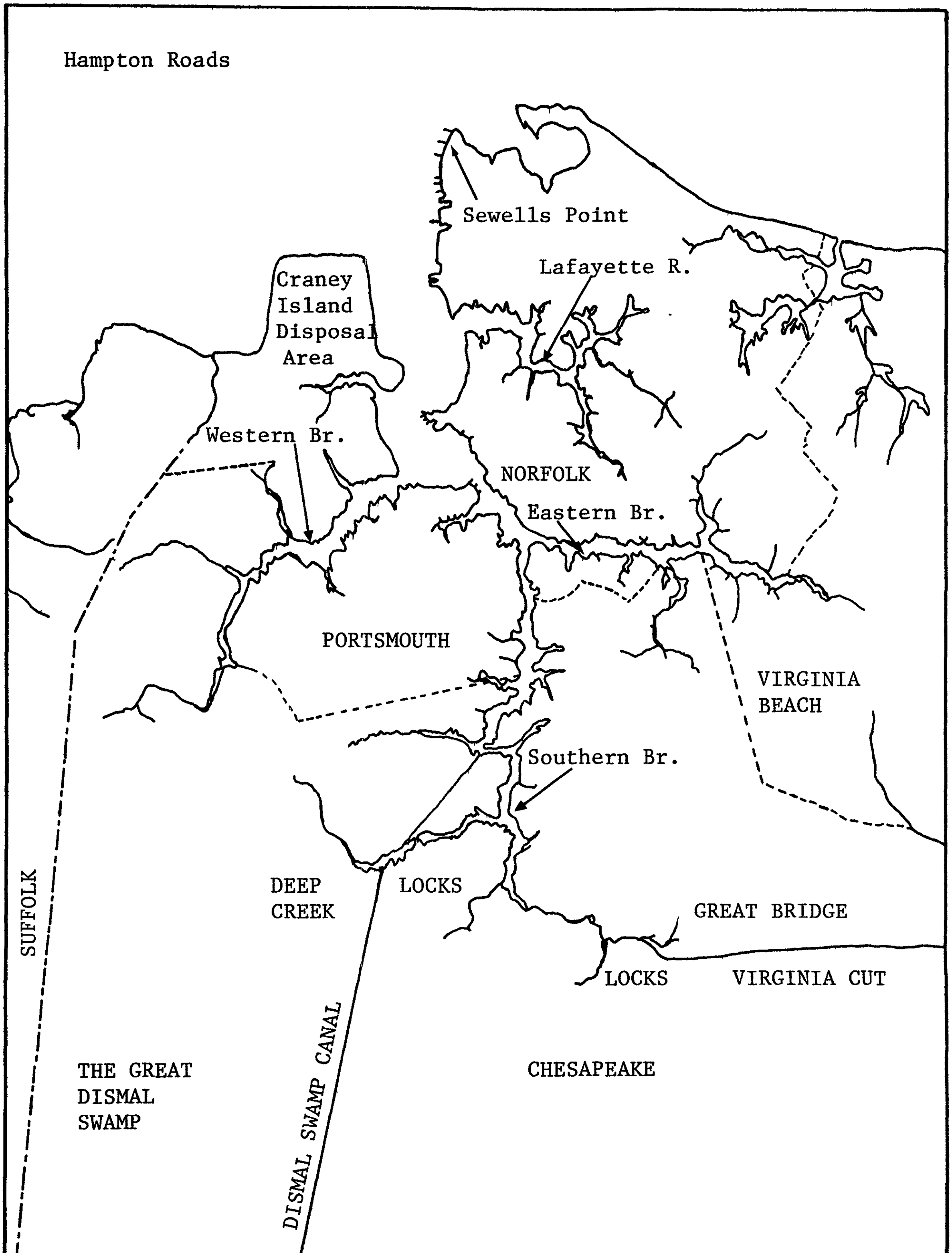

Figure 1. The Elizabeth River basin.

passes through the canal locks. For much of the year, therefore, the system's circulation is dominated by tidal effects and flushing of pollutants is poor, contributing to degraded water quality.

During the summer of 1976, a series of water quality surveys was conducted in the Elizabeth River system: an intensive survey on July 7-8, and a pair of less comprehensive slackwater surveys on August 23-24. The results of these surveys are summarized in Chapter I and illustrated in Figures 7 through 55.

Based on the results of these surveys, a mathematical ecosystem model of the river system was calibrated and verified. The results of the model application and its use in analyzing the factors affecting water quality of the Elizabeth are included in the Chapter I summary. Additional details of the model formulation are presented in Chapter II. Chapters III and IV detail the parameter evaluation, calibration, and verification of the model while Chapter V illustrates the model sensitivity to selected parameters.

I. SUMMARY AND CONCLUSIONS

A. Water Quality Surveys

The results of the intensive survey of July 7-8 are presented graphically in Figs. 7-16 for the Southern Branch and Main Stem, in Figs. 17-26 for the Eastern Branch, in Figs. 27-36 for the Western Branch, and in Figs. 37-46 for the Lafayette River. The slackwater surveys of August 23-24 were conducted only in the Southern Branch and Main Stem and the results are presented in Figs. 47-55.

During the intensive survey, dissolved oxygen levels depressed below the 4 mg/ℓ level were noted in the Main Stem, Southern, and Eastern Branches with a large portion of the Main Stem and Southern Branch showing daily average D.O. levels below 5 mg/ℓ. All dissolved oxygen observations in the Western Branch and Lafayette River were above 4 mg/ℓ and daily average values exceeded 5 mg/ℓ.

The wide fluctuations and minimum D.O. values which occurred in the Southern and Eastern Branches may be attributed to photosynthetic activity. A bloom was occurring in the Southern Branch and Chl. 'a' values in excess of 100 μg/ℓ were noted. The daily average Chl. 'a' concentrations were in the 70-80 μg/ℓ range. The model calibration also indicated the potential for a bloom in the Lafayette River due to its shallow depth and low turbidity but no excessive Chl. 'a' concentrations were noted at the time of the survey.

Elevated fecal coliform levels occurred throughout the system. Concentrations in excess of 3000 mpn/100mℓ were sampled and daily average values in excess of 100 mpn/100mℓ were noted in the Main Stem, the Southern and Eastern Branches, and in the Lafayette River.

During the slackwater surveys, dissolved oxygen concentrations differed from those observed in the intensive sampling. D.O. levels in the Southern Branch and Main Stem were generally above 5 mg/ℓ. Sampling was conducted during daylight hours and thus these values may be elevated by photosynthetic activity but the D.O. levels still appear to be significantly higher than those observed in the intensive survey.

These elevated D.O. levels may be the result of a density-driven circulation which flushes water from the Elizabeth and brings highly oxygenated water in from Hampton Roads. During the slackwater survey, salinity stratification was greater than during the intensive and thus increased circulation would be expected to occur prior to the slackwater sampling.

Chlorophyll 'a' levels were approximately equivalent during the intensive and slackwater surveys except in the upstream portion of the Southern Branch where somewhat lower levels were observed in the latter surveys. A bloom still persisted, however, and concentrations as high as 80 μg/ℓ were noted.

Fecal coliform levels during the slackwater surveys were in the same range as the daily average values noted during the intensive survey: 100-1000 mpn/100mℓ. The extremely high values present in the intensive survey were not noted but this may be an artifice of the slackwater sampling scheme since fewer samples were taken than during the intensive survey.

B. Model Application

A real-time ecosystem model has been applied to the Elizabeth River system. The model treats each branch of the river as a one-dimensional body and predicts longitudinal variations in salinity, organic, ammonia and nitrate nitrogen, ortho- and organic phosphorous, CBOD, dissolved oxygen, chlorophyll 'a', and fecal coliforms. The model is denoted a "branched" ecosystem model since it joins the one-dimensional models of each branch of the river into a unified representation of the entire river system.

The model is calibrated based on field data collected during the intensive water quality survey conducted July 7-8, 1976. Agreement between the model predictions and the field data is generally good except for ammonia nitrogen. Here, the disagreement is most likely due to interference in the laboratory analysis of the ammonia samples. Reasonable values have been assumed for the nitrogen kinetic parameters which determine the ammonia concentrations and the model sensitivity to these assumptions has been shown to be minimal.

The model was verified against a second data set collected during the slackwater surveys on August 23 and 24, 1976. The verification is less successful than the calibration, especially for the salinity and dissolved oxygen parameters.

The discrepancy between the predicted and sampled values of salinity suggests the circulation structure of the river is not being well-described. The Elizabeth exhibits variable longitudinal and vertical salinity structures which are influenced by tidal mixing, freshwater inflows, and stratification in Hampton Roads. These variable salinity structures cause a gravity-induced circulation of water out of the system near the surface and into the system near the bottom. This circulation is best described with a two-dimensional model capable of predicting vertical variations in density and velocity.

In many cases, a one-dimensional, vertically averaged, model can account for this two-dimensional circulation through the use of a dispersion parameter which is fitted to the observed salinity distribution. In the absence of observations or under unsteady conditions, it is difficult to evaluate the dispersion and model predictions become less reliable. For optimum accuracy, therefore, use of this model should be limited to periods during which conditions similar to those which were observed during the intensive survey prevail. As additional data sets for verification and evaluation of dispersion become available, use of the model may be expanded.

C. Model Sensitivity

A sensitivity analysis was performed on the calibrated model both to determine the effect of variations in calibration parameters on the model results and to indicate the factors influencing water quality in the Elizabeth. The analysis shows the kinetic rate constants and other calibration parameters selected for use are satisfactory and provide the best agreement to the field data.

The factors determining the D.O. deficit detected during the July 7-8 survey were analyzed by alternately eliminating from the calibrated model point-source inputs, non-point source inputs, and benthal demand. The results indicate that benthal oxygen demand was the largest single factor contributing to the deficit noted during the survey period. Following this demand in influence were point source and non-point source inputs. The apparent insignificance of non-point sources should be viewed with caution since a different set of storm conditions preceeding the survey may have produced different results.

The model run without non-point source inputs also resulted in a decline in the excessive chlorophyll levels noted in the upstream sections of the Southern Branch suggesting that the bloom is the result of non-point nutrient inputs.

Since the Elizabeth River system receives little or no freshwater input from upstream sources, the concept of a ten-year, seven-day low flow is not applicable. Roughly corresponding conditions were simulated, however, by running the model with no stormwater input and at the elevated temperature of 30^{o}C. Dissolved oxygen concentrations declined throughout the river by approximately 0.5 mg/ℓ primarily due to a temperature induced increase in benthal demand concurrent with a reduction in the saturated dissolved oxygen concentration.

II. THE MATHEMATICAL MODEL

The water quality model used for this study is a one-dimensional, intra-tidal model which simulates the longitudinal distribution of cross-sectional average concentrations of water quality measures, including the temporal variation of these concentration fields in response to tidal oscillation. The water quality measures simulated in the model include dissolved oxygen, carbonaceous oxygen demand, organic nitrogen, ammonia nitrogen, nitrite-nitrate nitrogen, organic phosphorus, inorganic phosphorus, phytoplankton (quantified as chlorophyll 'a'), coliform bacteria, and salinity. Temperature, turbidity, and light intensity are important parameters for the biochemical interactions taking place, but are not modeled directly. Instead the values for these parameters are specified as inputs to the model. Their influence on the biochemical reaction rates is taken into account mathematically, as indicated below.

A. Basic Equations

The model is based on the one-dimensional equation describing the mass-balance of a dissolved or suspended substance in a water body.

$$\frac{\partial}{\partial t}(AC) + \frac{\partial}{\partial x}(QC) = \frac{\partial}{\partial x}\left(EA\frac{\partial C}{\partial x}\right) + A \cdot Se + A \cdot Si \quad (1)$$

where

t is time,

x is the distance along the axis of the estuary, A is the cross sectional area,

Q is discharge,

C is the concentration of dissolved or suspended substance,

E is the dispersion coefficient,

Se is the time rate of external addition (or withdrawal) of mass across the boundaries, i.e. free surface, bottom, and lateral boundary,

Si is the time rate of increase or decrease of mass of a particular substance by biochemical reaction processes.

The advective transport term, the second term on the left hand side of the equation, represents advection of mass by water movement; the dispersive transport term, the first term on the right hand side, represents dispersion of mass by turbulence and shearing flow. These two terms represent the physical transport processes in the flow field and are identical for all dissolved and suspended substances in the water. The last two terms of the equation represent the external additions and internal biochemical reactions and differ for different substances.

The model treats nitrogen, phosphorus, oxygen demanding material and dissolved oxygen through an interacting system of eight components as shown in the schematic diagram (Figure 2). Each rectangular box represents one component being simulated by the model, with its name in the computer program shown in parentheses. The arrows between components represent the biochemical transformation of one substance to

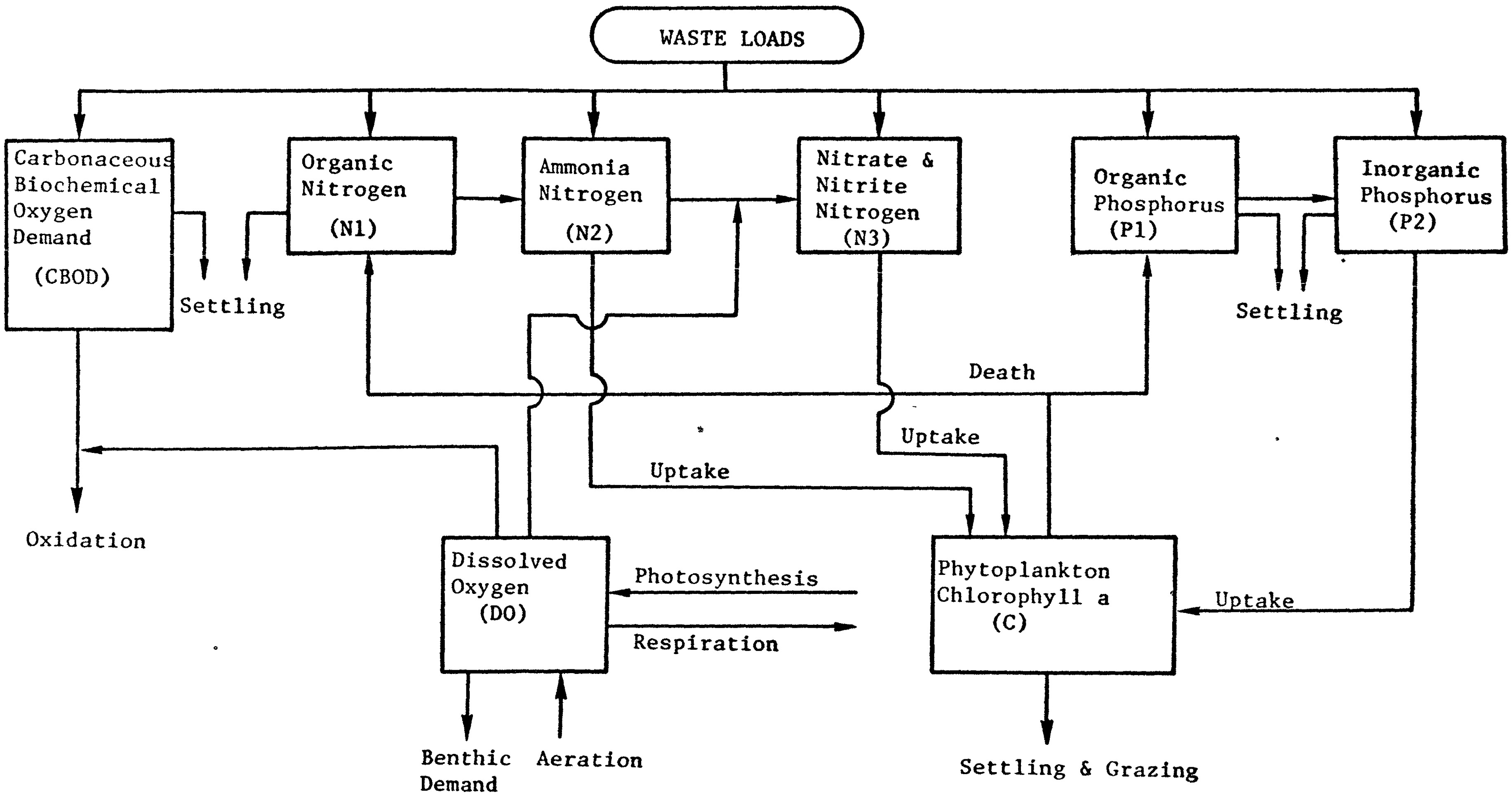

Figure 2. Schematic diagram of interaction of Ecosystem Model.

the other. An arrow with one end unattached represents an external source (or sink) or an internal source (or sink) due to some biochemical reaction. The mathematical expressions for the terms Se and Si for each of the eight components are the following:

(1) Phytoplankton concentration, C, measured as μg/ℓ of chlorophyll 'a'

$$Se = -k_{cs} \cdot C$$

where k_{cs} is the settling rate of phytoplankton.

$$Si = (g-d-kg)C$$

where g and d are the growth and endogenous respiration rates of phytoplankton respectively, kg is the grazing of phytoplankton by zooplankton.

(2) Organic Nitrogen, N1 in mg/ℓ

$$Se = W_{n1} - k_{n11} \cdot N1$$

where W_{n1} is the wasteload from point and non-point sources and k_{n11} is the settling rate.

$$Si = -k_{n12} \cdot N1 + a_n \cdot (d + 0.4\ kg) \cdot C$$

where k_{n12} is the hydrolysis rate of organic nitrogen to ammonia nitrogen and a_n is the ratio of nitrogen to chlorophyll 'a' in mg-N/μg-C. The factor of 0.4 in the last term of the equation is based on the assumption that 40% of the organic material consumed by zooplankton is excreted.

(3) Ammonia Nitrogen, N2 in mg/ℓ

$$Se = W_{n2}$$

where W_{n2} is the wasteload from point and non-point sources.

$$Si = k_{n12} \cdot N1 - k_{n23} \cdot N2 - a_n \cdot g \cdot C \cdot P_r$$

where k_{n23} is the NH_3 to NO_3 nitrification rate, P_r is ammonia preference of phytoplankton given by

$$P_r = \frac{N2}{N2 + K_{mn}}$$

K_{mn} is the Michaelis constant.

(4) Nitrite - Nitrate Nitrogen, N3 in mg/ℓ

$$Se = W_{n3} - k_{n33} \cdot N3$$

where W_{n3} is wasteload from point and non-point sources, k_{n33} represents nitrate removal by settling and denitrification.

$$Si = k_{n23} \cdot N2 - (1-P_r) \cdot a_n \cdot g \cdot C$$

where the first term represents the nitrification of ammonia nitrogen and the second term represents the uptake by phytoplankton.

(5) Organic Phosphorus, P1 in mg/ℓ

$$Se = W_{p1} - k_{p11} \cdot P1$$

where W_{p1} is wasteload from point and non-point sources, k_{p11} is the settling rate.

$$Si = -k_{p12} \cdot P1 + a_p \ (d + 0.4\ kg) \cdot C$$

where k_{p12} is the organic P to inorganic P conversion rate, a_p is the phosphorus to chlorophyll ratio, in mg-P/μg-C.

(6) Inorganic Phosphorus, P2 in mg/ℓ

$$Se = W_{p2} - k_{p22} \cdot P2$$

where W_{p2} is wasteload from point and non-point sources, k_{p22} is settling rate.

$$Si = k_{p12} \cdot P1 - a_p \cdot g \cdot C$$

where the first term represents the hydrolysis of organic phosphorus to inorganic phosphorus, the second term represents the uptake by phytoplankton.

(7) Carbonaceous Biochemical Oxygen Demand, CBOD in mg/ℓ

$$Se = W_b - k_s \cdot CBOD$$

where W_b is the wasteload from point and non-point sources, k_s is the settling rate.

$$Si = -k_1 \cdot CBOD + 2.67\ a_c \cdot 0.4\ kg \cdot C$$

where k_1 is the oxidation rate of CBOD, a_c is the carbon-chlorophyll ratio.

(8) Dissolved Oxygen, DO in mg/ℓ

$$Se = k_2 \cdot (DO_s - DO) - BEN$$

where k_2 is reaeration rate, DO_s is the saturated oxygen concentration, BEN is the benthic oxygen demand.

$$Si = -k_1 \cdot CBOD - 4.57 \cdot k_{n23} \cdot N2$$
$$+ a_d \cdot g \cdot C - a_r \cdot d \cdot C$$

where the first two terms represent the oxygen demands by oxidation of CBOD and by nitrification of ammonia nitrogen, the last two terms represent the source and sink due to photosynthesis and respiration of phytoplankton, a_d (or a_r) is the amount of oxygen produced (or consumed) per unit of chlorophyll synthesized (or respired) in the photosynthesis (or respiration) process.

The model treats salinity and fecal coliforms as independent systems. The simulation of salinity distribution verifies that the model is reproducing the prototype hydraulic regime and also provides data to calculate dispersion and the saturation concentration of oxygen in saline water.

(9) Salinity, S in parts per thousand

$$Se = 0$$
$$Si = 0$$

(10) Fecal Coliform Bacteria, BAC in MPN/100mℓ

$$Se = W_{bac}$$

where W_{bac} is the loading from point and non-point sources.

$$Si = -k_b \cdot BAC$$

where k_b is the die-off rate.

B. Evaluation of Parameters and Rate Constants

(1) Velocity U: In an estuary, the current velocity may be divided into two parts,

$$U_m(t) = UF_m + Ut_m(t) \qquad (2)$$

where UF is the non-tidal component generated by freshwater discharge and Ut is the oscillating tidal component. In the model, the tidal current is approximated by a sinusoidal function of time with period T and phase ϕ

$$Ut_m(t) = UT_m \sin \left\{ \frac{2\pi}{T} t + \phi_m \right\} \qquad (3)$$

where UT is the amplitude. UT_m and ϕ_m are obtained from field data. The non-tidal component UF is calculated by the equation

$$UF_m = \frac{Q_m}{AC_m} \qquad (4)$$

where Q_m is the freshwater discharge from a drainage area up-stream of the mth transect, and AC_m is the conveyance cross-sectional area of the mth transect.

(2) Dispersion coefficient E: The dominant mechanism of longitudinal dispersion is the interaction between turbulent diffusion and shearing current. Taylor's (1954) formulation of one-dimensional dispersion has been successfully modified

and extended to homogeneous estuaries (Holley, et al., 1970; Harleman, 1971). The dispersion coefficient in the fresh-water portion of a tidal estuary may be expressed as

$$E = 77n|U|R^{5/6} \tag{5}$$

where n is Manning's friction coefficient, $|U|$ is the absolute value of velocity, and R is the hydraulic radius. It is known that the presence of density stratification due to salinity intrusion enhances vertical shear while suppressing turbulence, and therefore, increases the dispersion coefficient. Equation (5) is modified to

$$E = 77n|U|R^{5/6}(1 + \nu'S) \tag{6}$$

where ν' is a constant and S is the salinity. The constant is determined by model calibration, i.e. adjusting ν' until the model results agree with the salinity distribution observed in the field.

(3) Reaeration coefficient k_2: O'Connor and Dobbins (1958) presented a theoretical derivation of the reaeration coefficient based on the concept of surface renewal of a liquid film through internal turbulence. They hypothesized that the reaeration coefficient was proportional to the square root of a surface renewal rate which was in turn proportional to the ratio of a characteristic velocity and a characteristic mixing length

$$k_2 = f(\sqrt{r}) \tag{7}$$

where r = surface renewal rate, $r = g(u/\ell)$

As the characteristic velocity, they chose the depth-average velocity of the stream and as the mixing length they chose the total depth resulting in the well-known O'Connor-Dobbins formulation. In the English system, this formula is

$$(k_2)_{20} = \frac{12.9\ U^{\frac{1}{2}}}{H^{3/2}} \tag{8}$$

For the Elizabeth River, however, this formulation is not directly applicable and predicts a reaeration rate which is far too low. This is because the mixing length of the river is less than the total depth (which is 30-40 ft. in deeper sections), and the velocity near the surface, where reaeration takes place, is greater than the depth-average velocity. The smaller mixing length and larger velocity result in a greater surface renewal rate and increased reaeration. Reaeration is also enhanced by the heavy boat traffic which occurs in the Elizabeth. The frequent passage of large vessels serves to stir the water column and increase turbulence beyond the range expected to result from natural conditions.

Increased reaeration is included in the model by multiplying the O'Connor-Dobbins reaeration term by an amount ε which is obtained via model calibration. The formulation used in the model is then

$$(k_2)_{20} = \frac{12.9\ \varepsilon\ U^{\frac{1}{2}}}{H^{3/2}} \tag{9}$$

To adjust k_2 for temperatures other than $20^{o}C$, the ASCE (1961) formula is utilized.

$$k_2 = (k_2)_{20} \cdot 1.024^{(T-20)} \qquad (10)$$

where T is the water temperature in centigrade degrees.

(4) CBOD oxidation rate, k_1: The oxidation rate of CBOD (carbonaceous biochemical oxygen demand) normally ranges from 0.1 to 0.5 per day, and also depends on water temperature. The following formula is used for this temperature dependence:

$$k_1 = (k_1)_{20} \cdot 1.047^{(T-20)} \qquad (11)$$

(5) CBOD settling rate, k_s: k_s is usually negligible.

(6) Saturated oxygen content, DO_s: The saturation concentration of dissolved oxygen depends on both the temperature and salinity of the water. From tables of saturation concentration (Carritt and Green, 1967) a polynomial equation was determined by a least-squares method.

$$DO_s = 14.6244 - 0.367134T + 0.0044972T^2 - 0.0966S + 0.00205TS + 0.0002739S^2 \qquad (12)$$

where S is salinity in parts per thousand and DO_s is in mg/liter.

(7) Benthic oxygen demand, BEN: The bottom sediment of an estuary may vary from deep deposits of organic matter (which may arise from sewage disposal, industrial waste or be of natural origin) to beds of sand and rocks. The oxygen

consumption rate of the bottom deposits is best determined with field measurements, whenever possible. A value of 1.0 $gm/m^2/day$ at 20^oC is a "typical value" for most estuaries. The effect of temperature on benthal demand is given by Thomann (1972).

$$BEN = (BEN)_{20} \cdot 1.065^{(T-20)} \qquad (13)$$

where $(BEN)_{20}$ is the benthic demand at 20^oC.

(8) Coliform bacteria dieoff rate, k_b

$$k_b = (k_b)_{20} \cdot 1.040^{(T-20)} \qquad (14)$$

where $(k_b)_{20}$ is the dieoff rate at 20^oC and T is temperature in degrees centigrade. The normal range of $(k_b)_{20}$ is 0.5-4.0/day.

(9) Settling rate of organic nitrogen, k_{n11}

k_{n11} is of order of 0.1/day

(10) Organic N to NH_3 hydrolysis rate, k_{n12}

$$k_{n12} = aT$$

where a is of order of 0.007/day/degree.

(11) NH_3 to NO_3 nitrification rate, k_{n23}

$$k_{n23} = aT$$

where a is of order of 0.01/day/degree

(12) NO_3 removal rate, k_{n33}

where k_{n33} is of order of 0.1/day

(13) Organic phosphorus settling rate, k_{p11}

k_{p11} is order of 0.1/day

(14) Organic P to inorganic P hydrolysis rate, k_{p12}

$k_{p12} = aT$

where a is of order of 0.007/day/degree

(15) Inorganic phosphorus settling rate, k_{p22}

k_{p22} is of order of 0.1/day

(16) Nitrogen-chlorophyll ratio, a_n

a_n is of order of 0.01 mg N/μg Chlorophyll 'a'

(17) Phosphorus-chlorophyll ratio, a_p

a_p is of order of 0.001 mg P/μg Chlorophyll 'a'

(18) Carbon-chlorophyll ratio, a_c

a_c is of order of 0.05 mg carbon/μg chlorophyll 'a'

(19) Oxygen produced per unit of chlorophyll growth, a_d

$a_d = 2.67 \cdot a_c \cdot PQ$

where PQ is photosynthesis quotient, $PQ = 1 \sim 1.4$.

(20) Oxygen consumed per unit of chlorophyll respired, a_r

$a_r = 2.67 \cdot a_c/RQ$

where RQ is respiration ratio.

(21) Zooplankton grazing, k_g: In reality, k_g should depend solely on the concentration of herbivorous zooplankton biomass. In order to avoid adding an additional trophic level to the model, however, k_g is considered to be proportional to phytoplankton concentration C. A Michaelis-Menten type

function is hypothesized

$$k_g = \frac{k_g' C}{k_{gm} + C} \qquad (15)$$

k_g is the zooplankton predation rate, k_g' is the maximum predation rate, and k_{gm} is a predation half-saturation constant. This functional form results in a low predation rate when the phytoplankton population is small and in a maximum predation rate when the phytoplankton population is large.

(22) Endogenous respiration rate, R_s

$$R_s = aT$$

where a is of order of 0.005/day/degree

(23) Growth rate, G_c: The growth rate expression was developed by DiToro, O'Connor and Thomann (1971) and, as used in this model, is given by

$$G_c = \underbrace{k_{gr} T}_{\text{temperature effect}} \cdot \underbrace{I\,(I_a, I_s, k_e, C, h)}_{\text{light effect}} \cdot \underbrace{N(N2, N3, P2)}_{\text{nutrient effect}} \qquad (17)$$

where k_{gr} is the optimum growth rate of the order of 0.1/day/degree. The functional form, I, for the light effect incorporates vertical extinction of solar radiation and the self-shading effect. The form is

$$I = \frac{2.718}{k_e h} \left(e^{-\alpha_1} - e^{-\alpha_o}\right) \qquad (18a)$$

$$k_e = k_e' + 0.0088 \cdot C + 0.054 \cdot C^{0.66} \qquad (18b)$$

$$\alpha_1 = \frac{I_a}{I_s} e^{-k_e h} \tag{18c}$$

$$\alpha_o = \frac{I_a}{I_s} \tag{18d}$$

k_e' is the light extinction coefficient at zero chlorophyll concentration, k_e is the overall light extinction coefficient, I_a is the incoming solar radiation and I_s is the optimum light intensity, about 300 langleys per day. The nutrient effect makes use of product Michaelis-Menton kinetics and is given by

$$N = \frac{N2 + N3}{k_{mn} + N2 + N3} \cdot \frac{P2}{k_{mp} + P2} \tag{19}$$

where k_{mn} is the half saturation concentration for total inorganic nitrogen and k_{mp} is the half saturation concentration for phosphorus. Literature values for k_{mn} and k_{mp} are about 0.01 - 0.03 and 0.005 mg/ℓ respectively.

C. Solution to the Governing Equation

The model is implemented by solving Equation (1) based on combinations of parameters x, Q, E, A, Se, and Si. The classical solution to Equation (1) involves integration which results in an expression for the dissolved substance as a function of distance and time. Three constants of integration including two boundary conditions and an initial condition are needed to solve the equation. Analytical solutions obtained through integration are only available, however, for simplistic cases. In most actual modelling efforts, non-uniform initial conditions and variations in flow, cross-section and other parameters which do not fit convenient mathematical forms make an analytical solution impossible to obtain. Therefore, Equation (1) must be solved by approximate numerical means.

The most common numerical approach to solving Equation (1) is the finite difference method in which the continuum of the water body is divided into a number of discrete sections and derivatives are replaced by the ratios of change in the appropriate variables across these sections. The resulting finite-difference equations are then solved by a suitable algorithm on a high speed computer. For details of the implicit numerical scheme used in this model, see Hyer, Kuo and Neilson (1977).

III. MODEL PARAMETER EVALUATION

Implementation of the mathematical model outlined in Chapter II requires the identification and evaluation of a large number of parameters of three basic types: physical, calibration, and input. Physical parameters are the measurements (e.g. channel cross section) which define the physical characteristics of the river system. Under this heading also are the dimensions such as segment length needed for the finite difference solution. Calibration parameters are the biochemical rate constants (e.g. BOD decay rate) and inputs which cannot be measured in the field. They are initially obtained from literature values and from experience in the analysis of similar water bodies and are adjusted, within reasonable limits, to improve the predictive capability of the model. Input parameters (e.g. point-source discharges) are a set of conditions upon which the modeller wishes to base a water quality prediction.

A. Physical Parameters

1. Finite Sections

The Main Stem and Southern Branch of the Elizabeth were divided into 18 segments approximately one mile (1.6 km) each in length and numbered from one at the upstream end to eighteen at the downstream end. The Eastern and Western Branches of the Elizabeth and the Lafayette River each were divided into three reaches numbered from one at the upstream

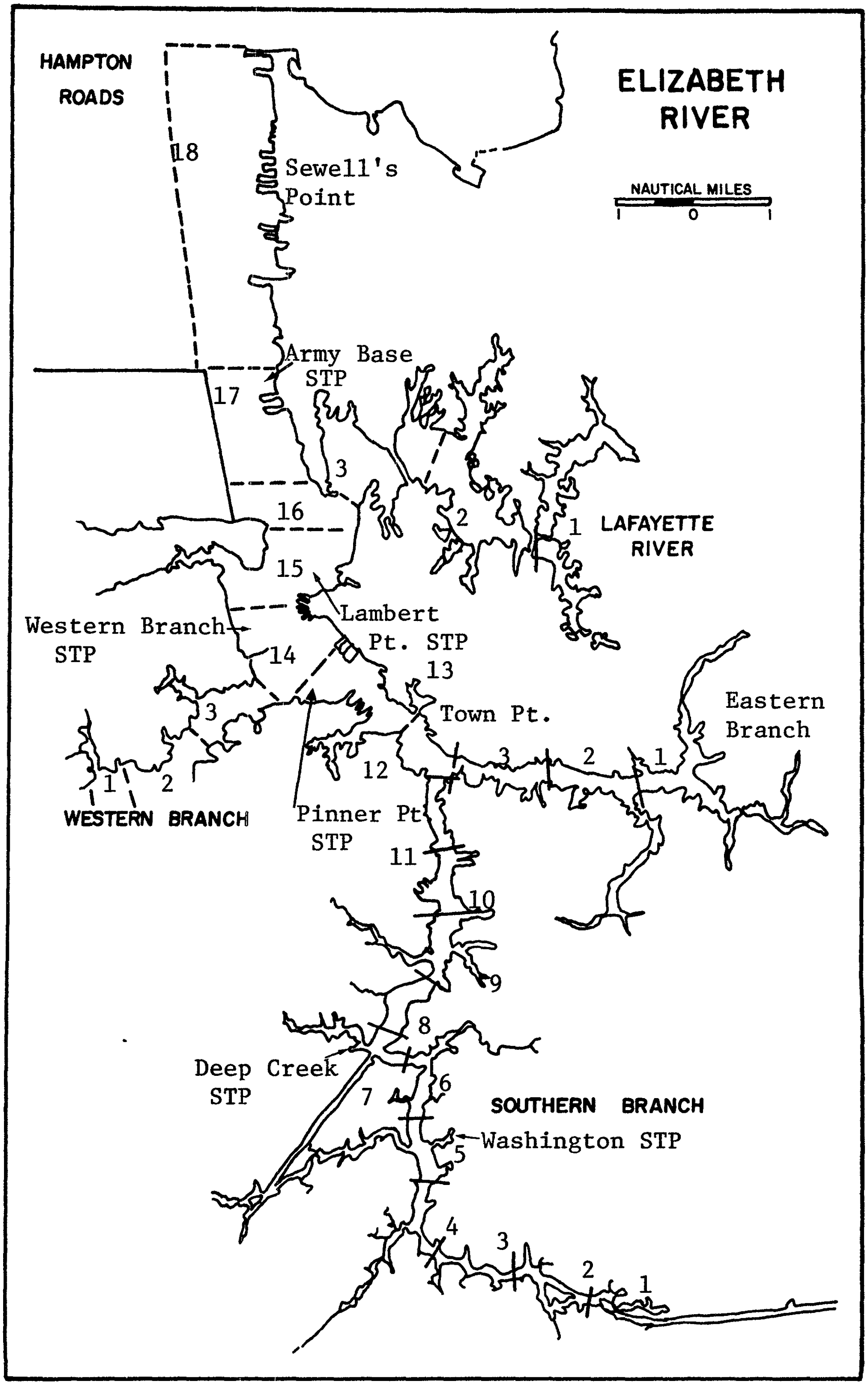

Figure 3. Segmentation of the Elizabeth River into finite sections.

end to three at the junction with the main branch. The first segment of the Southern Branch is a dummy segment, required by an artifice of the computer program, and is excluded from further analysis. The remaining reaches are shown in Figure 3 and their physical parameters including the river mile of each transect as measured from the mouth at Sewell's Pt., the transect cross sectional area, the transect and reach average depth and the reach volume are summarized in Table 1. These parameters were derived from National Ocean Survey Maps of Norfolk Harbor and the Elizabeth River and from a VIMS bathymetry survey conducted in July, 1978.

2. Tidal Velocity and Phase Difference

Tidal phase and velocity parameters are needed to correctly reproduce the prototype flow field in the model. Initial values of tidal velocity were derived from current meter data obtained in September of 1974. These values were refined via model calibration until an agreement of field data and predicted salinities was obtained. The tidal phase difference is negligible and assumed to be zero.

The tidal velocities obtained for each transect are presented in Table 2.

B. Calibration Parameters

The calibration parameters required by the model include the quantities needed to evaluate the dispersion coefficient in Equation (6), the reaeration parameter ε in

Table 1. Physical Characteristics of Finite Sections
English Units

Transect	River Mile of Transect	Transect Cross Section $10^4 ft^2$	Transect Depth ft	Reach Depth ft	Reach Volume $10^8 ft^3$	Reach
Dimensions of Southern Branch and Main Stem						
1	20.9	0.0	0.0	4.3	0.07	1
2	20.0	0.28	8.5	8.0	0.25	2
3	18.9	0.57	7.5	8.7	0.33	3
4	17.7	0.46	9.8	8.5	0.33	4
5	16.5	0.61	7.2	8.1	0.37	5
6	15.4	0.74	8.9	13.7	0.70	6
7	14.5	1.93	18.4	20.3	1.47	7
8	13.4	3.50	22.3	27.1	1.89	8
9	12.4	3.32	31.8	27.9	1.66	9
10	11.3	2.71	24.0	34.2	1.55	10
11	10.3	2.99	44.3	41.2	2.25	11
12	9.3	5.15	38.1	34.0	3.49	12
13	8.1	6.76	29.9	30.1	6.31	13
14	6.9	12.67	30.2	24.5	7.06	14
15	5.7	9.82	18.7	16.9	5.43	15
16	4.7	10.98	15.1	15.8	6.11	16
17	3.7	12.40	16.4	18.7	8.52	17
18	2.6	15.67	21.0	21.0	21.4	18
19	0	15.67	21.0			
Eastern Branch						
1	13.1	0.92	4.9	7.2	0.71	1
2	12.1	1.57	9.5	12.3	1.37	2
3	10.7	2.15	15.1	19.6	2.30	3
4	9.2	3.79	24.0			

Table 1 (Cont'd)

Transect	River Mile of Transect	Transect Cross Section $10^4 ft^2$	Transect Depth ft	Reach Depth ft	Reach Volume $10^8 ft^3$	Reach
		Western Branch				
1	11.5	0.32	3.9	4.4	0.48	1
2	10.0	0.90	4.9	6.1	0.86	2
3	8.6	1.46	7.2	7.4	0.97	3
4	7.7	2.25	7.5			
		Lafayette River				
1	10.6	0.0	0.0	3.1	0.55	1
2	8.7	1.07	5.9	4.5	0.53	2
3	7.2	0.74	3.9	3.6	0.78	3
4	5.4	0.93	3.3			

Table 1 (Cont'd) Physical Characteristics of Finite Sections
Metric Units

Transect	Kilometer of Transect	Transect Cross Section $10^3 m^2$	Transect Depth m	Reach Depth m	Reach Volume $10^6 m^3$	Reach
	Dimensions of Southern Branch and Main Stem					
1	33.6	0	0	1.3	.20	1
2	32.2	.26	2.6	2.4	.71	2
3	30.4	.53	2.3	2.7	.93	3
4	28.5	.43	3.0	2.6	.93	4
5	26.6	.57	2.2	2.5	1.05	5
6	24.8	.69	2.7	4.2	1.98	6
7	23.3	1.79	5.6	6.2	4.16	7
8	21.6	3.25	6.8	8.3	5.35	8
9	20.0	3.08	9.7	8.5	4.70	9
10	18.2	2.52	7.3	10.4	4.39	10
11	16.6	2.78	13.5	12.6	6.37	11
12	15.0	4.78	11.6	10.4	9.88	12
13	13.0	6.28	9.1	9.2	17.86	13
14	11.1	11.78	9.2	7.5	19.99	14
15	9.2	9.13	5.7	5.2	15.37	15
16	7.6	10.20	4.6	4.8	17.30	16
17	6.0	11.52	5.0	5.7	24.12	17
18	4.2	14.56	6.4	6.4	60.58	18
19	0	14.56	6.4			
	Dimensions of Eastern Branch					
1	21.1	.85	1.5	2.2	2.01	1
2	19.5	1.46	2.9	3.7	3.88	2
3	17.2	2.00	4.6	6.0	6.51	3
4	14.8	3.52	7.3			

Table 1 (Cont'd)

Transect	Kilometer of Transect	Transect Cross Section $10^3 m^2$	Transect Depth m	Reach Depth m	Reach Volume $10^6 m^3$	Reach
		Western Branch				
1	18.5	.30	1.2			
				1.3	1.36	1
2	16.1	.84	1.5			
				1.9	2.43	2
3	13.8	1.36	2.2			
				2.3	2.75	3
4	12.4	2.09	2.3			
		Lafayette River				
1	17.1	0	0			
				0.9	1.56	1
2	14.0	.99	1.8			
				1.4	1.50	2
3	11.6	.69	1.2			
				1.1	2.21	3
4	8.7	.86	1.0			

Table 2. Tidal Velocities

Southern Branch and Main Stem

Transect	2	3	4	5	6	7	
Velocity	0.0	0.30	0.67	0.74	0.84	0.42	ft/sec
	0.0	0.09	0.20	0.23	0.26	0.13	m/sec
Transect	8	9	10	11	12	13	
Velocity	0.30	0.40	0.57	0.57	0.36	0.69	ft/sec
	0.09	0.12	0.17	0.17	0.11	0.21	m/sec
Transect	14	15	16	17	18	19	
Velocity	0.44	0.86	0.89	1.06	0.96	1.11	ft/sec
	0.13	0.26	0.27	0.32	0.29	0.34	m/sec

Eastern Branch

Transect	1	2	3	4	
Velocity	0.0	0.56	0.76	0.63	ft/sec
	0.0	0.17	0.23	0.19	m/sec

Western Branch

Transect	1	2	3	4	
Velocity	0.0	0.61	0.77	0.75	ft/sec
	0.0	0.19	0.23	0.23	m/sec

Lafayette River

Transect	1	2	3	4	
Velocity	0.0	0.58	1.37	1.89	ft/sec
	0.0	0.18	0.42	0.58	m/sec

Equation (9), the biochemical kinetics parameters outlined in subsections 4-15 of Chapter II, the phytoplankton related parameters of Chapter II, subsections 16-24, and the turbidity.

1. Dispersion Parameters

The dispersion parameters were obtained via a recursive process in which the parameters were modified until the predicted salinity distribution matched the field data. Manning's n was assumed to be 0.03 and a best fit was obtained for $\nu' = 0.55$.

2. Reaeration Parameter

Values of the reaeration parameter, ε, obtained by calibration are reported in Table 3.

3. Biochemical Kinetics

Biochemical rate parameters were obtained in a calibration process similar to that used to derive dispersion constants. Typical literature values were assumed and modified, within reported limits, until a best fit was obtained. These parameters were allowed to vary throughout the system to reflect the varying properties of loadings (e.g. natural and industrial) and other system characteristics. The values of the biochemical rate parameters used in the model are presented in Table 4.

4. Phytoplankton Related Parameters

Phytoplankton related parameters are considered to be uniform throughout the system. Their values, except for

Table 3. The Reaeration Parameter

Southern Branch and Main Stem

Reach	1	2	3	4	5	6
ε	2	2	2	2	2	2
Reach	7	8	9	10	11	12
ε	2	3	3	3	4	4
Reach	13	14	15	16	17	18
ε	4	4	4	4	4	4

Eastern Branch

Reach	1	2	3
ε	3	3	3

Western Branch

Reach	1	2	3
ε	3	3	3

Lafayette River

Reach	1	2	3
ε	2	2	2

Table 4. Biochemical Rate Parameters

Southern Branch and Main Stem

Segment	k_1 (1/day)	k_s (1/day)	k_b (1/day)	k_{n11} (1/day)	k_{n12} (1/day-^oC)	k_{n23} (1/day-^oC)	k_{n33} (1/day)	k_{p11} (1/day)	k_{p12} (1/day-^oC)	k_{p22} (1/day)
2	0.10	0.0	0.1	0.0	0.008	0.012	0.3	0.0	0.003	0.0
3	0.10	"	"	"	"	"	"	"	"	"
4	0.10	"	"	"	"	"	"	"	"	"
5	0.10	"	"	"	"	"	"	"	"	"
6	0.12	"	"	"	"	"	"	"	"	"
7	"	"	"	"	"	"	"	"	"	"
8	"	"	"	"	"	"	"	"	"	"
9	"	"	"	"	"	"	"	"	"	"
10	"	"	"	"	"	"	"	"	"	"
11	"	"	"	"	"	"	"	"	"	"
12	"	"	"	"	"	"	"	"	"	"
13	"	"	"	"	"	"	"	"	"	"
14	"	"	"	"	"	"	"	"	"	"
15	"	"	"	"	"	"	"	"	"	"
16	"	"	"	"	"	"	"	"	"	"
17	"	"	"	"	"	"	"	"	"	"
Eastern Branch										
1-3	0.12	0.0	0.1	0.0	0.008	0.012	0.3	0.0	0.003	0.0
Western Branch										
1-3	0.05	0.0	0.1	0.0	0.008	0.012	0.3	0.0	0.003	0.0
Lafayette River										
1-3	0.05	0.0	0.1	0.0	0.008	0.012	0.3	0.0	0.003	0.0

average light intensity, are obtained through the calibration procedure and are reported in Table 5.

5. Turbidity

The turbidity parameter, sampled in-situ with a secchi disk, is a measure of the rate of light extinction in the water column. The rate of extinction of sunlight striking the surface of the water, in turn, affects the growth rate of the phytoplankton population.

Sverdrup, et al. (1970) give a formula for converting secchi readings to extinction coefficients as

$$k_e = \frac{1.7}{D_d} \qquad (19)$$

k_e is the extinction coefficient (meter^{-1}) and D_d is the secchi depth (meter). Because light attenuation due to self-shading of phytoplankton is calculated in the model from the predicted time-varying chlorophyll concentrations, field measures of light extinction cannot be used directly, however. The field measures must be corrected to reflect only the non-phytoplankton related turbidity. Riley (1956) gives this correction factor as

$$k_e' = k_e - 0.0088C - 0.054C^{0.66} \qquad (20)$$

k_e is the in-situ extinction coefficient (obtained from Equation (19)), k_e' is the extinction coefficient at zero chlorophyll concentration, and C is the ambient chlorophyll concentration in μg/ℓ.

Corrected values of the extinction coefficients used in the model are reported in Table 6.

Table 5. Phytoplankton Related Parameters

a_n	a_p	a_c	PQ	RQ	k_{gm}	k'_g	a	I_a	I_s	k_{mn}	k_{mp}
$\frac{mgN}{\mu g\ Chl}$	$\frac{mgP}{\mu g\ Chl}$	$\frac{mgC}{\mu g\ Chl}$			$\frac{\mu g\ Chl}{\ell}$	$\frac{1}{day}$	$\frac{1}{day\text{-}C^{o}}$	$\frac{langleys}{day}$	$\frac{langleys}{day}$	$\frac{mgN}{l}$	$\frac{mgP}{l}$
$5x10^{-3}$	$5x10^{-4}$	$2.5x10^{-2}$	1.0	1.0	10	0.1	0.015	392	280	0.015	0.005

Table 6. Extinction Coefficient (meter^{-1})

Southern Branch and Main Stem

Segment	2	3	4	5	6	7	8	9	
Coefficient	1.0	1.0	1.0	1.0	1.0	1.0	1.0	1.0	
Segment	10	11	12	13	14	15	16	17	18
Coefficient	1.0	1.0	1.0	1.0	1.0	1.0	1.0	1.0	1.0

Eastern Branch

Segment	1	2	3
Coefficient	2.0	1.5	1.0

Western Branch

Segment	1	2	3
Coefficient	3.0	3.0	1.5

Lafayette River

Segment	1	2	3
Coefficient	2.5	2.0	2.0

C. Input Parameters

Parameters input to the model include the location and magnitude of point and non-point sources of pollutants, the amount of daily solar radiation, benthic demand, freshwater inflow, the temperature, and a set of boundary conditions.

1. Point Sources of Pollution

Data on point source inputs to the Elizabeth River System were obtained primarily from the Hampton Roads Sanitation District, from Betz Environmental Engineers (a subcontractor of HRWQA), and from NPDES reports. In a number of cases, data from sewage treatment plants discharging into the river was incomplete and was synthesized either from monthly averages or from the reported pollutant concentrations at other plants.

The locations and wasteflows of significant point source discharges are presented in Table 7. Several smaller sources have been omitted.

2. Non-Point Sources of Pollution

Non-point sources of pollution generated by storm runoff form a significant input to the Elizabeth River System. They are included both to aid in calibration and to increase the capacity of the model in dealing with transient conditions involving both point and non-point loadings. Data on non-point sources was generated by use of the U. S. Army Corps of Engineers "STORM" model as executed by Malcolm Pirnie

Table 7. Point Source Discharges to Southern Branch and Main Stem

Model Segment	Discharger	Q (cfs)	Org N lb/day	NH_4 lb/day	NO_3 lb/day	Org P lb/day	Inorg P lb/day	BOD_u lb/day	Coliform 10^9/day
5	Washington STP	0.84	21	101	3	11	11	1928	0.41
7	Deep Creek STP	0.88	22	106	3	11	12	958	0.43
9	Texaco	0.0						208	
10	Norfolk Naval Shipyard	4.01	1	6	2	2	4	475	
13	Pinner Pt. STP	14.8	437	1629	6	103	104	37225	7.2
14	Western Branch STP	2.6	30	374	1	34	34	4662	1.3
15	Lambert's Point STP	41.5	1117	5402	19	676	677	108862	20.4
15	Virginia Chemical	2.0	5	81	4		1	1930	
17	Army Base STP	17.5	499	1784	6	283	284	36255	8.6

Note: No major discharges on the other branches.

Engineers, Inc. (MPEI), in a non-point source study conducted for the Hampton Roads Water Quality Agency. Table 8 presents the total mass of pollutants estimated to have entered the Elizabeth River System during the thirty-day period prior to the intensive field survey upon which the model calibration is based. MPEI allocated these masses to the river by dividing the total drainage area into sub-basins which were further subdivided by VIMS into areas contributing to each model segment. A matrix showing the proportion of total mass allocated to each model segment is given as Table 9.

3. Sunlight

An average light intensity of 392 langleys per day for the calibration period was derived from pyreheliometer data provided by Langley Air Force Base, Hampton, Virginia. This value was arbitrarily halved on days in which precipitation occurred.

4. Benthic Demand

Values of benthic demand were obtained from VIMS field surveys on July 7 and 10, 1976, at the sites shown in Figure 4. These point values of benthic demand were assumed to apply to the stretches of river adjacent to each station. Table 10 gives the benthic demand allocated to each model segment and the field station from which this value was obtained.

Table 8. Non-point Source Inputs During Calibration Period June - July, 1976

Date	Runoff $10^6 ft^3$	Org N lb	NH_4^--N lb	NO_3^--N lb	Org P lb	Inorg P lb	CBOD lb	Coliform 10^9
June 17	6.1	271	67	145	35	16	3190	43563
June 19	16.3	1674	417	557	286	117	9444	92605
June 20	16.6	1673	421	548	292	119	7958	63404
July 3	54.9	10119	2550	3204	1790	769	43443	293575
July 4	41.1	5844	1457	1811	1016	440	20756	87869

Table 9. Percentages of Total Runoff Allocated to Model Segments

Segment	Runoff	Org N	NH_4	NO_3	Org P	Inorg P	CBOD	Coliform
Southern Branch								
2	10.7	23.2	23.3	10.4	27.5	27.3	18.7	21.3
3	1.4	3.0	3.1	1.4	3.5	3.6	2.4	2.8
4	4.0	8.5	8.7	3.9	10.1	10.0	6.9	7.9
5	4.9	10.6	10.7	4.7	12.5	12.5	8.6	9.7
6	5.0	6.7	6.7	5.1	7.2	7.0	6.1	6.2
7	3.2	2.0	2.0	3.5	1.5	1.4	2.5	1.9
8	0.0	0.0	0.0	0.0	0.0	0.0	0.0	0.0
9	5.9	3.7	3.7	6.4	2.7	2.7	4.5	3.5
10	0.9	0.6	0.5	0.9	0.4	0.4	0.7	0.5
11	2.0	1.2	1.2	2.1	0.9	0.9	1.5	1.2
12	0.0	0.0	0.0	0.0	0.0	0.0	0.0	0.0
13	4.6	2.7	2.7	4.6	2.0	1.8	3.3	2.7
14	0.9	0.8	0.8	1.3	0.6	0.5	1.0	0.9
15	1.8	0.9	0.4	1.5	0.7	0.7	1.1	0.9
16	0	0	0	0	0	0	0	0
17	0	0	0	0	0	0	0	0
18	0	0	0	0	0	0	0	0
Eastern Branch								
1	17.5	9.0	9.0	15.5	6.5	6.4	11.2	11.0
2	4.2	2.2	2.1	3.8	1.6	1.6	2.7	2.7
3	2.4	1.2	1.2	2.1	0.9	0.9	1.5	1.5
Western Branch								
1	13.4	13.1	13.0	14.3	14.7	14.6	13.8	12.5
2	4.5	2.8	2.7	4.7	2.0	2.0	3.5	2.9
3	2.3	1.4	1.4	2.5	0.2	0.9	1.8	1.5
Lafayette River								
1	6.8	4.2	4.3	7.3	3.1	3.0	5.3	5.5
2	1.3	0.8	0.8	1.4	0.6	0.7	1.0	1.1
3	2.3	1.4	1.4	2.5	1.1	1.1	1.8	1.9

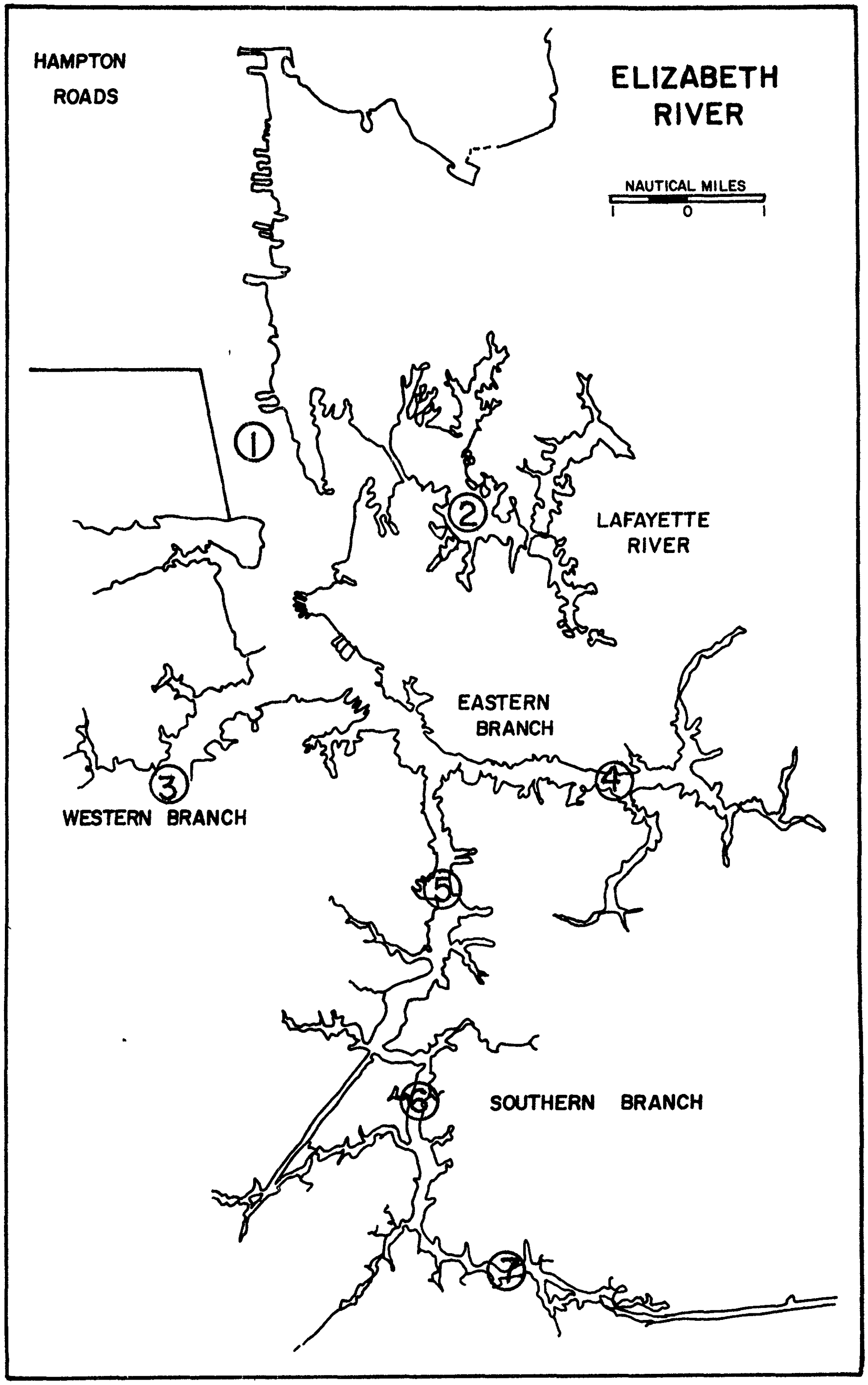

Figure 4. Benthic sampling stations.

Table 10. Benthic Demand (gm $O_2/m^2/day$)

Southern Branch and Main Stem

Segment	2	3	4	5	6	7	8	9	
Demand	3.2	3.2	3.2	1.6	1.6	1.6	1.6	1.8	
Field Station	7	7	7	6	6	6	6	5	
Segment	10	11	12	13	14	15	16	17	18
Demand	1.8	1.8	1.8	1.8	1.8	1.8	1.8	1.8	1.8
Field Station	5	5	5	1	1	1	1	1	1

Eastern Branch

Segment	1	2	3
Demand	3.8	3.8	3.8
Field Station	4	4	4

Western Branch

Segment	1	2	3
Demand	3.8	3.8	3.8
Field Station	3	3	3

Lafayette River

Segment	1	2	3
Demand	3.2	3.2	3.2
Field Station	2	2	2

5. Freshwater Inflow

There are no major freshwater streams draining from upland areas into the Elizabeth River System. Potential sources of freshwater inflow are limited to advection from the Dismal Swamp Canal and the Virginia Cut and to stormwater runoff.

Neilson (1975) cites a U. S. Army Corps of Engineers communication in which the net flow through the Virginia Cut is estimated to be zero and this value is assumed in the model. Net flow through the Dismal Swamp Canal is also assumed to be negligible. Estimates of storm runoff volume (from Malcolm Pirnie Engineers) are given in Table 8.

6. Temperature

The average temperature of the Elizabeth River System during the July, 1976, field survey was 25°C and this value is used in the model calibration.

7. Boundary Conditions

The model requires a set of boundary conditions at the upstream end of each river branch and at the downstream end of the main channel. At the upstream boundaries, conditions of zero mass flux, corresponding to the absence of advective inflow, were set. At the downstream boundary, constituent concentrations were fixed at the values measured in Hampton Roads during the VIMS field survey. These concentrations, assumed constant over the calibration period, are reported in Table 11.

Table 11. Downstream Boundary Concentrations

Salinity (ppt)	Org N (ppm)	NH_4-N (ppm)	NO_3-N (ppm)	Org P (ppm)	Inorg P (ppm)	Chl'a' (ppm)	CBOD (ppm)	DO (ppm)	Coliform (mpn/100mℓ)
22.0	0.1	0.25	0.12	0.10	0.05	7.0	1.5	5.5	22

IV. MODEL CALIBRATION AND VERIFICATION

In the formulation of an ecosystem model, there are a number of parameters, especially biochemical rate constants, which cannot be assigned a priori values. The values of these parameters, specified in Section B of Chapter III, are obtained through the calibration procedure.

In this procedure predictions of water quality, based on calibration parameter values derived from literature or from experience, are compared with actual field data. The calibration parameters are then adjusted (within reasonable limits) in an iterative fashion until a satisfactory agreement between predicted water quality and field data is obtained.

Comparison of the calibrated model predictions with field measurements of water quality is one method of judging the applicability of a model. A more rigorous method is through the verification procedure in which the calibrated model, supplied with suitable input parameters, is used to provide a second set of water quality predictions for comparison with a second set of field data.

If the agreement between the second set of predictions and field data is good, the model is considered verified and confidence in its predictive capability is implied. If the agreement is poor, the model must be reexamined and recalibrated until a "best fit" to the field data is obtained.

A. Model Calibration

The Elizabeth River System model was calibrated using field data collected in an intensive river survey conducted on July 7-8, 1976. Twenty stations (Figures 5 and 6) were manned for 24-hour periods and sampled hourly for temperature, salinity, and dissolved oxygen. Total kjeldahl nitrogen, ammonia nitrogen, nitrate and nitrite nitrogen, total and soluble reactive phosphorus, $CBOD_5$, chlorophyll 'a' and fecal coliforms were sampled every three hours.

Values of each parameter sampled were temporally and depth averaged and, where necessary, converted to parameters used in the model via the following relationship:

Organic Nitrogen = Total Kjeldahl Nitrogen - Ammonia Nitrogen (21)

Inorganic Phosphorus = Soluble Reactive Phosphorus (S.R.P.) (22)

Organic Phosphorus = Total Phosphorus - S.R.P. (23)

$$CBOD_u = 2.0\ CBOD_5 \qquad (24)$$

The multiplicative factor of 2 used for converting $CBOD_5$ to $CBOD_u$ was obtained through analysis of field data taken during the intensive survey.

The intensive survey field data and results of the model calibration are presented graphically for the Main Stem and Southern Branch (Figures 7-16), Eastern Branch (Figures 17-26), Western Branch (Figures 27-36) and the

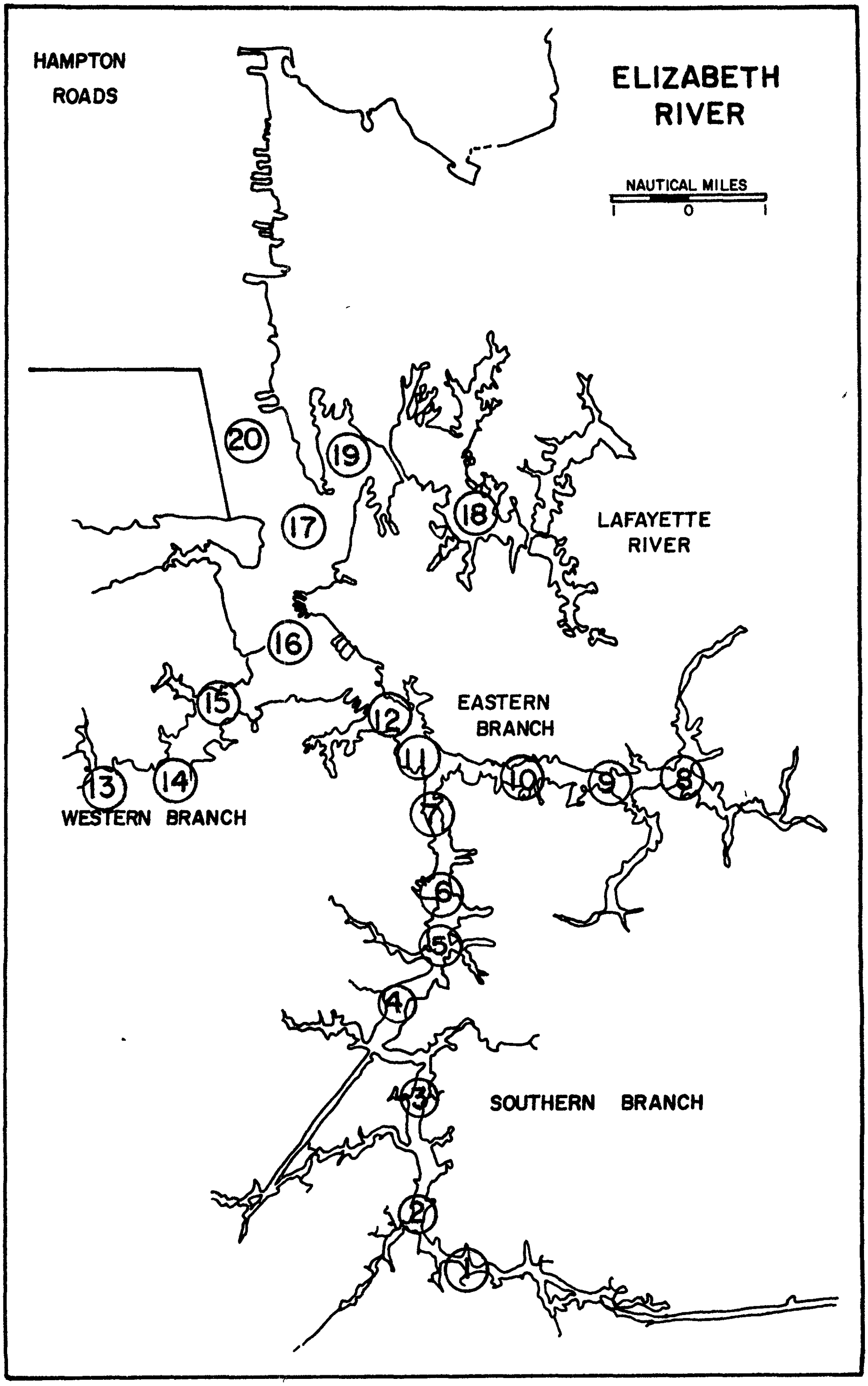

Figure 5. Plan view of intensive sampling stations.

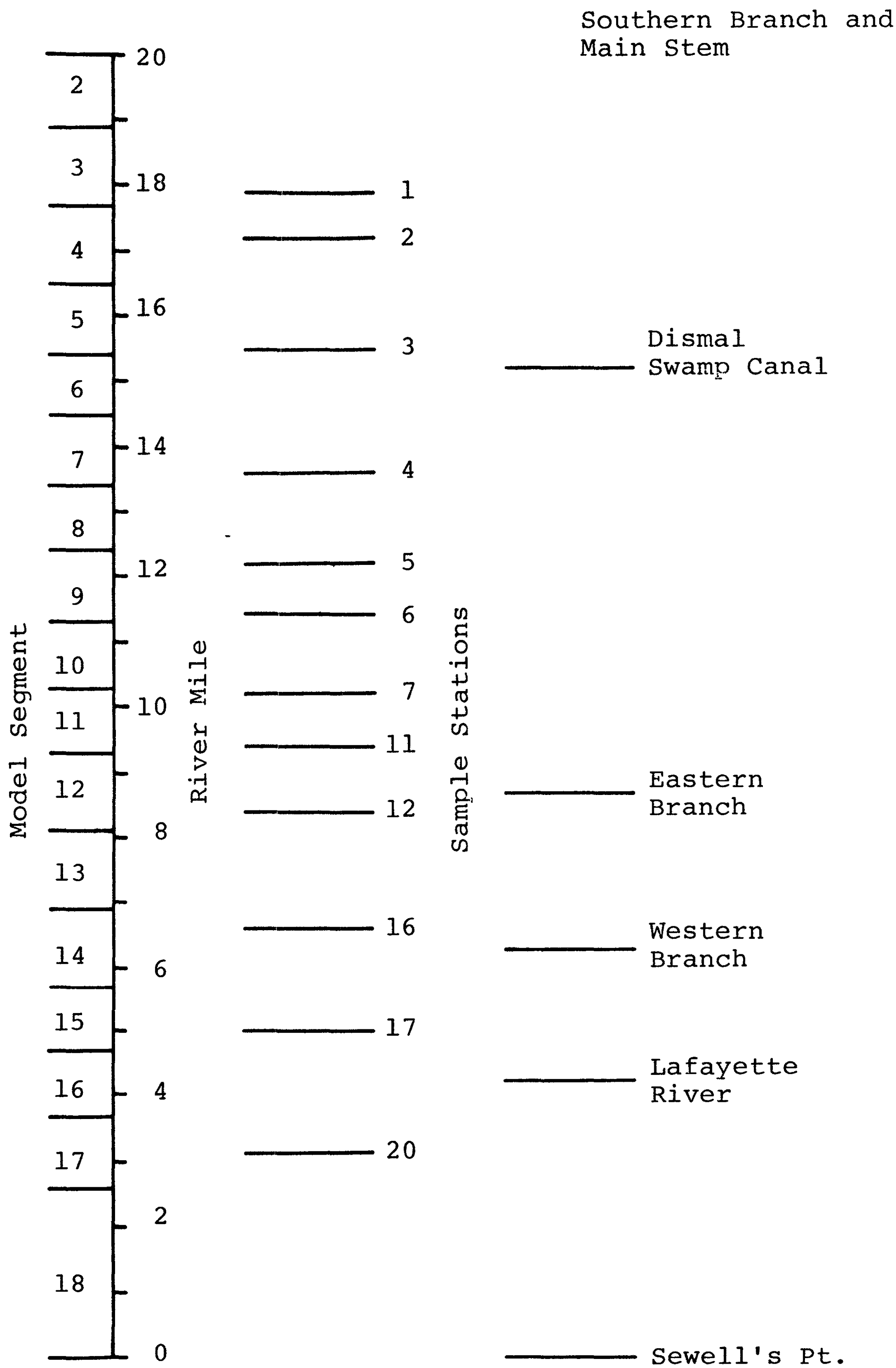

Figure 6. Location of intensive sampling stations.

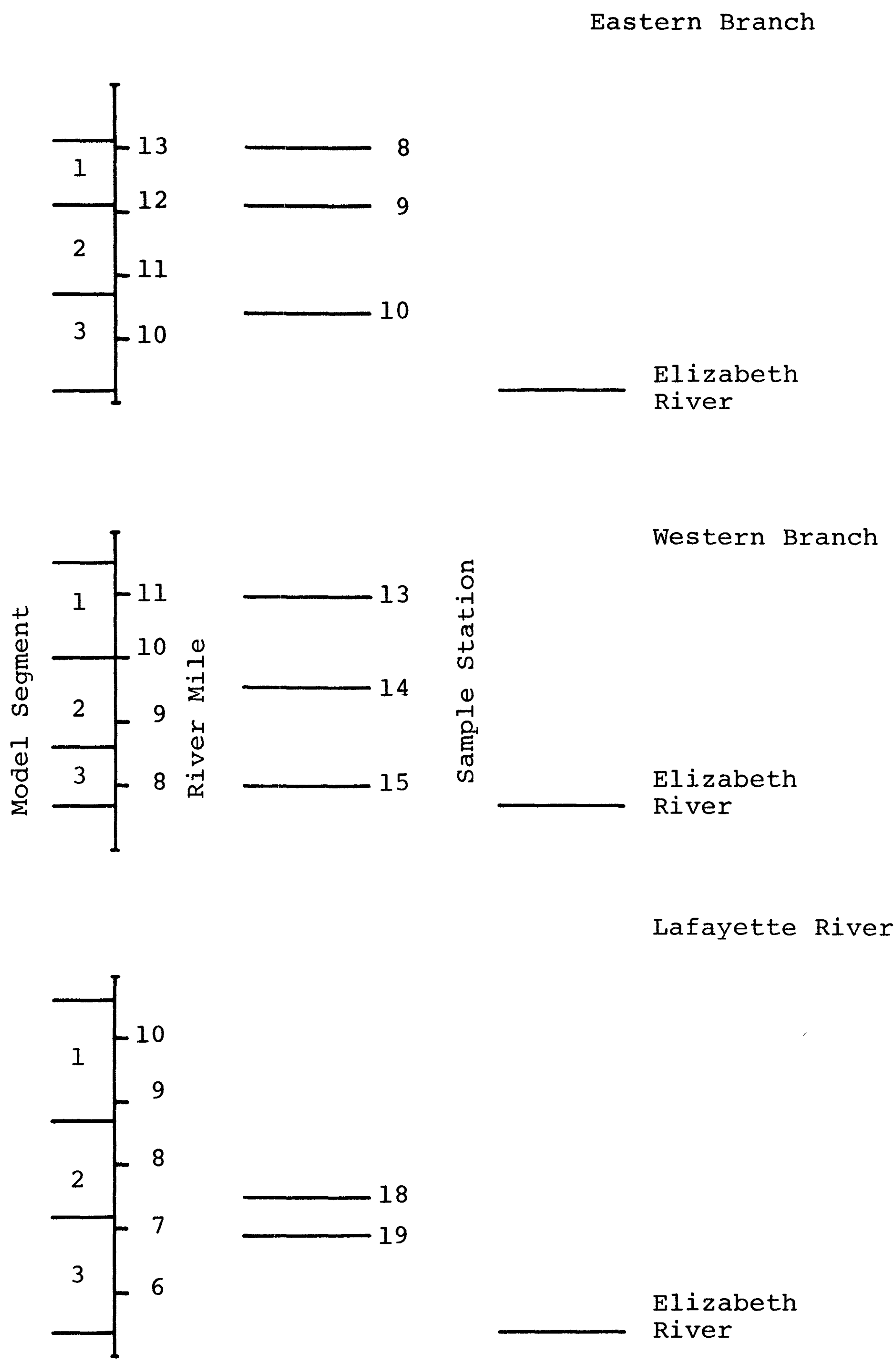

Figure 6. Continued

Lafayette River (Figures 37-46). Both the range of the field data and the average values (over depth and over two tidal cycles) are given, as well as the daily average of the values predicted by the model.

The calibration is generally satisfactory except for the ammonia nitrogen parameter. Field data for this parameter are consistently higher than the model predictions when reasonable values of k_{n12} and k_{n23} are utilized. The likelihood is that a salinity interference was present when the ammonia samples were analyzed and the field data are spurious. Therefore, values of k_{n12} and k_{n23} have been assumed based on values used in calibrated models of similar water bodies. The sensitivity of the results to these assumptions is tested in a subsequent section.

An alternative hypothesis is that a large source of ammonia nitrogen is absent from the input data. Sensitivity analysis shows, however, that doubling the point source inputs in the model is not enough to bring the predicted ammonia concentration into the range of the field data. It is unlikely that a source of this magnitude could be omitted.

B. Model Verification

The Elizabeth River System model was verified using field data from slack water surveys of August 23 and 24, 1976. On these days, eight stations on the Southern

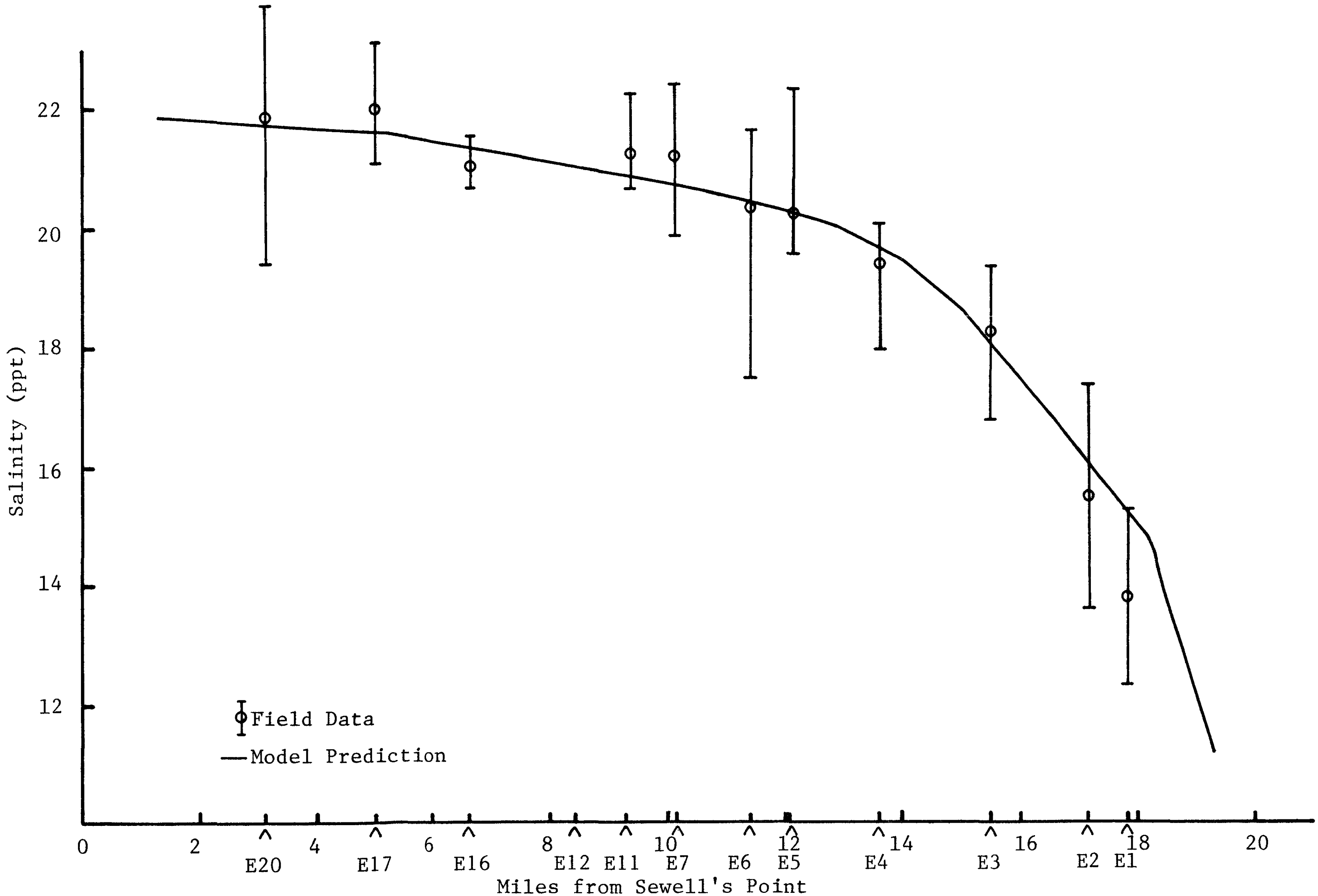

Figure 7. Results of salinity calibration for Southern and Main Branches.

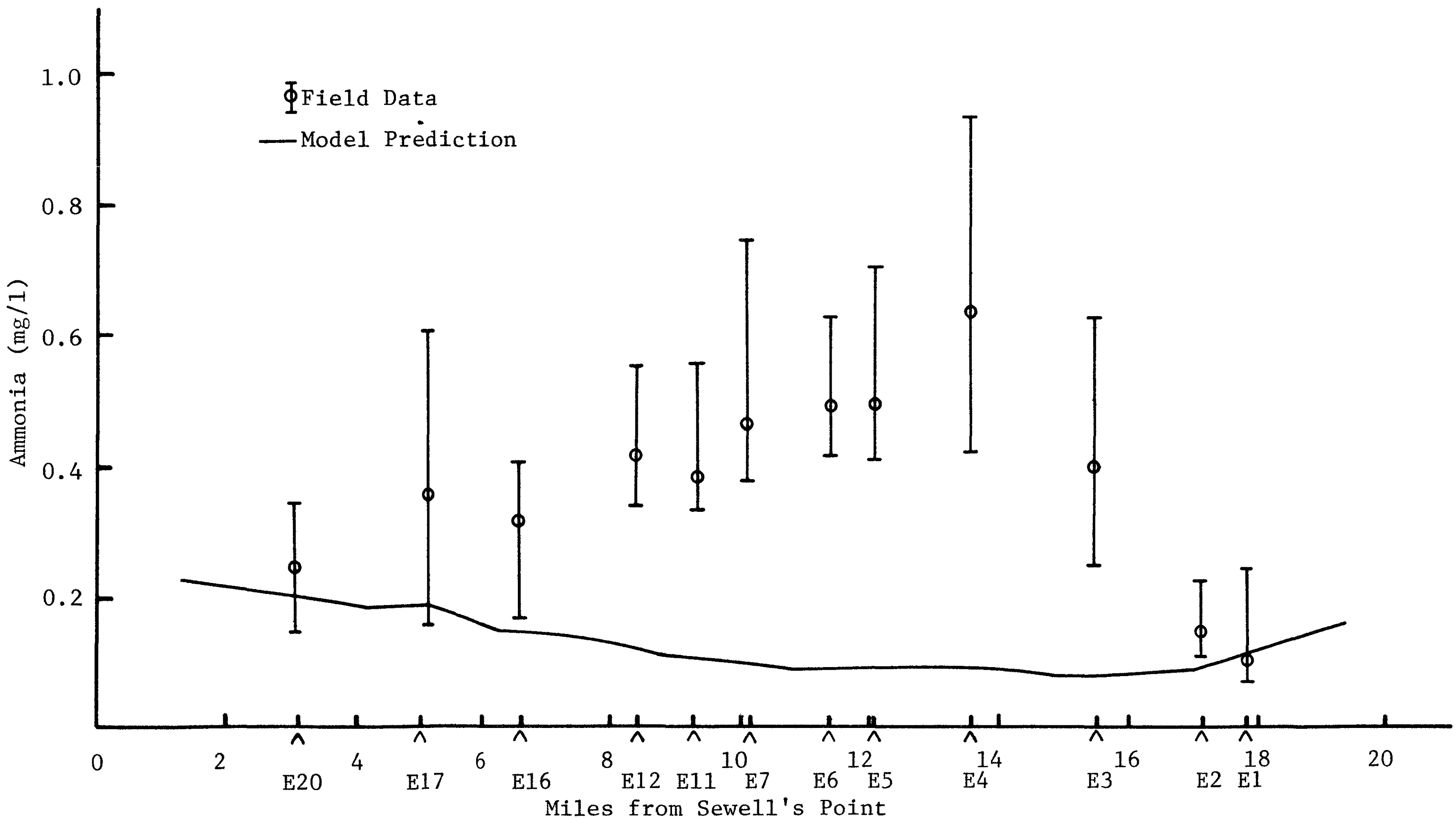

Figure 8. Results of ammonia calibration for Southern and Main Branches.

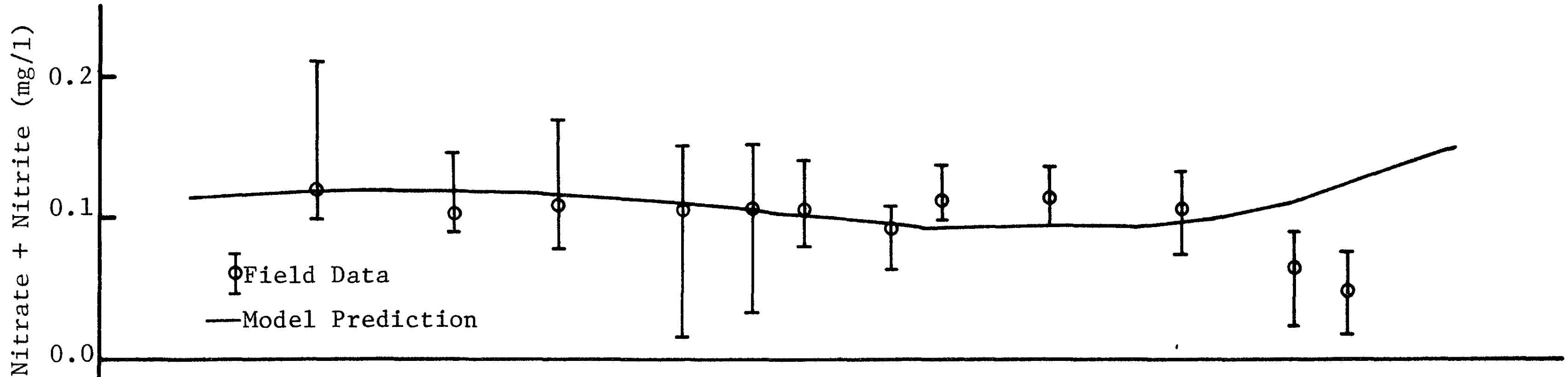

Figure 9. Results of nitrate calibration for Southern and Main Branches.

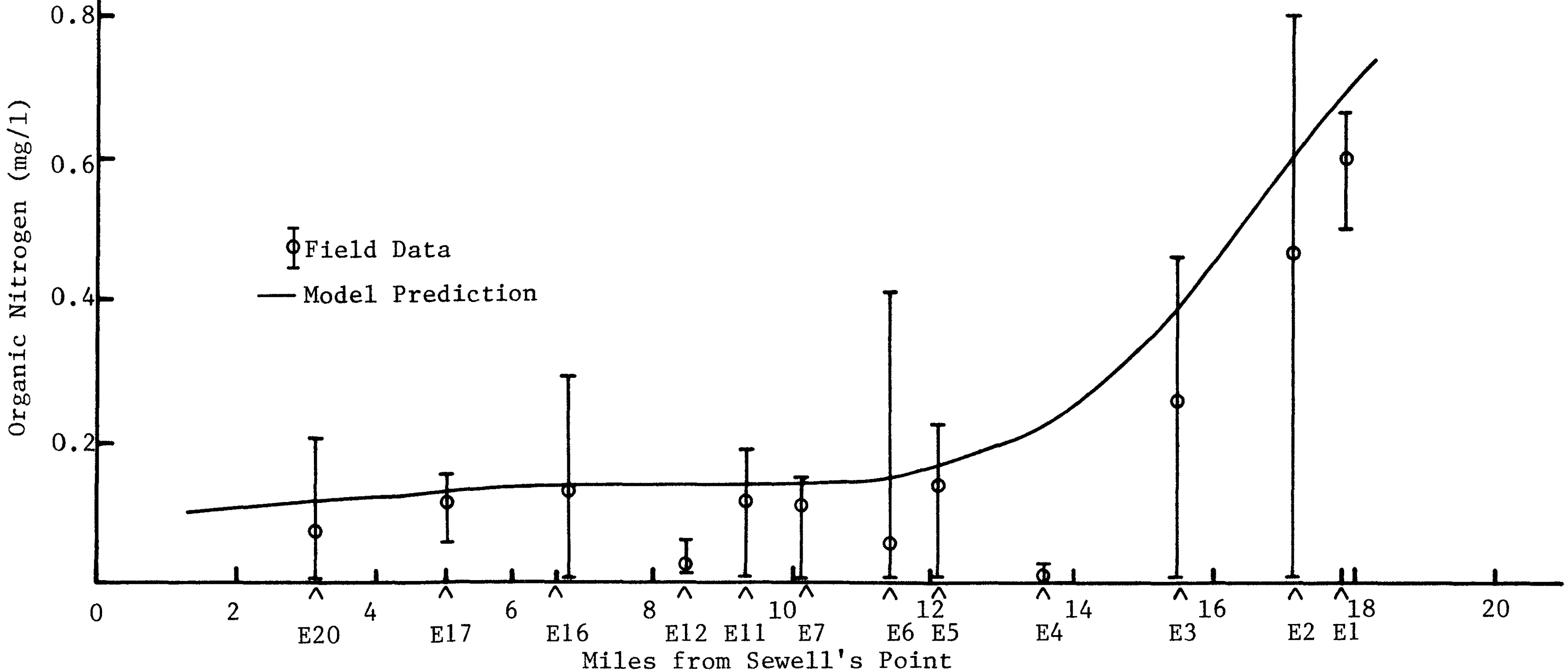

Figure 10. Results of organic nitrogen calibration for Southern and Main Branches.

Figure 11. Results of inorganic phosphorous calibration for Southern and Main Branches.

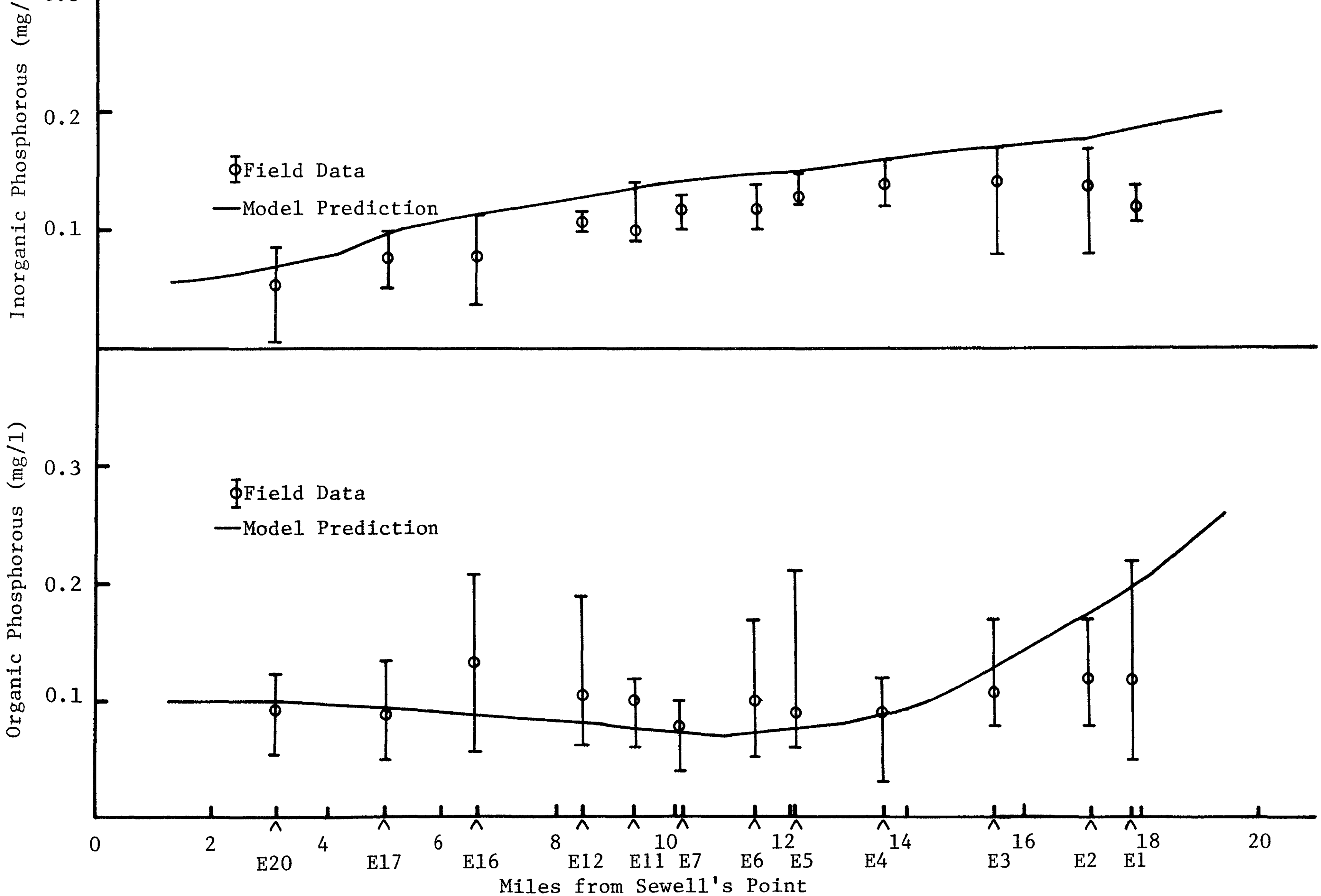

Figure 12. Results of organic phosphorous calibration for Southern and Main Branches.

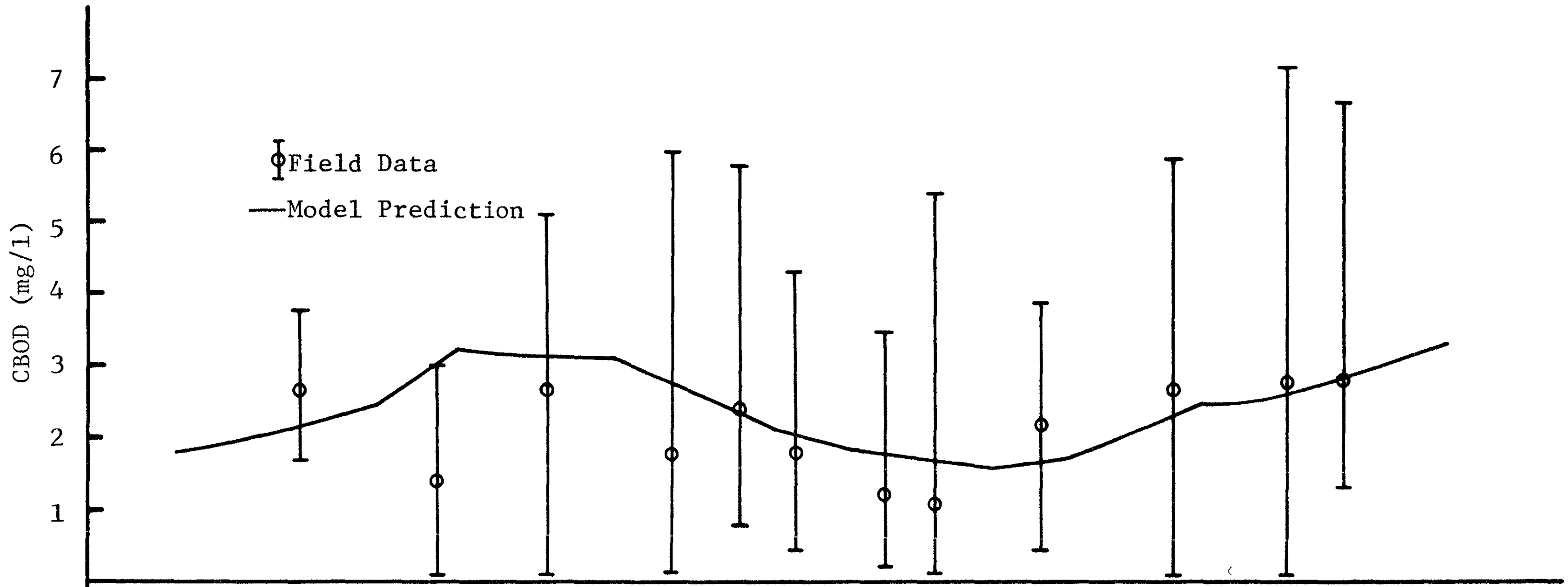

Figure 13. Results of CBOD calibration for Southern and Main Branches.

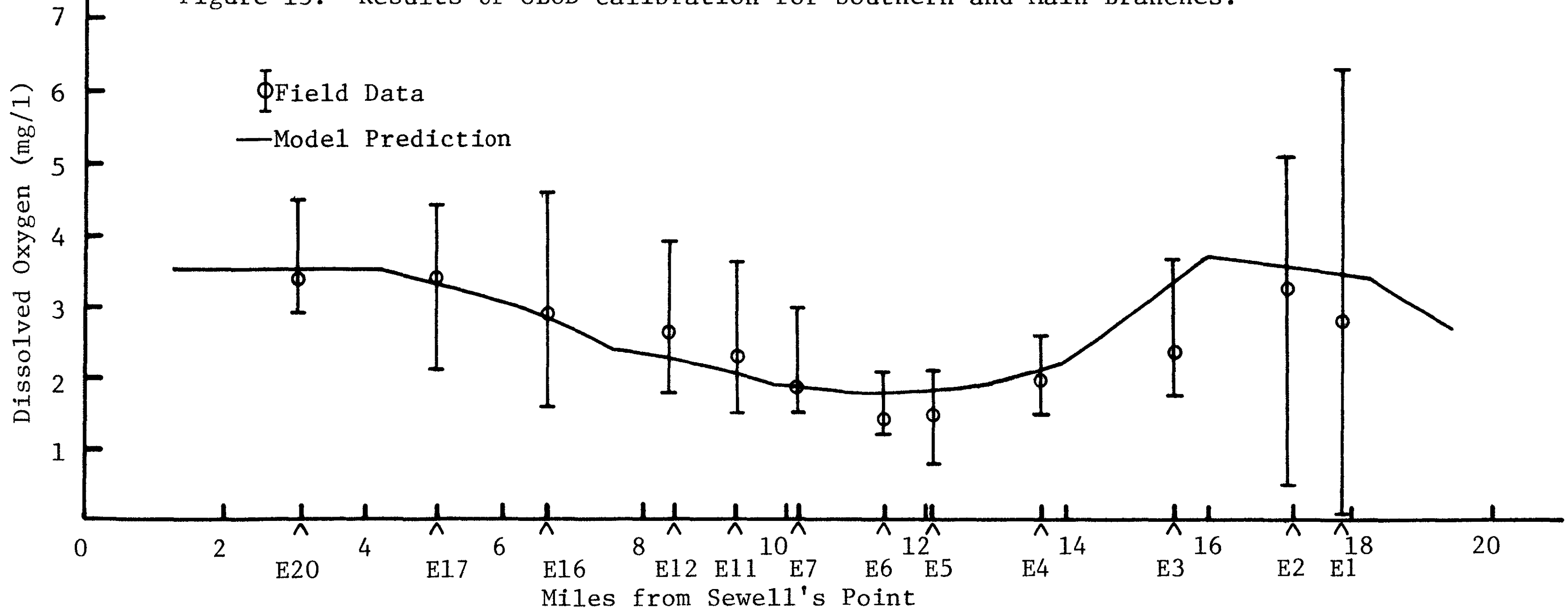

Figure 14. Results of dissolved oxygen calibration for Southern and Main Branches.

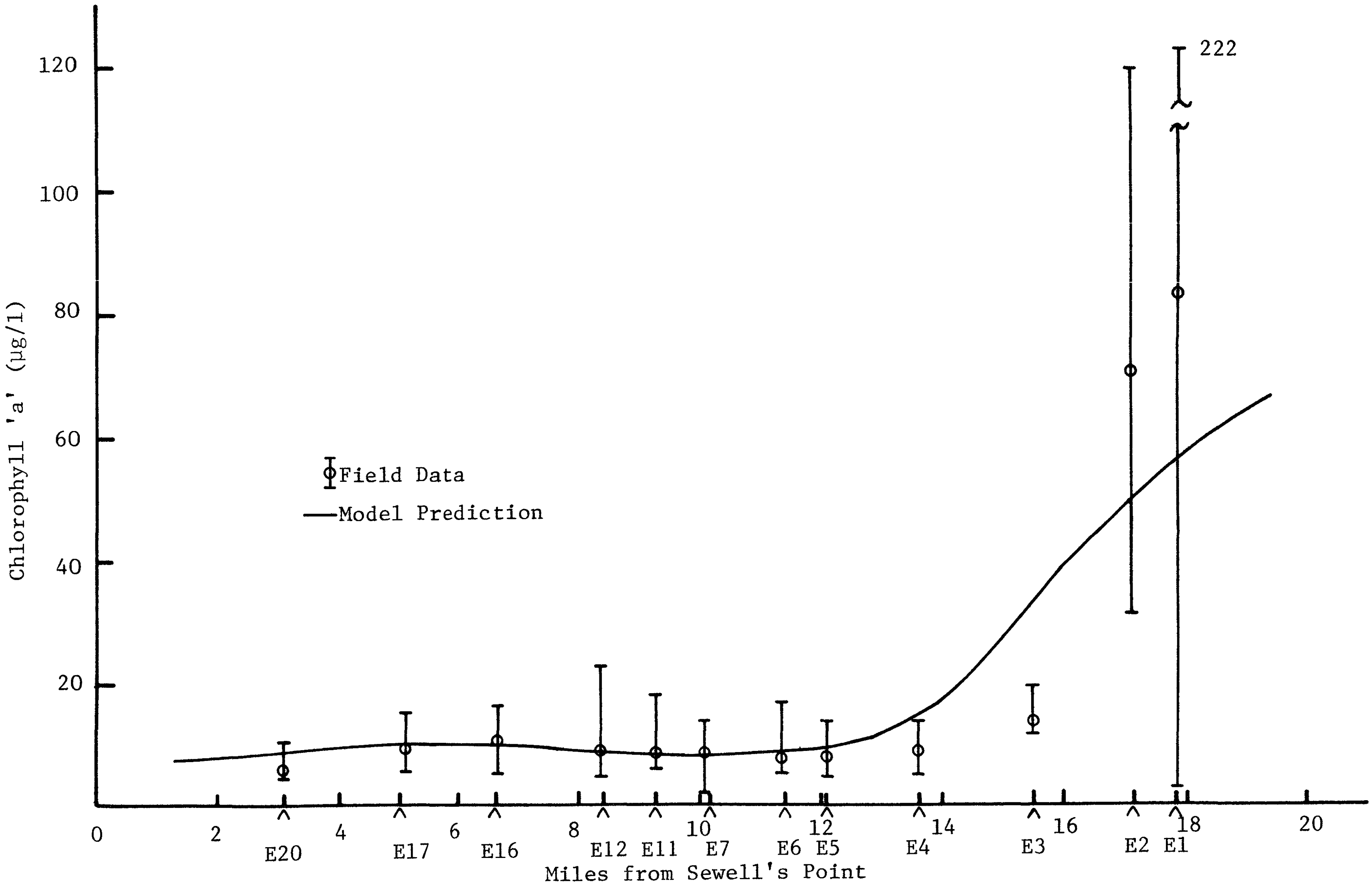

Figure 15. Results of chlorophyll 'a' calibration for Southern and Main Branches.

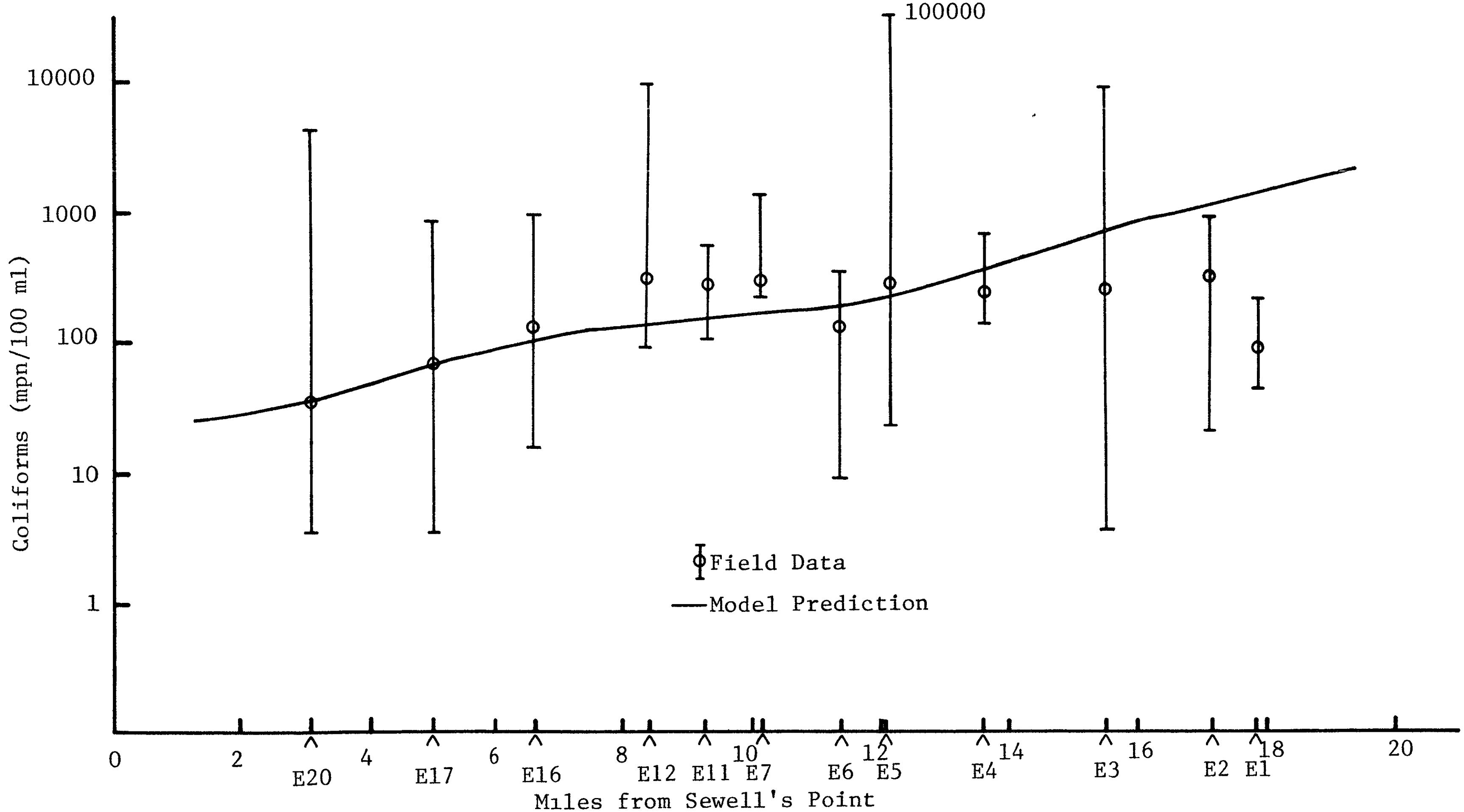

Figure 16. Results of fecal coliform calibration for Southern and Main Branches.

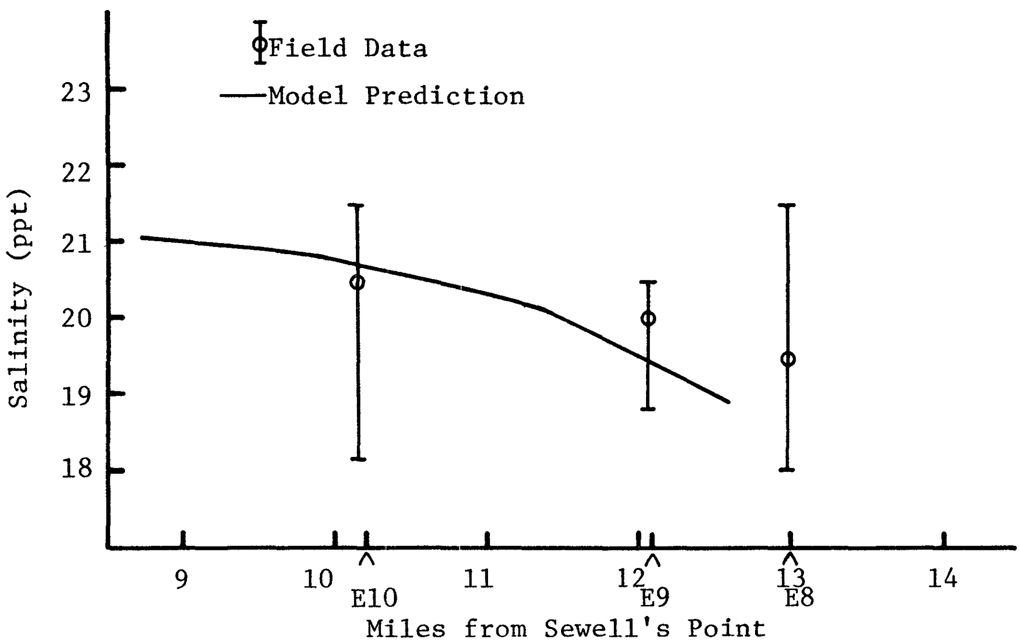

Figure 17. Results of salinity calibration for Eastern Branch.

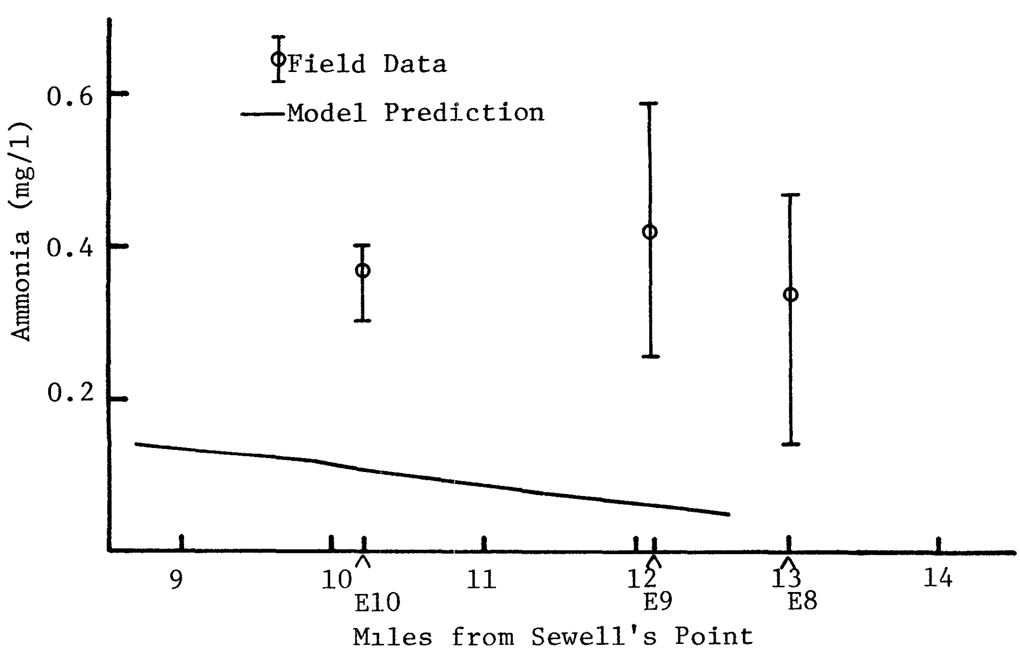

Figure 18. Results of ammonia calibration for Eastern Branch.

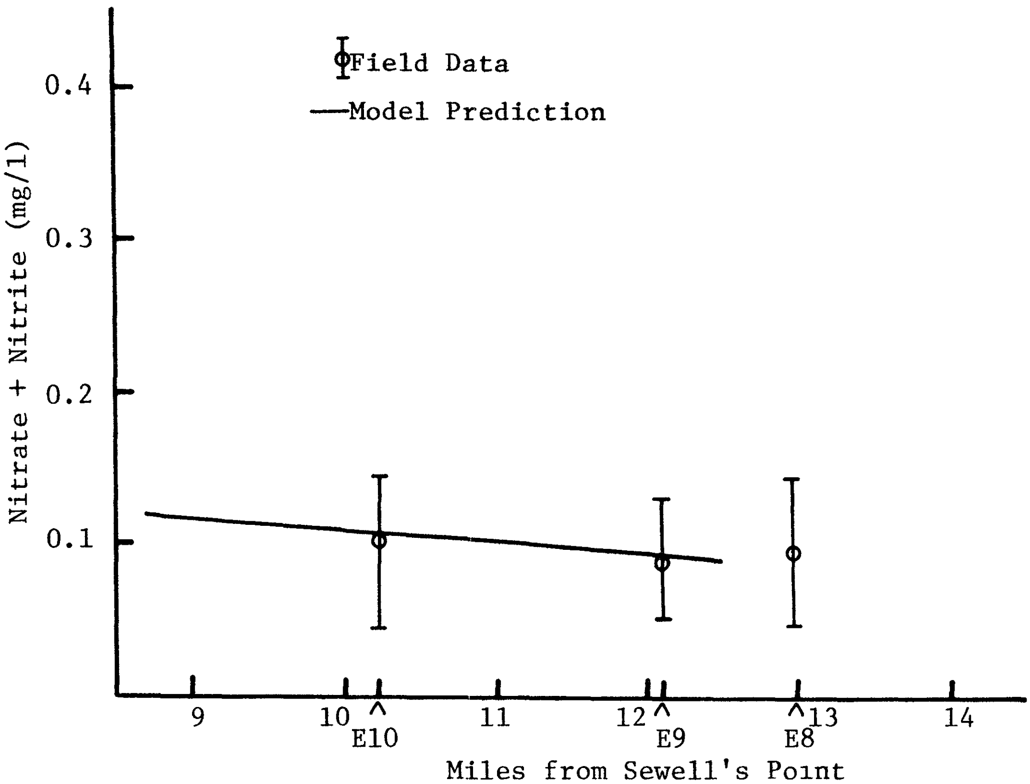

Figure 19. Results of nitrate calibration for Eastern Branch.

Figure 20. Results of organic nitrogen calibration for Eastern Branch.

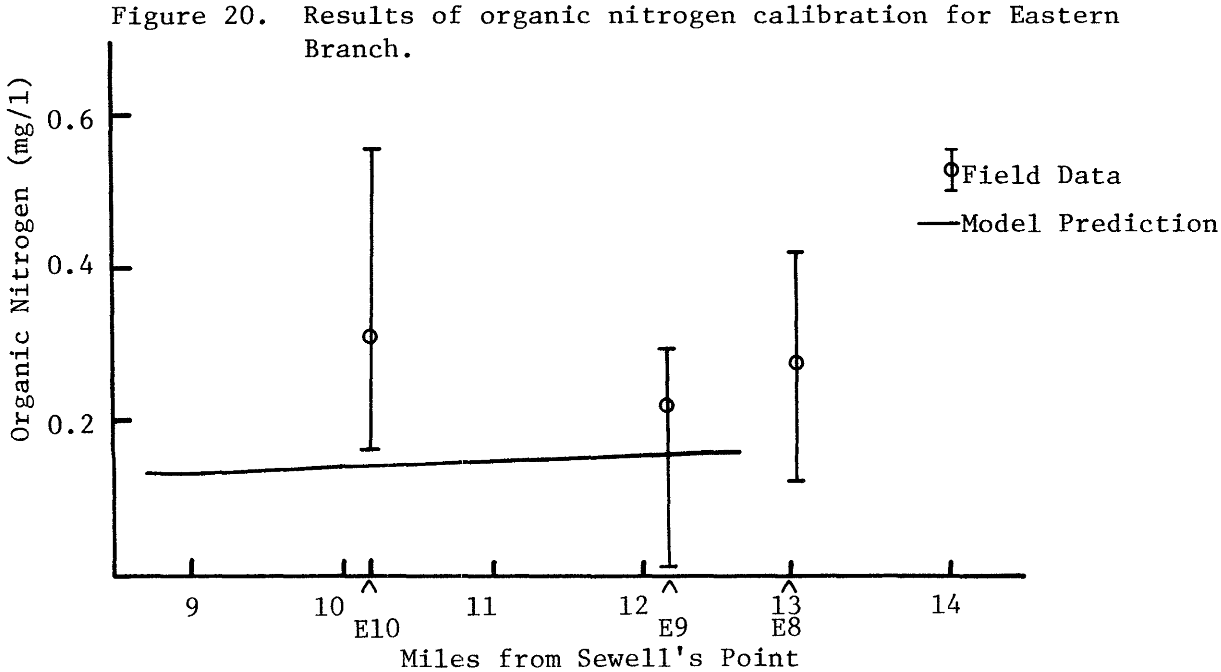

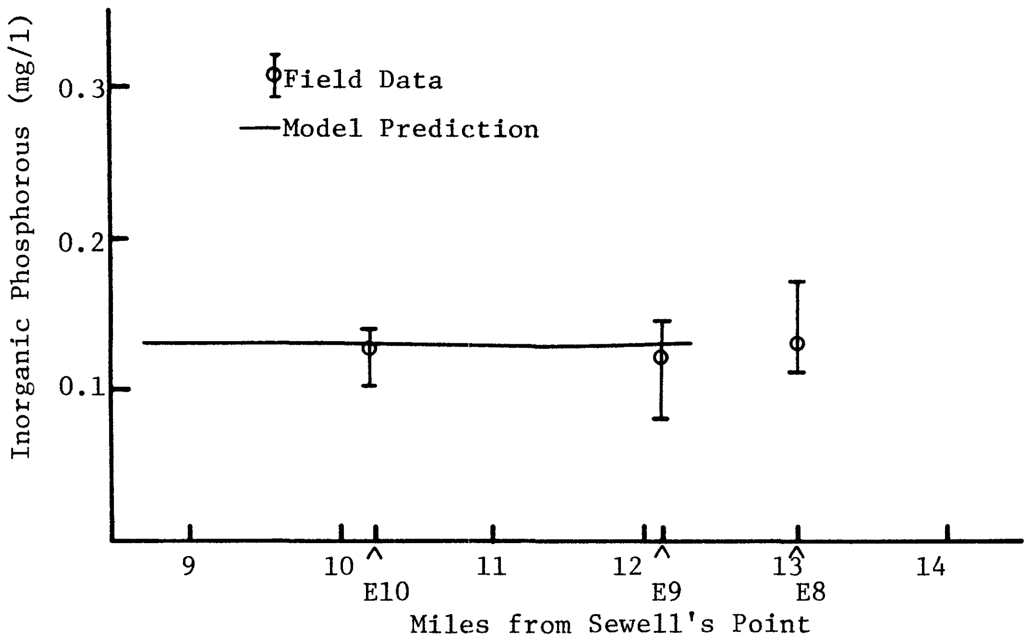

Figure 21. Results of inorganic phosphorous calibration for Eastern Branch.

Figure 22. Results of organic phosphorous calibration for Eastern Branch.

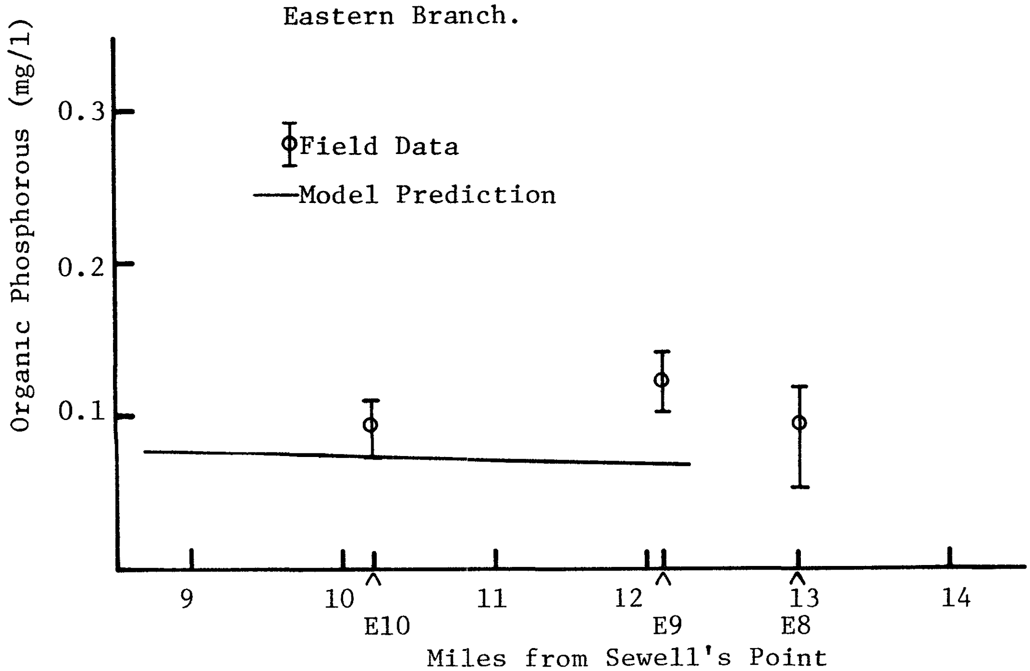

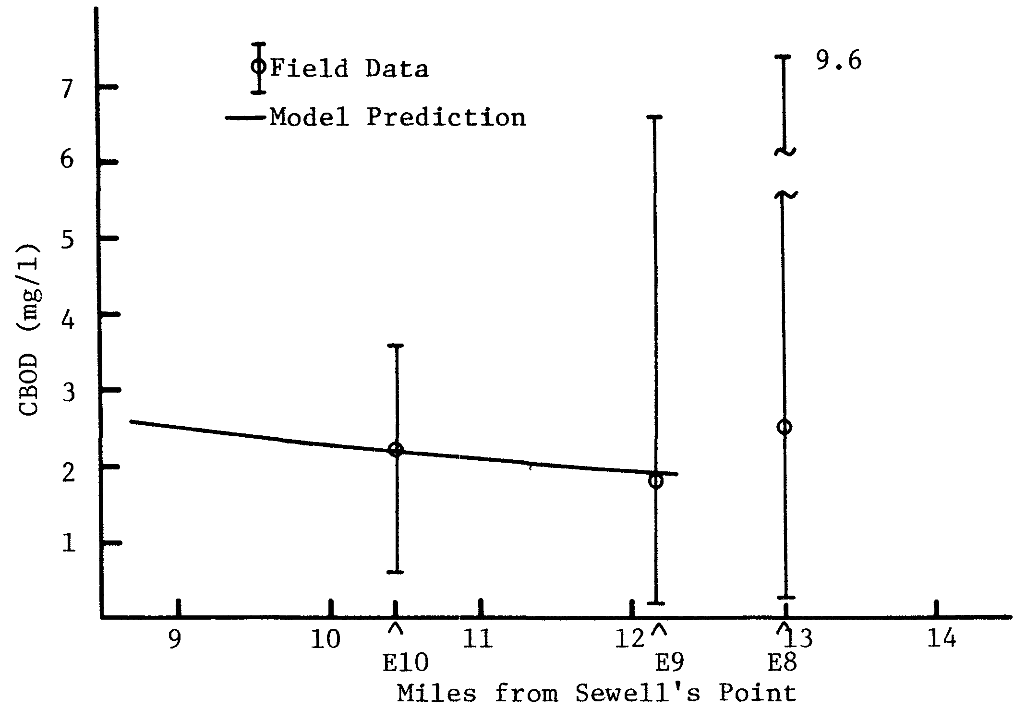

Figure 23. Results of CBOD calibration for Eastern Branch.

Figure 24. Results of dissolved oxygen calibration for Eastern Branch.

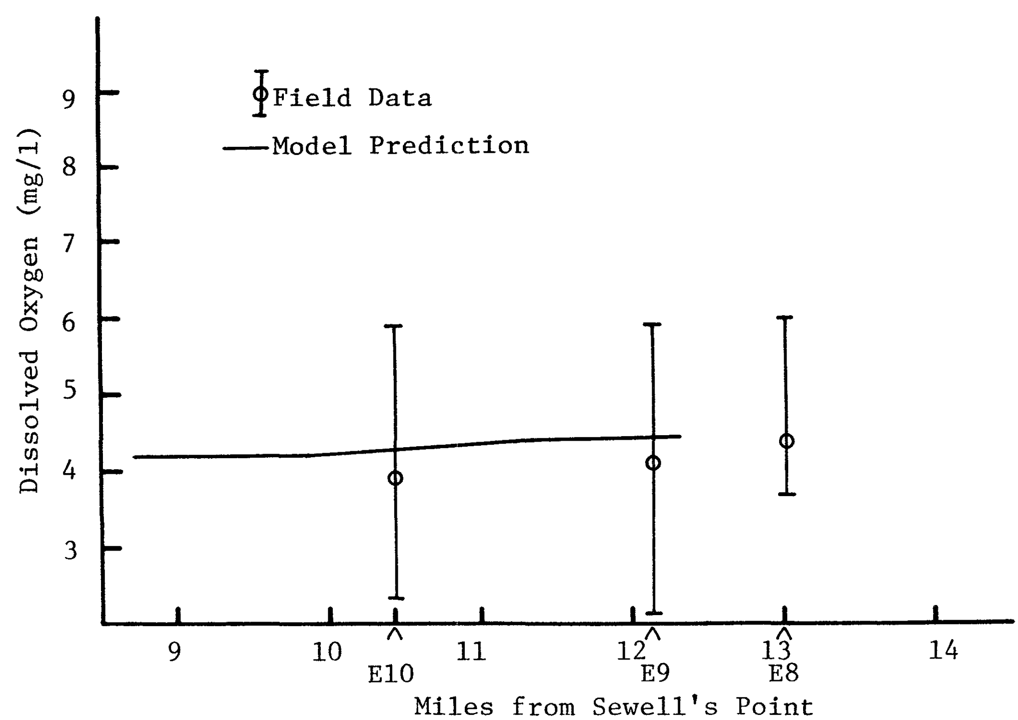

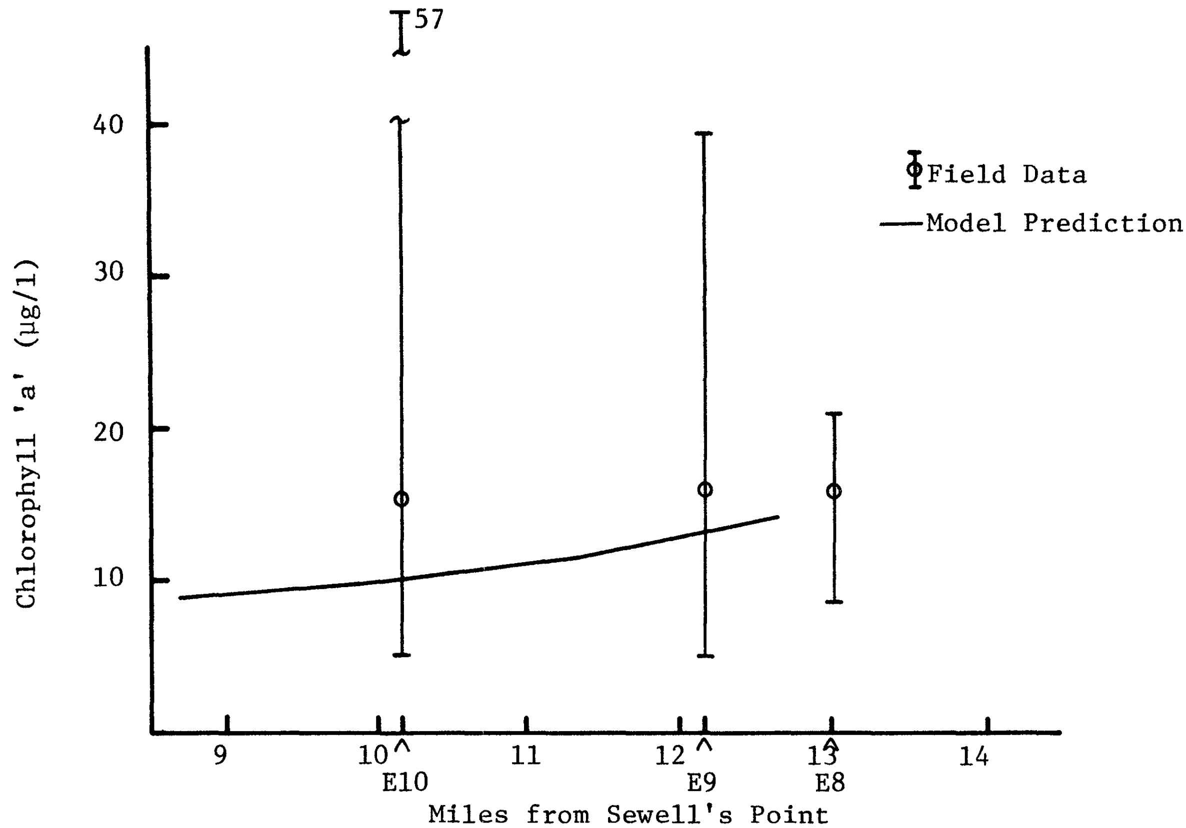

Figure 25. Results of chlorophyll 'a' calibration for Eastern Branch.

Figure 26. Results of fecal coliform calibration for Eastern Branch.

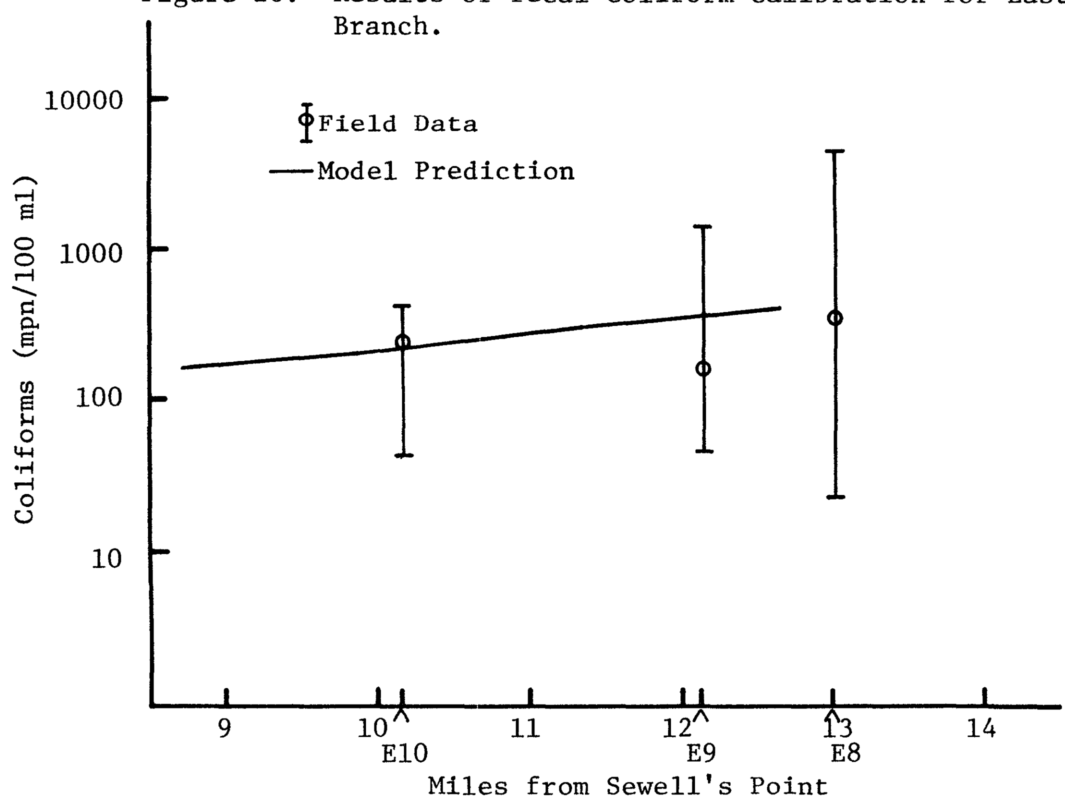

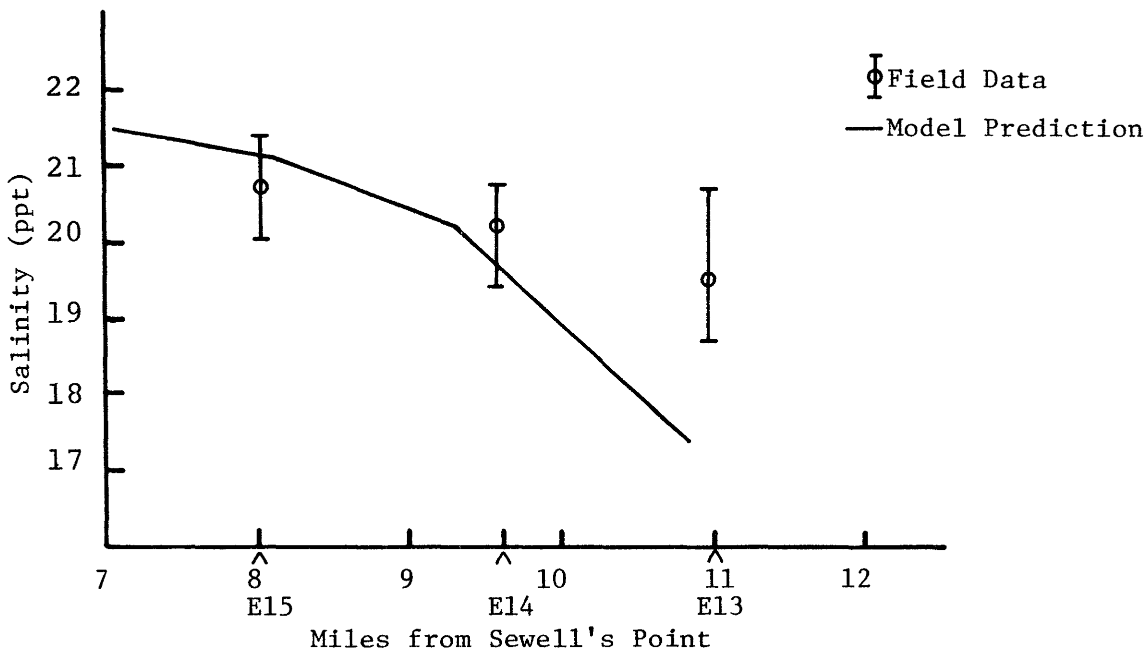

Figure 27. Results of salinity calibration for Western Branch.

Figure 28. Results of ammonia calibration for Western Branch.

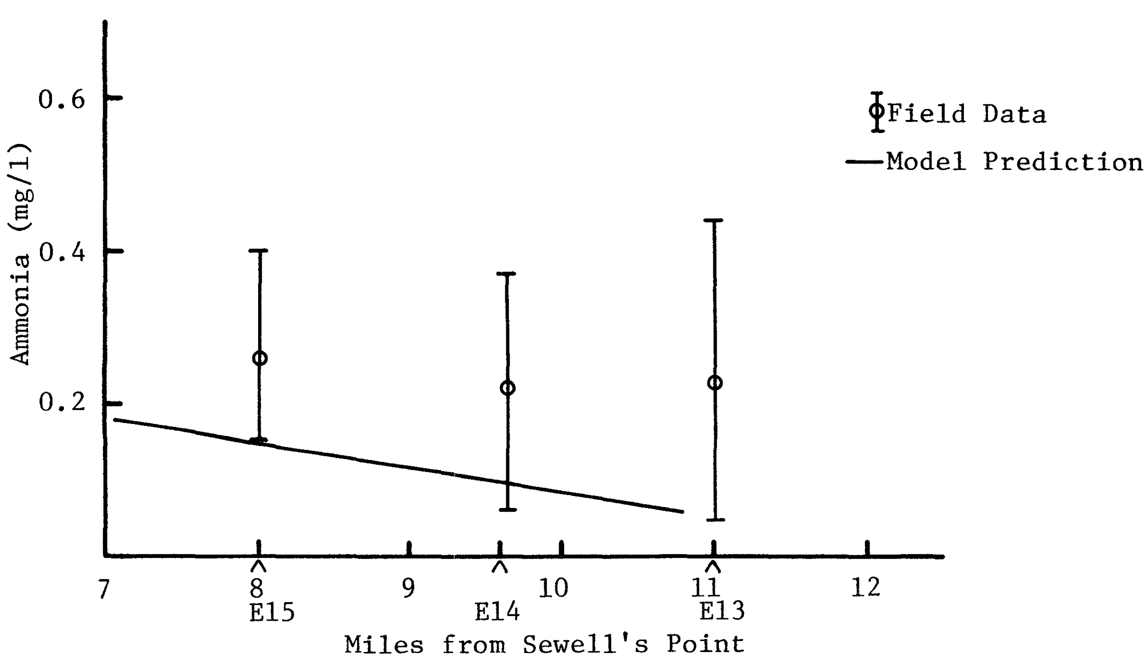

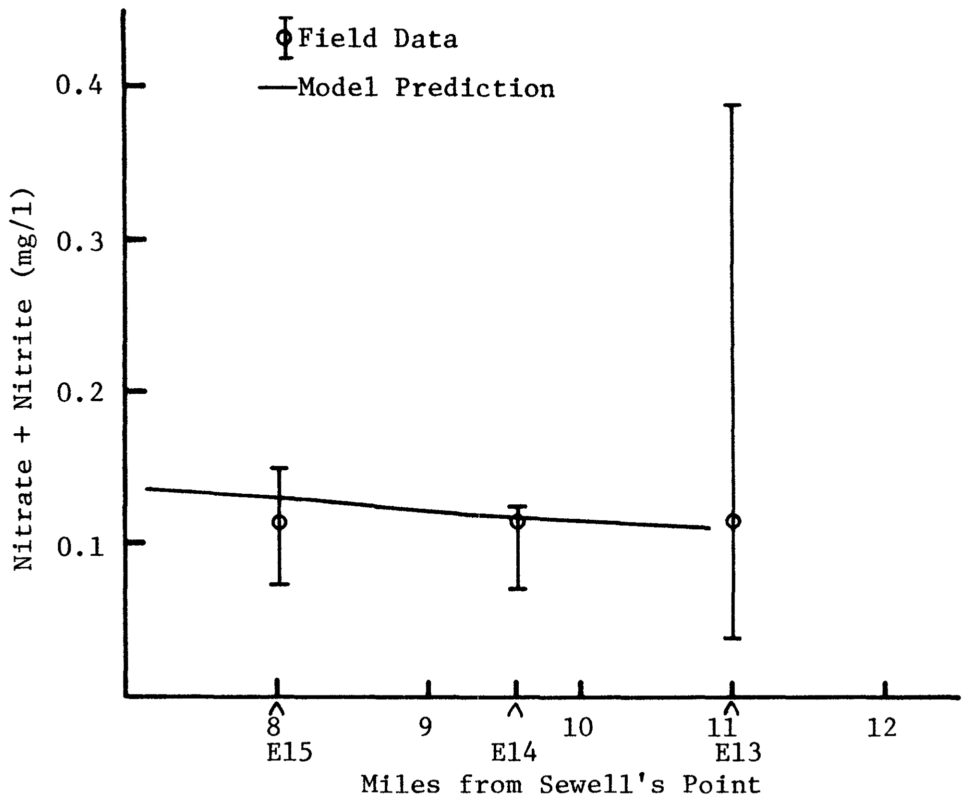

Figure 29. Results of nitrate calibration for Western Branch.

Figure 30. Results of organic nitrogen calibration for Western Branch.

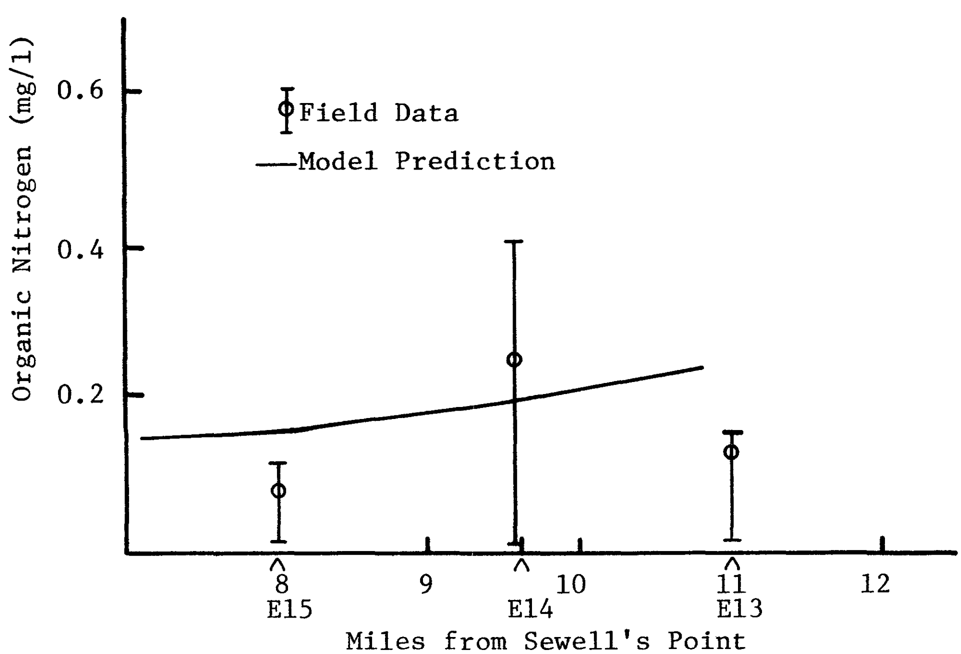

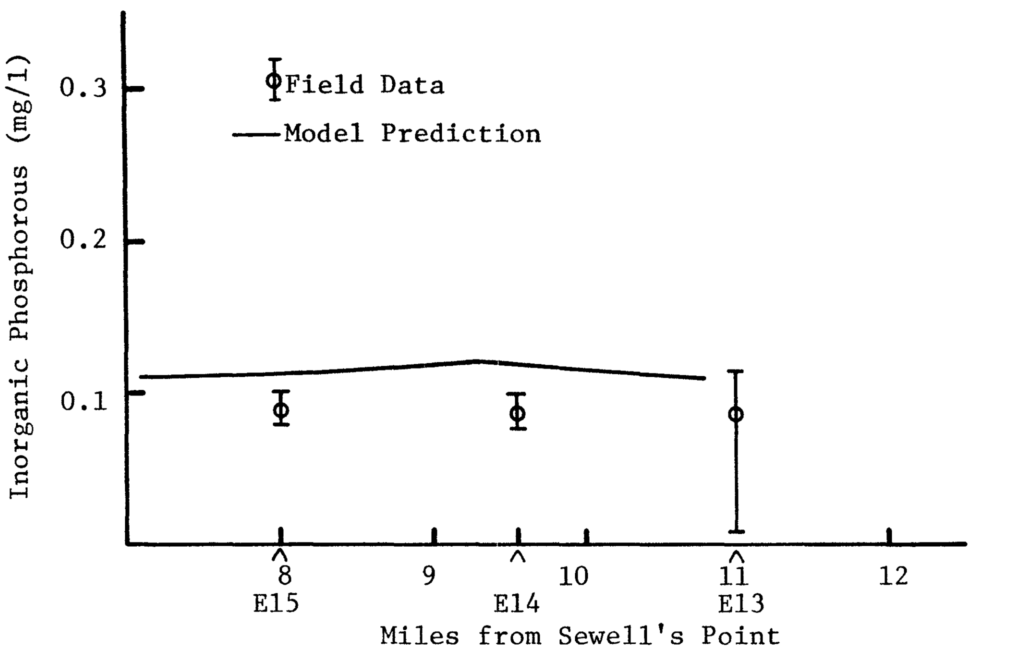

Figure 31. Results of inorganic phosphorous calibration for Western Branch

Figure 32. Results of organic phosphorous calibration for Western Branch

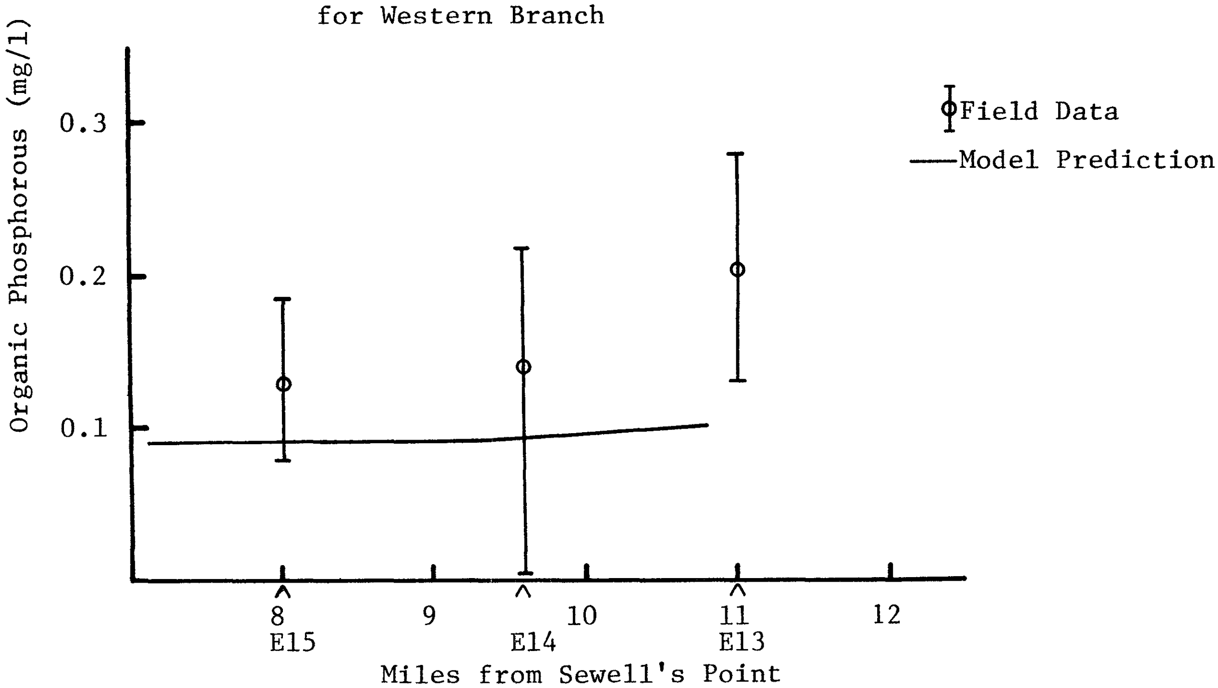

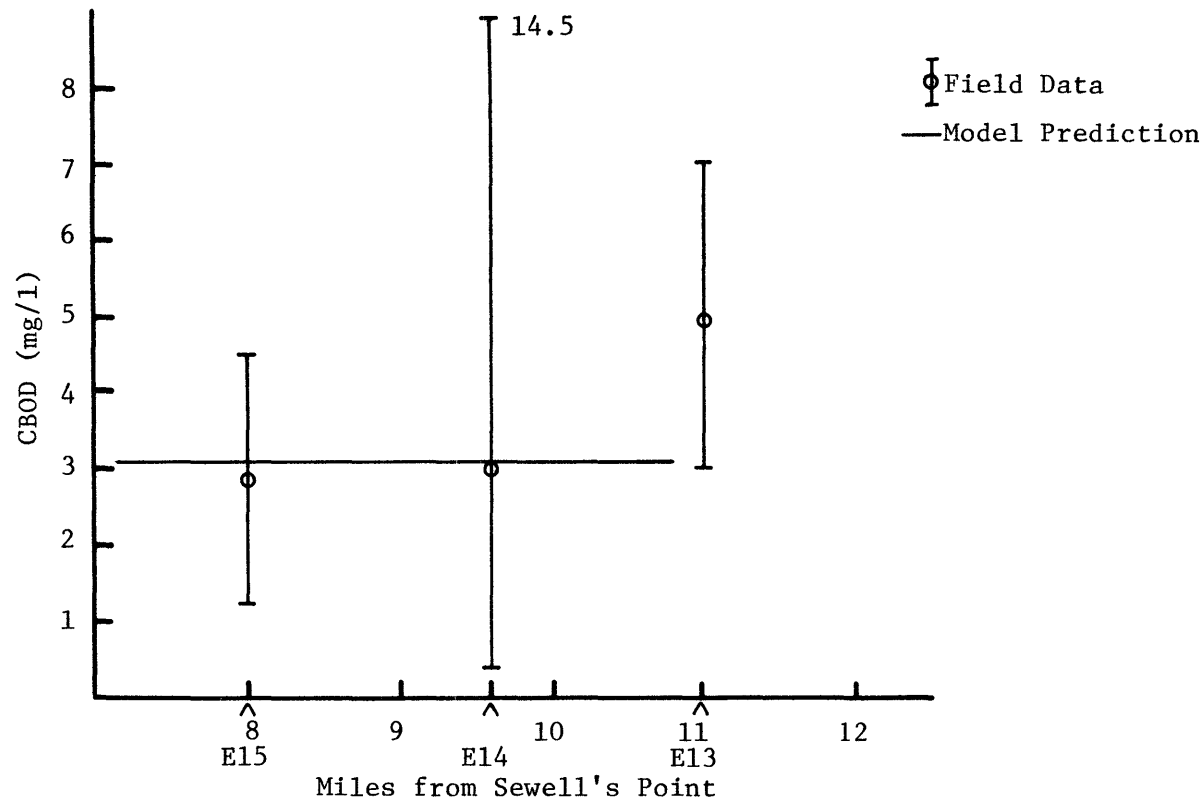

Figure 33. Results of CBOD calibration for Western Branch.

Figure 34. Results of dissolved oxygen calibration for Western Branch.

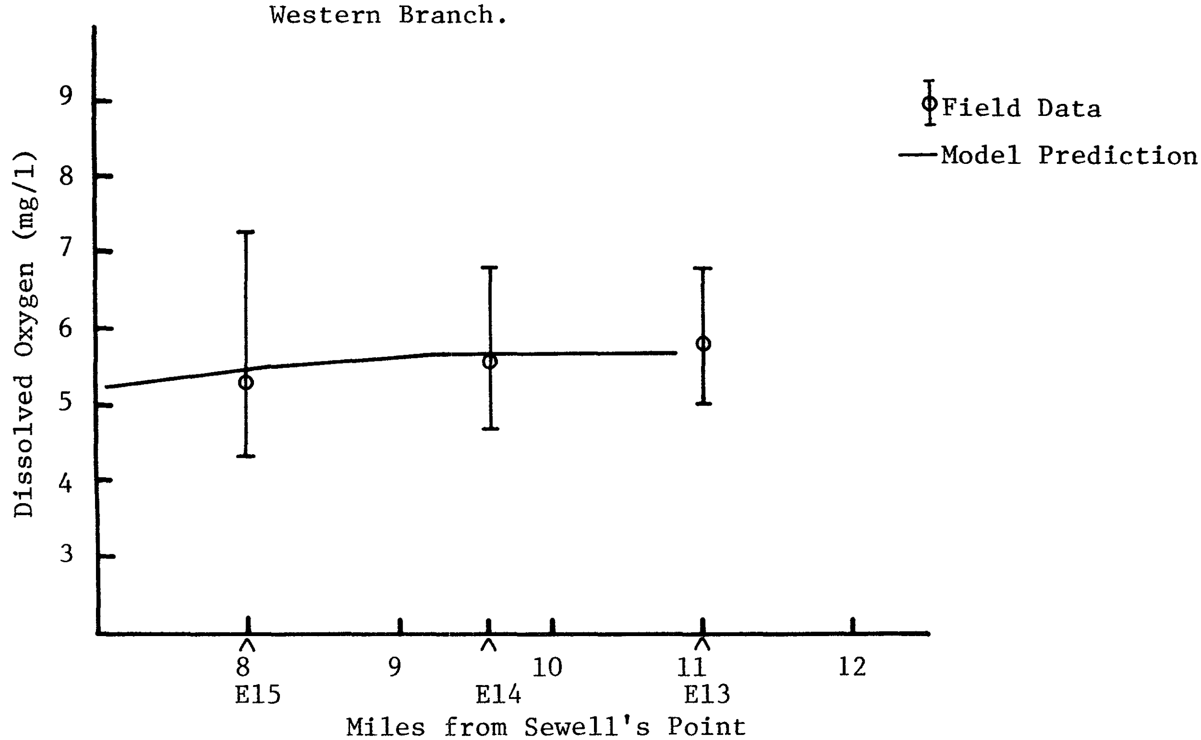

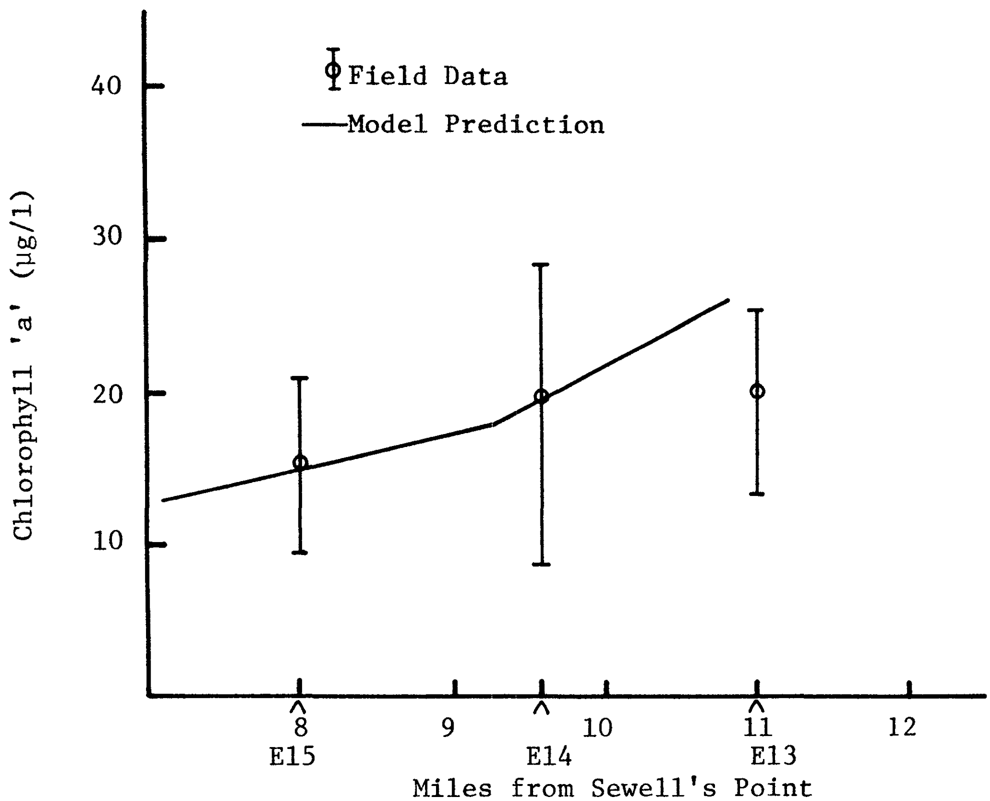

Figure 35. Results of chlorophyll 'a' calibration for Western Branch.

Figure 36. Results of fecal coliform calibration for Western Branch.

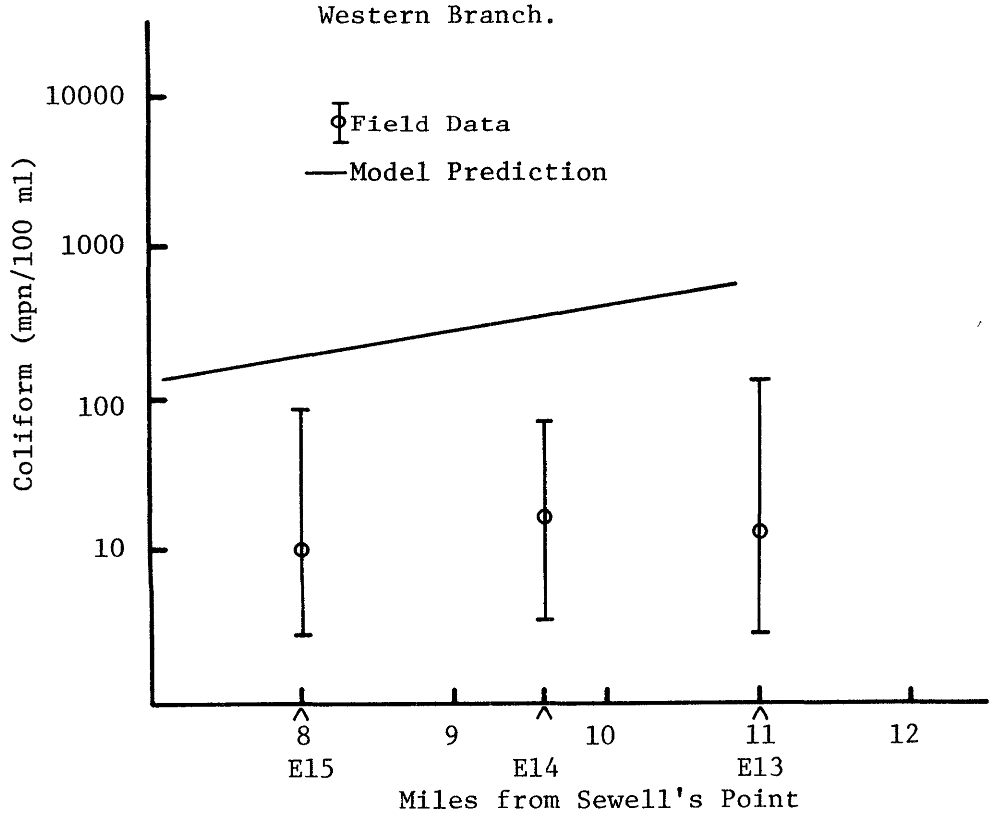

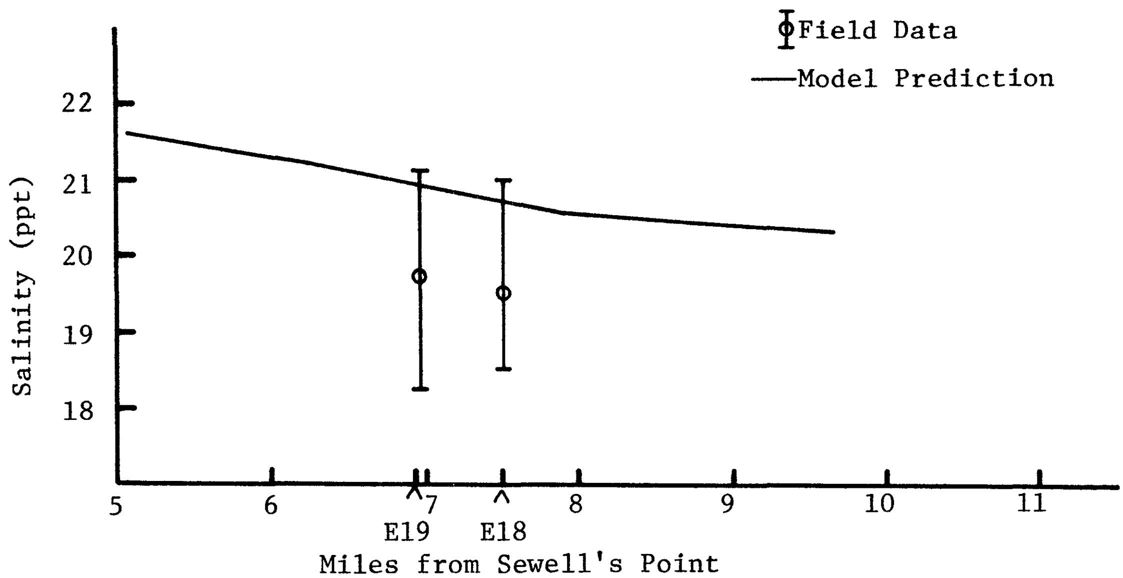

Figure 37. Results and salinity calibration for Lafayette River.

Figure 38. Results of ammonia calibration for Lafayette River.

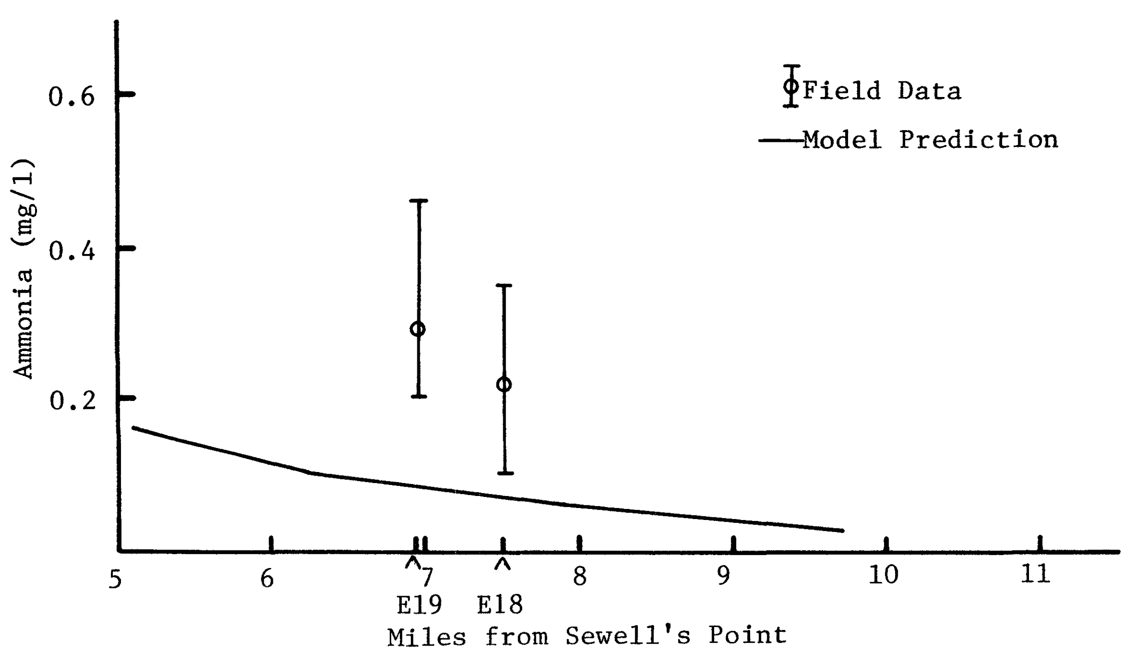

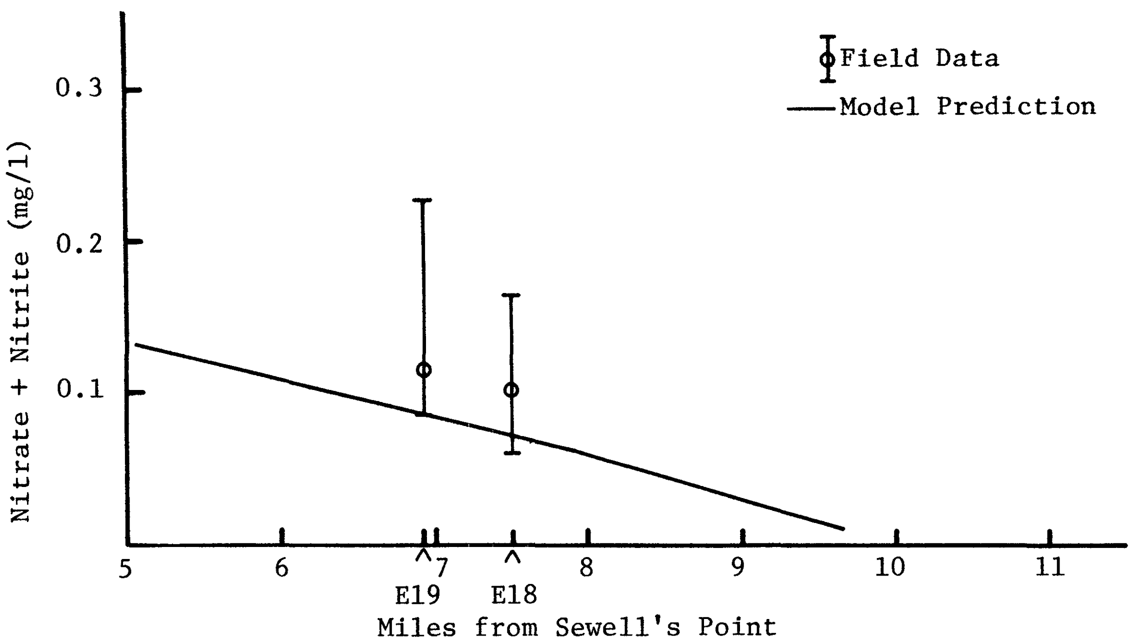

Figure 39. Results of nitrate calibration for Lafayette River.

Figure 40. Results of organic nitrogen calibration for Lafayette River.

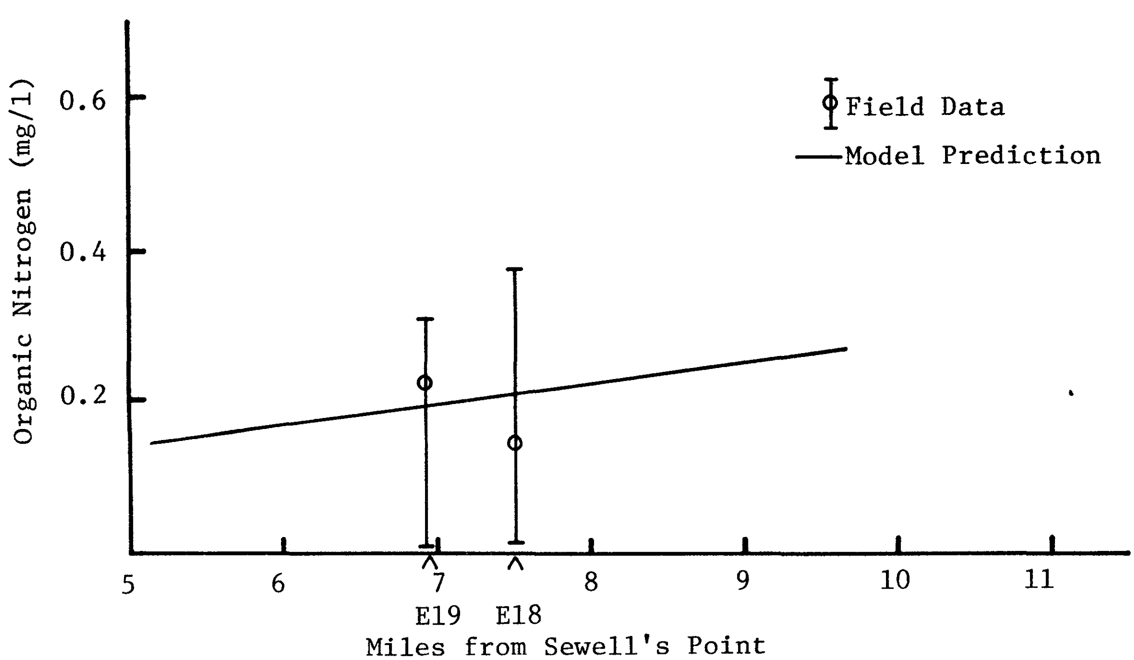

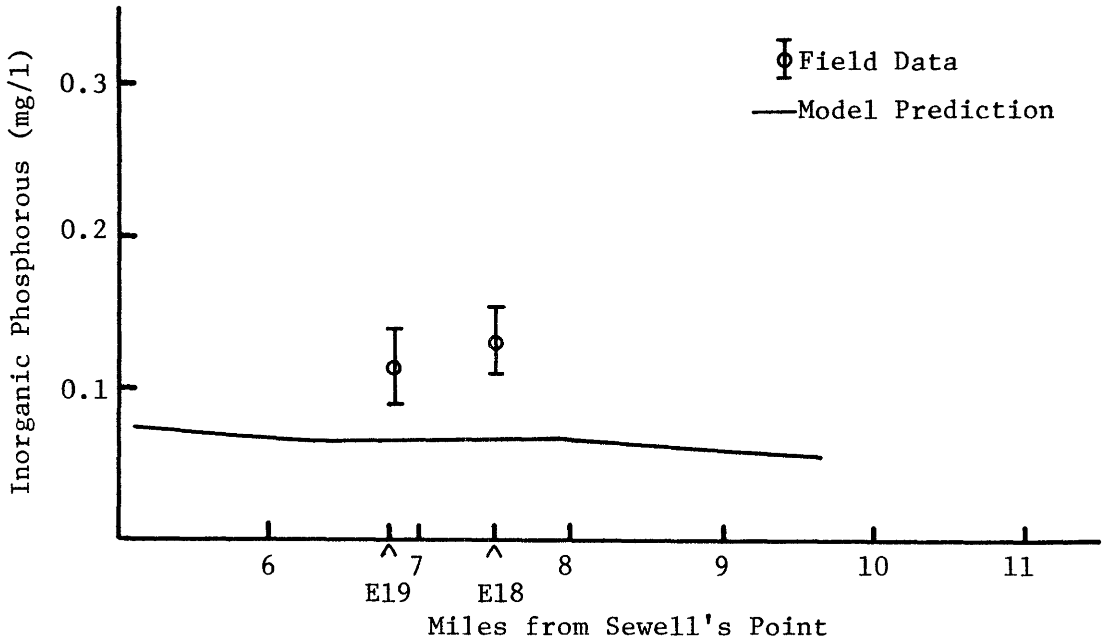

Figure 41. Results of inorganic phosphorous calibration for Lafayette River.

Figure 42. Results of organic phosphorous calibration for Lafayette River.

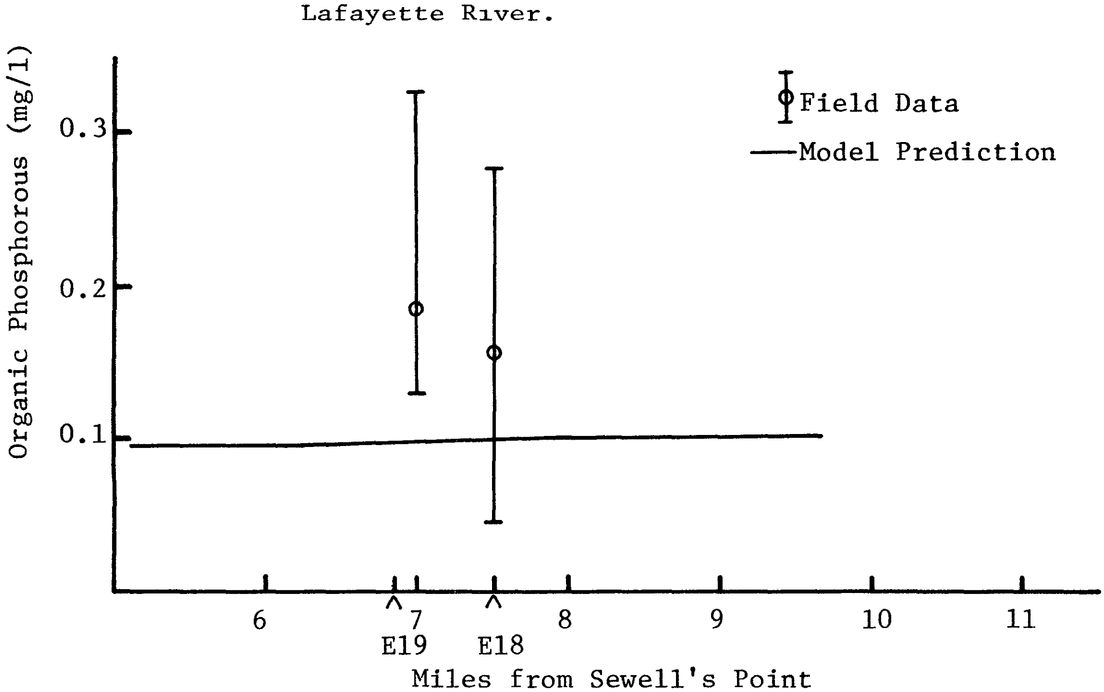

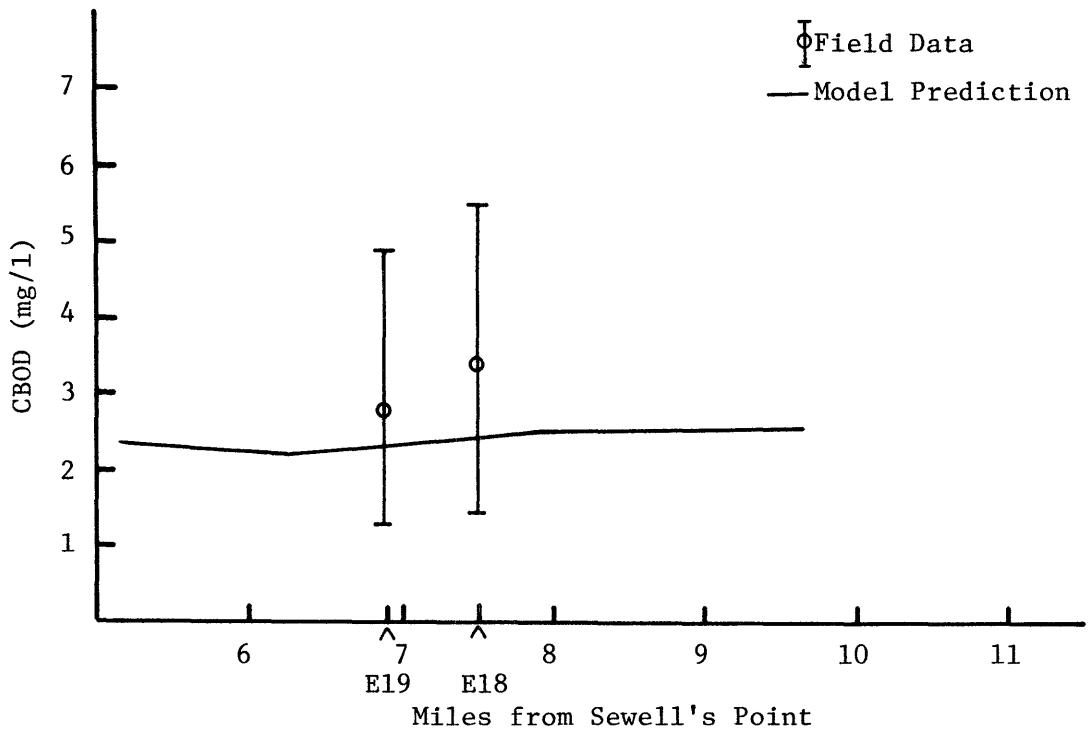

Figure 43. Results of CBOD calibration for Lafayette River.

Figure 44. Results of dissolved oxygen calibration for Lafayette River.

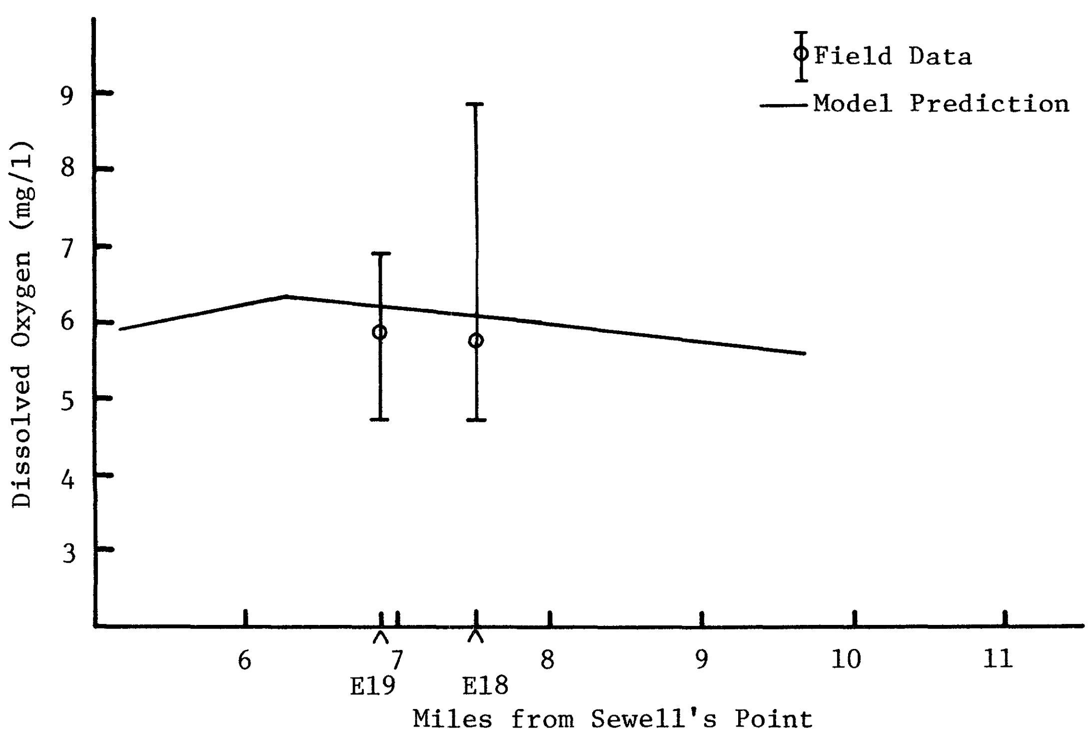

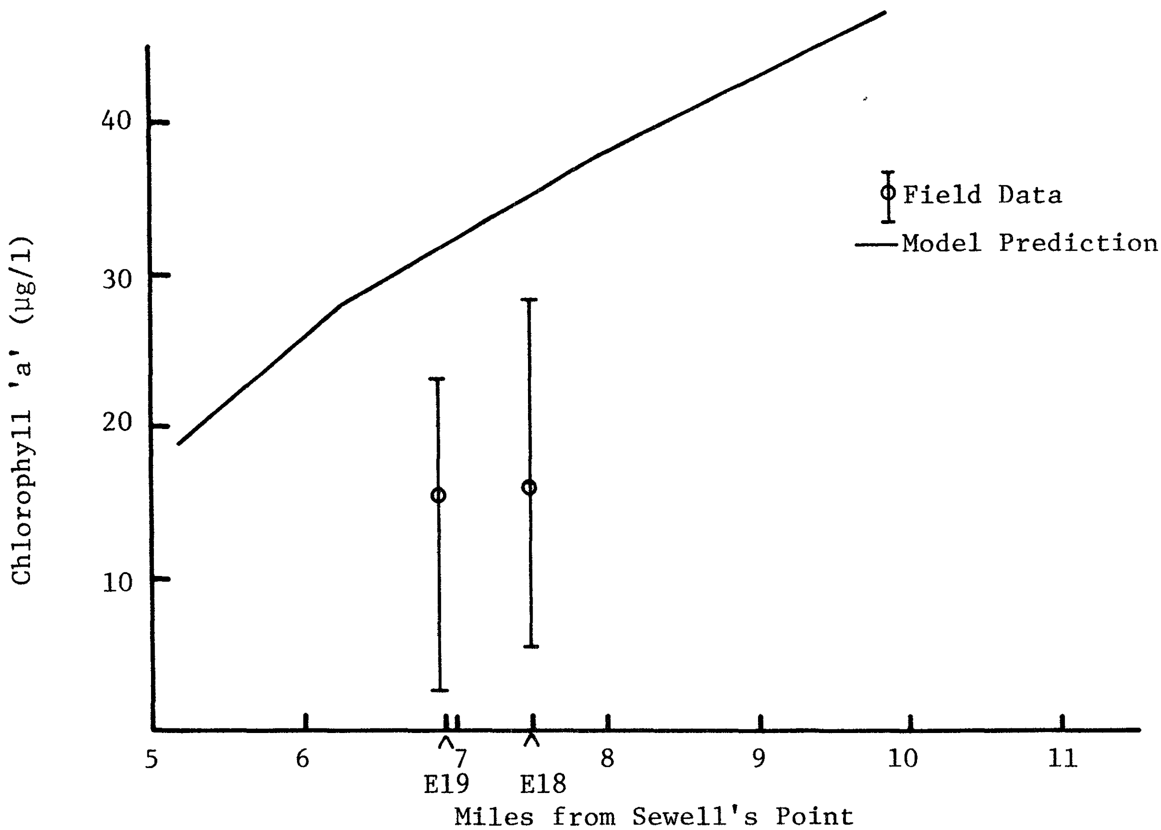

Figure 45. Results of chlorophyll 'a' calibration for Lafayette River.

Figure 46. Results of fecal coliform calibration for Lafayette River.

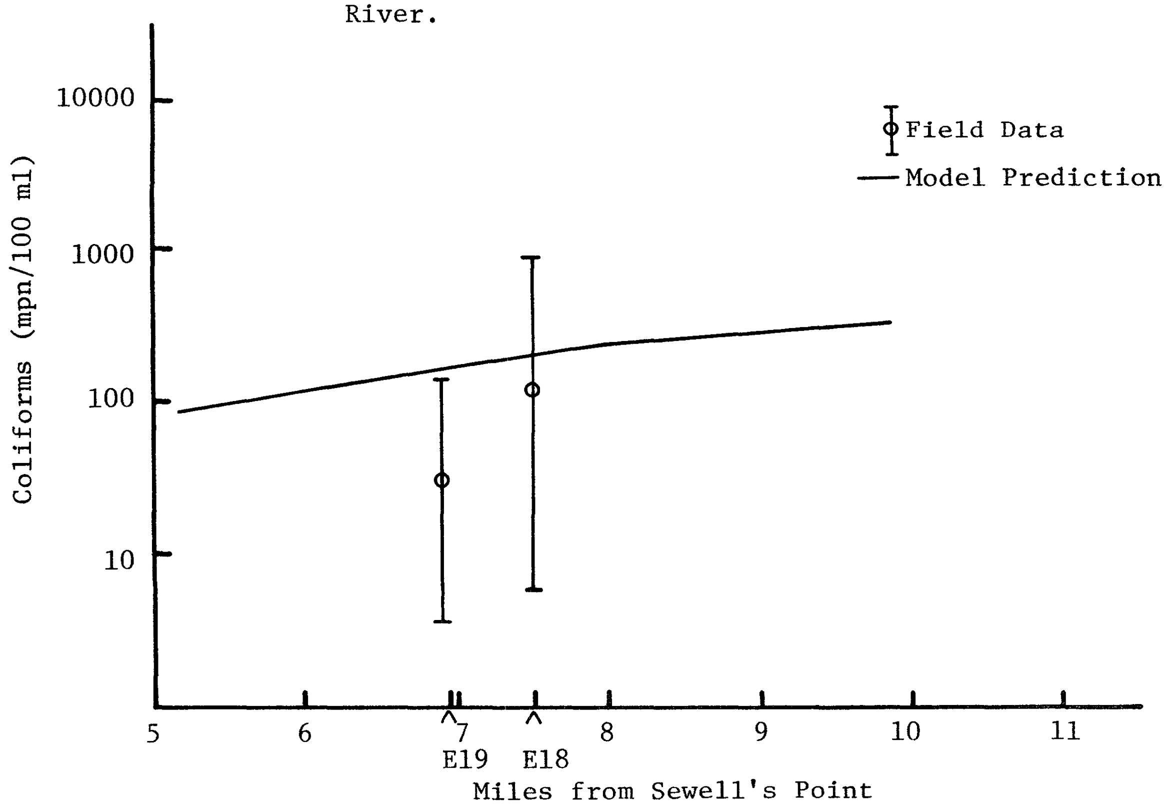

Branch and Main Stem were sampled during periods of high-water and low-water slacks. This provides a range of constituent concentrations, but no 24 hour averaging is possible. In addition, data on input parameters for point sources, with the exception of flow and BOD_5 were unavailable for this period and values of July inputs were used. These uncertainties in the data require the standard of comparison imposed on calibration field data and model predictions to be relaxed when examining verification field data and predictons. High- and low-water slack field data and time averaged model predictions for the verification period are presented in Figures 47-55.

The results of the verification are not as successful as the calibration. Discrepancies occur between the field data and the predictions due to the difficulties encountered in simulating two-dimensional circulation patterns with a one-dimensional model and to the transient nature of the two-dimensional circulations.

In the Elizabeth River, significant longitudinal and vertical salinity gradients (Fig. 56) may be set up by freshwater inflows or by stratification in Hampton Roads. The salinity gradients, in turn, cause a two dimensional circulation with fresher, less dense water flowing outward on the surface and more saline water flowing inward near the bottom. The mass transport caused by this two-dimensional flow is conventionally included in a one-dimensional model

Figure 47. Results of salinity verification for Southern and Main Branches.

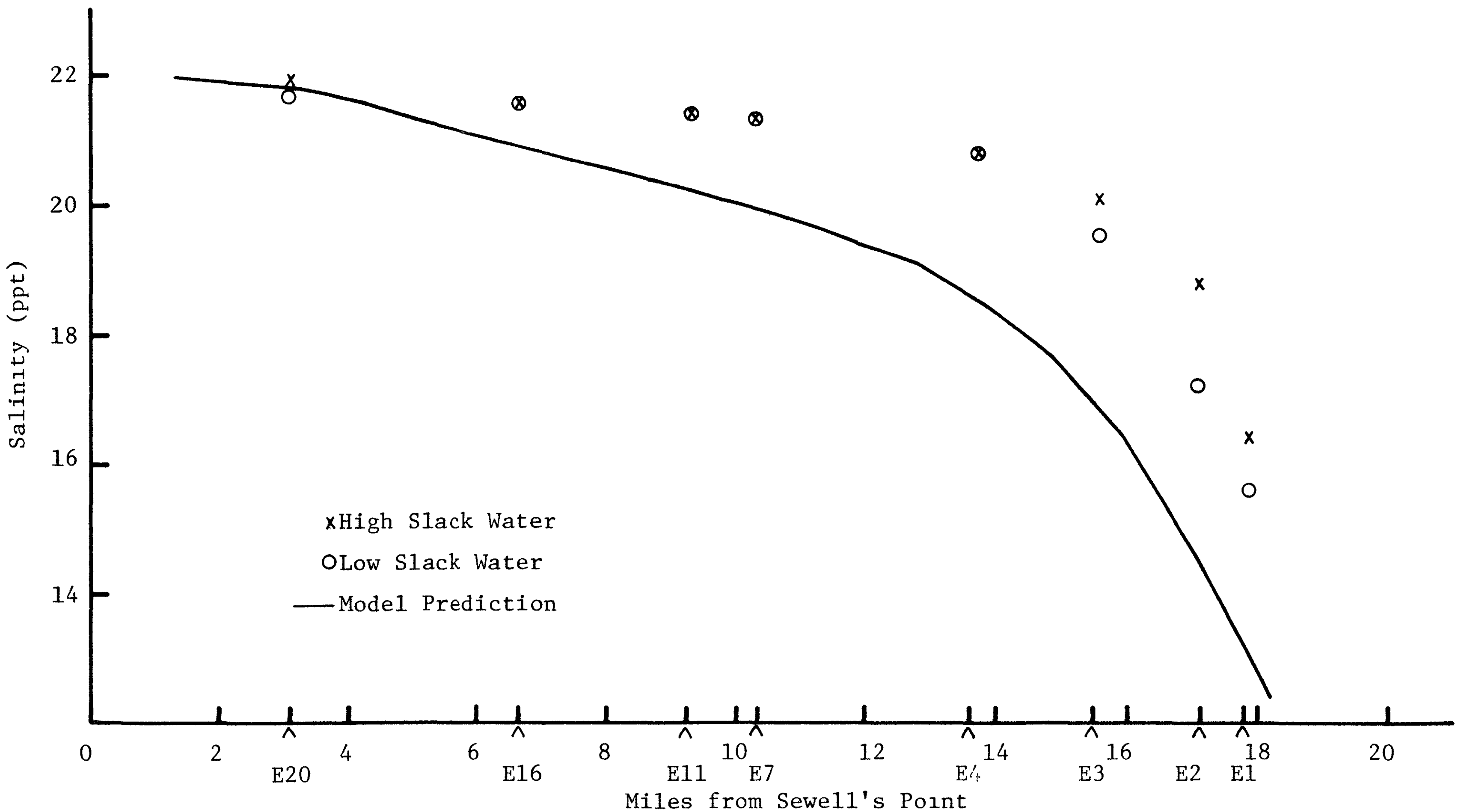

Figure 48. Results of ammonia verification for Southern and Main Branches.

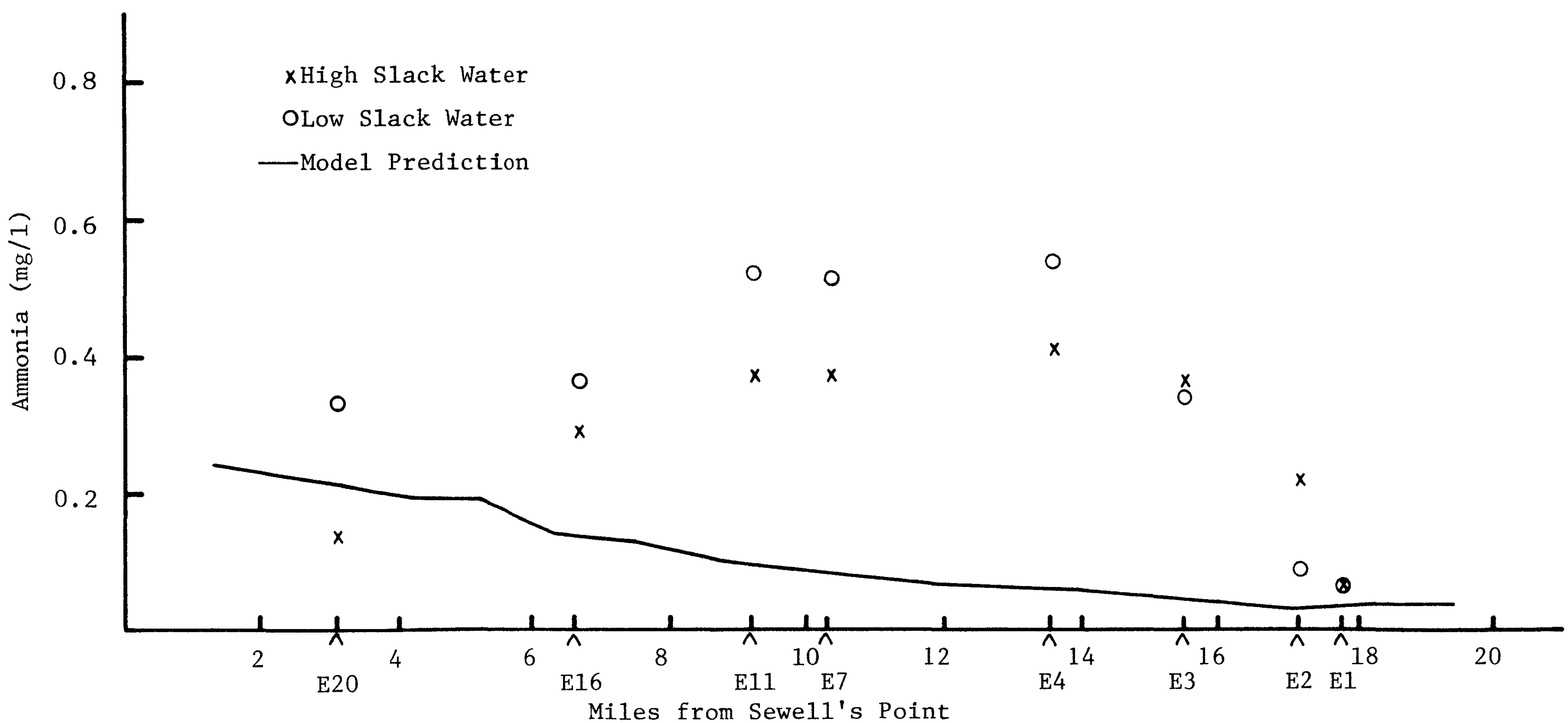

Figure 49. Results of nitrate verification for Southern and Main Branches.

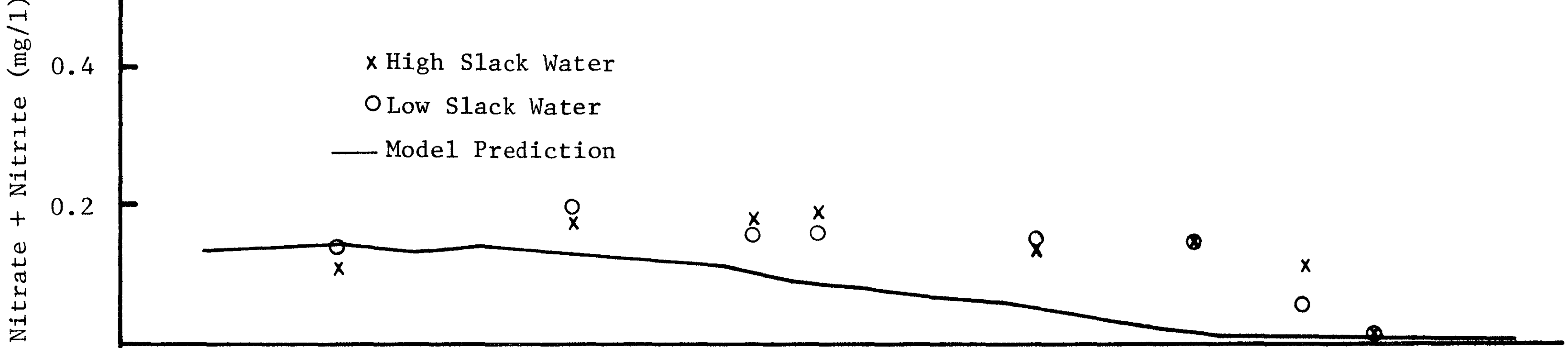

Figure 50. Results of organic nitrogen verification for Southern and Main Branches.

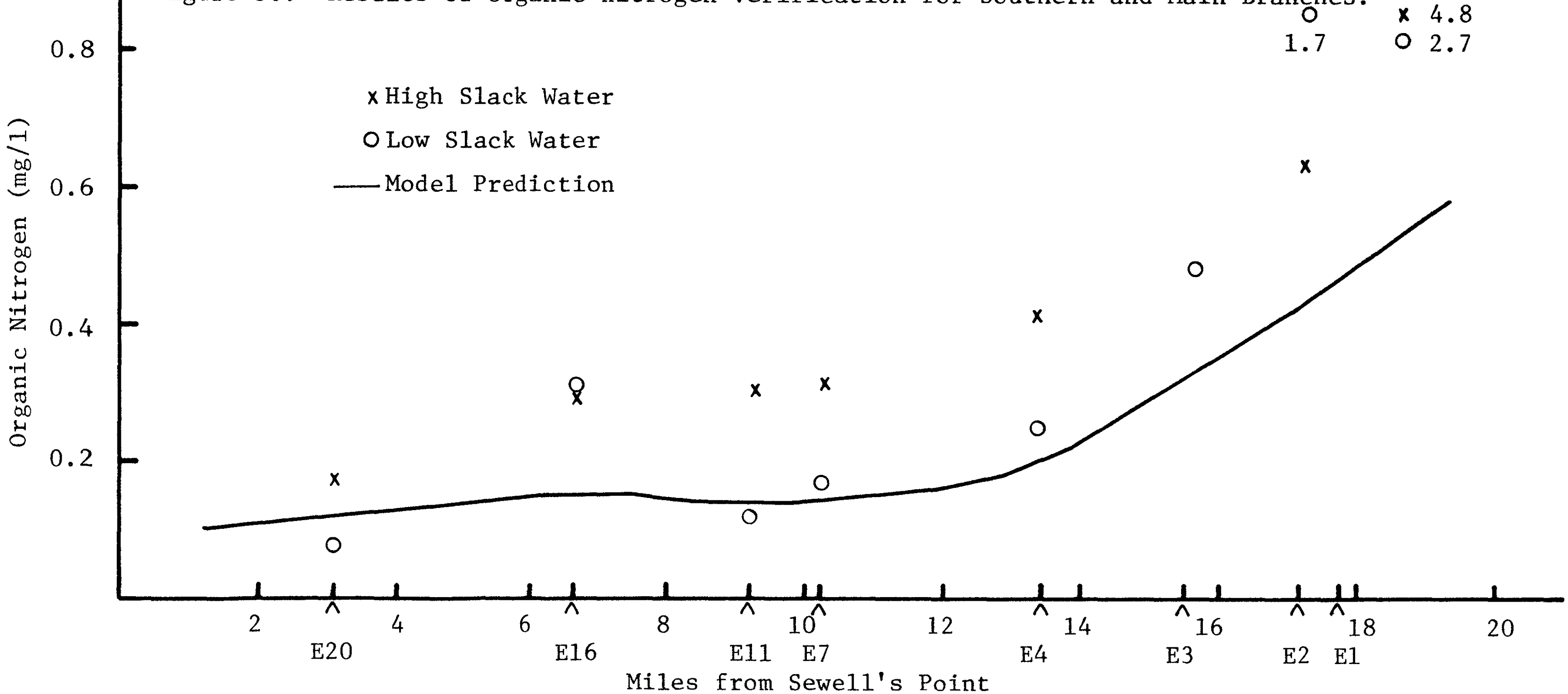

Figure 51. Results of total phosphorous verification for Southern and Main Branches.

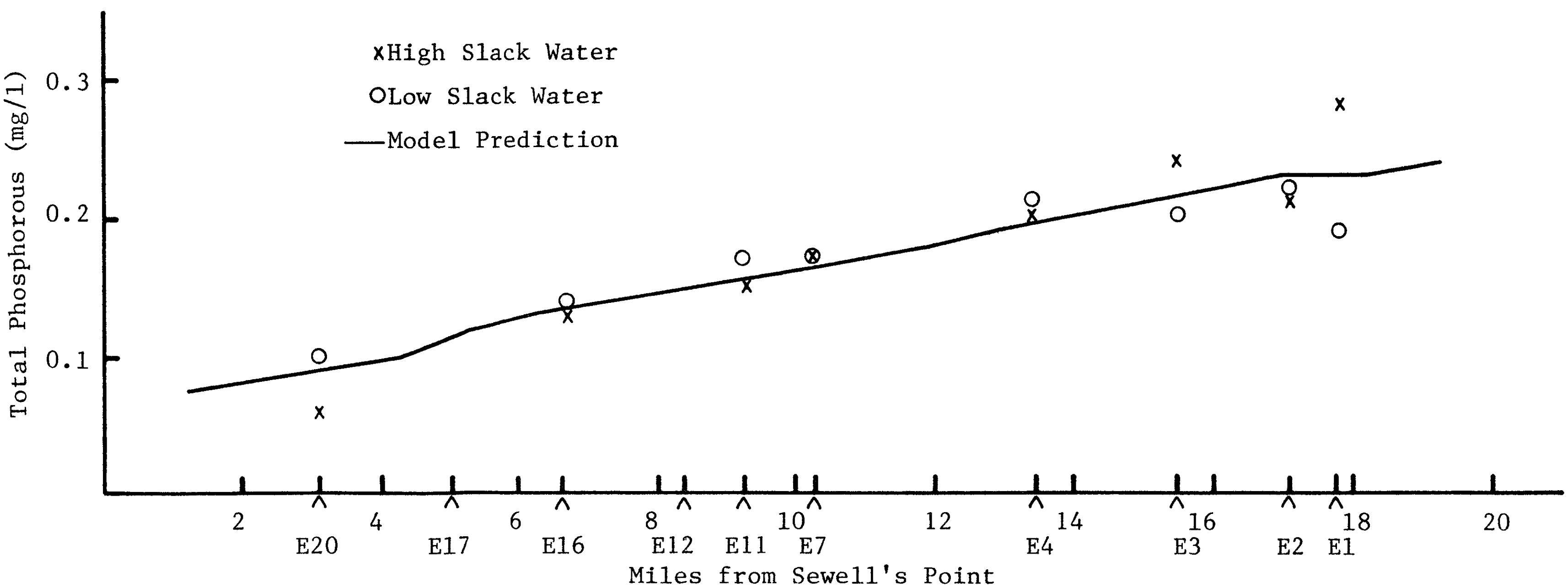

Figure 52. Results of CBOD verification for Southern and Main Branches

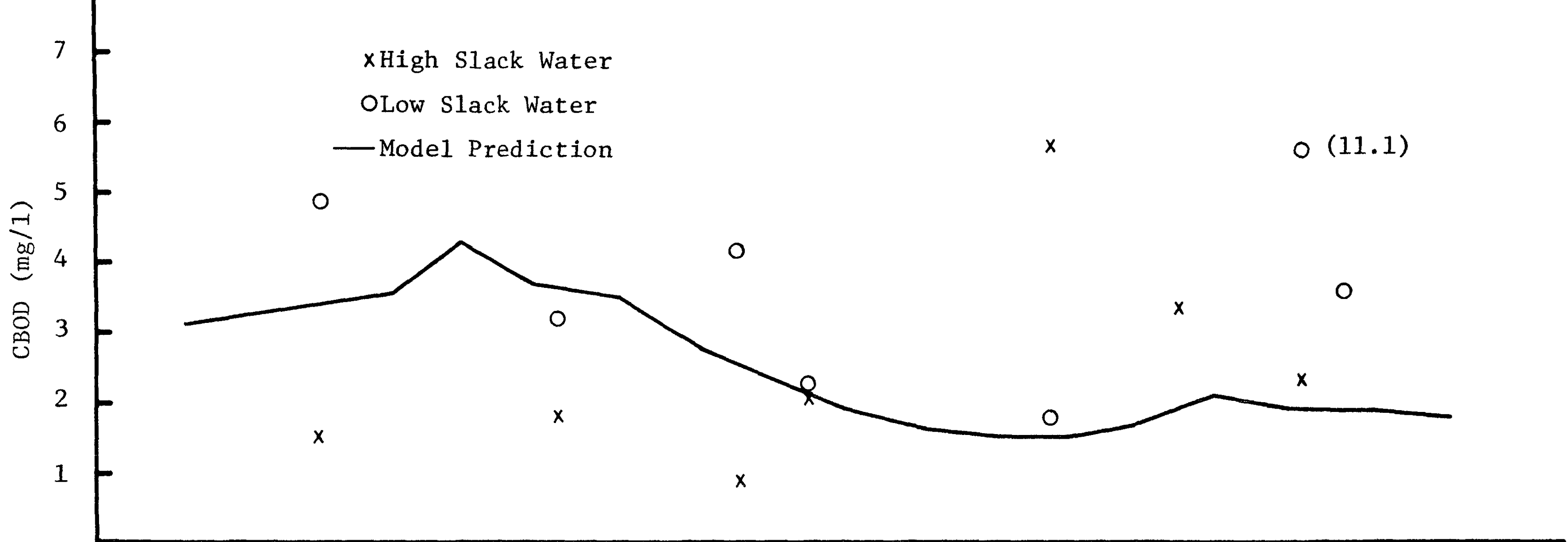

Figure 53. Results of dissolved oxygen verification for Southern and Main Branches.

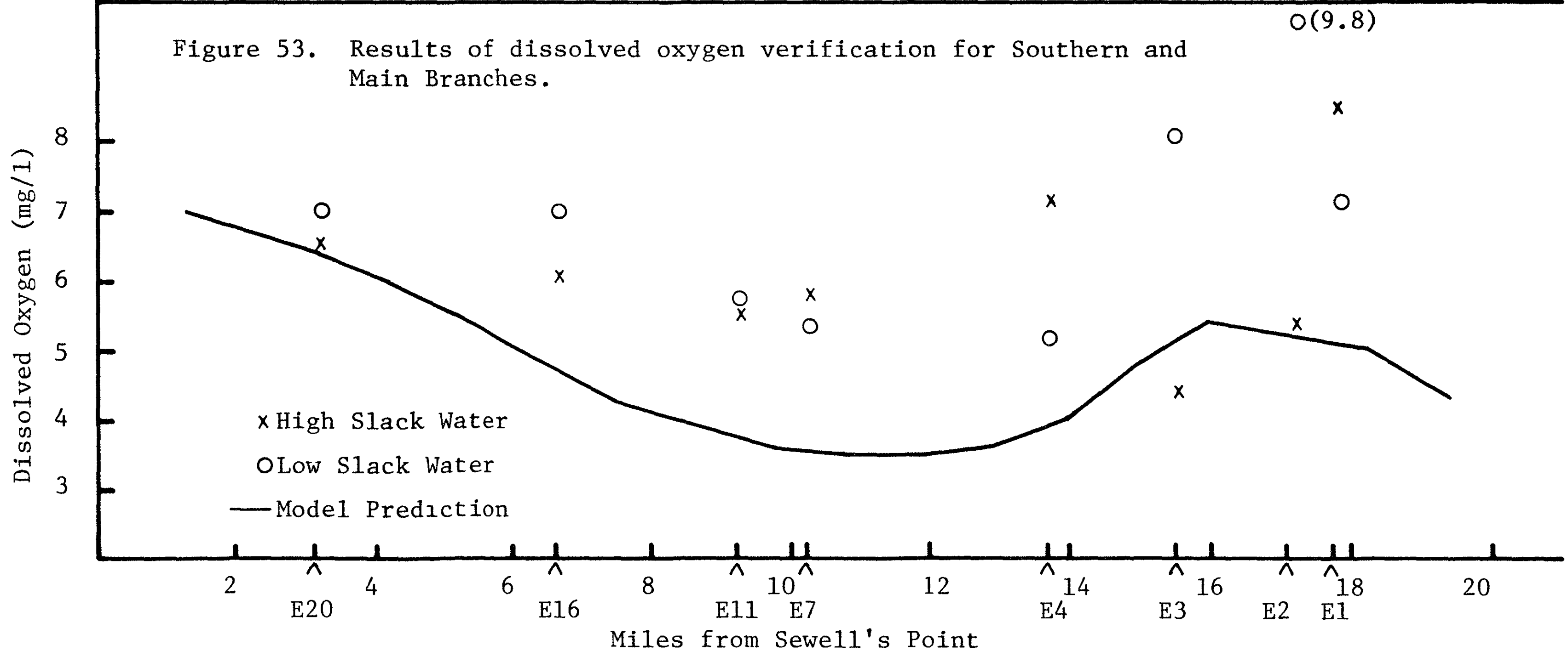

Figure 54. Results of chlorophyll 'a' verification for Southern and Main Branches.

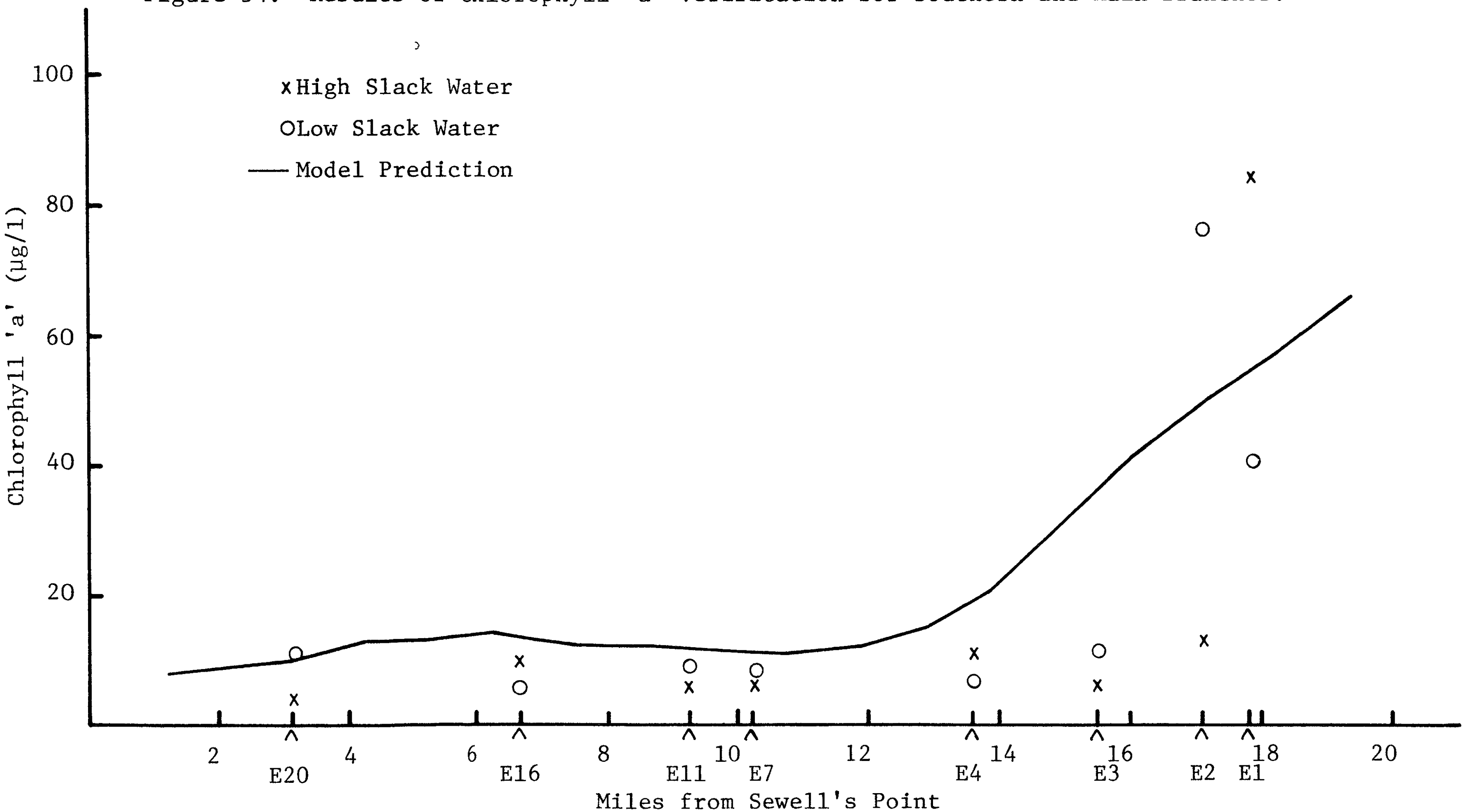

Figure 55. Results of fecal coliform verification for Southern and Main Branches.

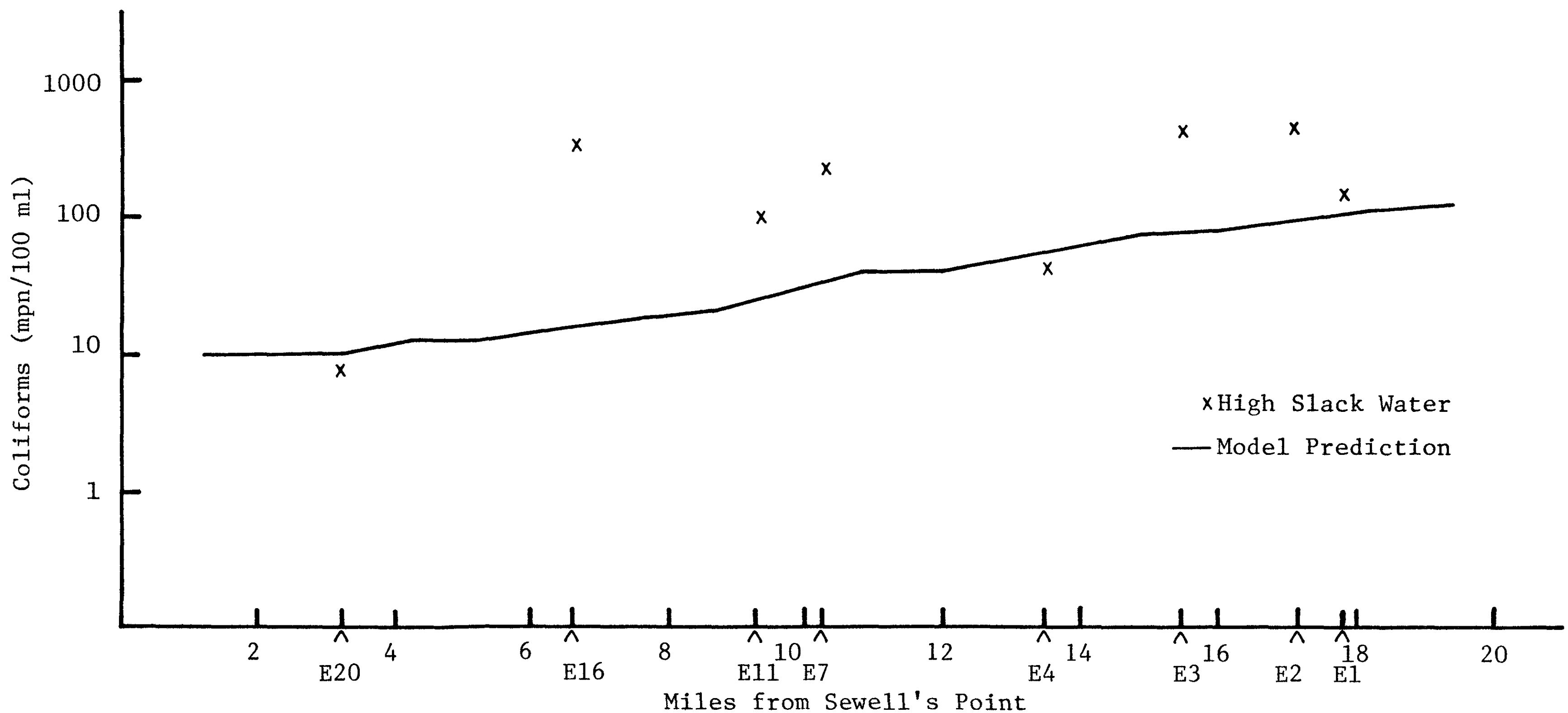

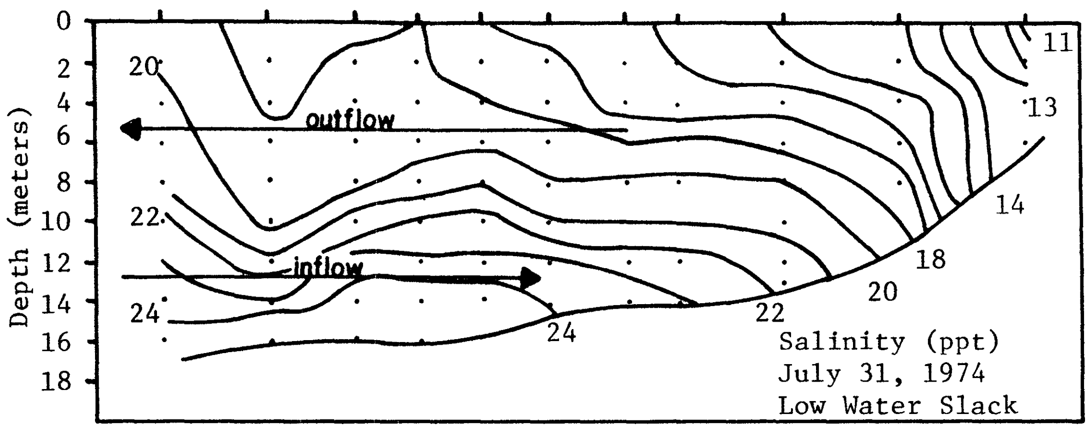

Figure 56. Elizabeth River stratification following rainstorm (from Neilson, 1975).

by use of a dispersion term with the dispersion coefficient proportional to the vertically averaged salinity and/or the longitudinal salinity gradient (Thatcher and Harleman, 1972).

The functional relationship of dispersion coefficient to salinity used in the model is given by equation (6). The parameter ν' should be related to the vertical salinity gradient, $\frac{\partial S}{\partial z}$, such that increased stratification causes increased dispersion. For conditions of relatively constant vertical salinity structure, ν' may be obtained from the model calibration procedure and employed with good results. During highly transient conditions, however, ν' varies as a function of the vertical salinity gradient. These variations in ν' are not included in the model nor can they be since no a priori knowledge of the vertical gradient is available. Neither can the variations in the vertical gradient be predicted in any longitudinal one-dimensional model.

During the summer of 1976, the Elizabeth River System was subject to a number of storm-generated freshwater inflows. As shown by Neilson (1975), these inflows result in vertical stratification which is gradually reduced through the action of tidal mixing. As the degree of stratification changes, the dispersion varies as well.

On July 3-4, 1976, four days prior to the intensive survey, the Elizabeth received an input of approximately

96 x $10^6 ft^3$ of stormwater resulting in the salinity structure during the calibration period shown in Fig. 57. No storm inputs were present immediately prior to the slackwater surveys, but two weeks prior to the survey, on August 8-10, stormwater flow of approximately 32 x $10^8 ft^3$ was input to the system resulting in the salinity structure during the verification period shown in Fig. 58.

The salinity structures during the two periods differ as do the resultant dispersion values. Thus the parameters derived from ambient conditions during the calibration survey are not directly applicable to the verification period.

The differences in dispersion and the resulting inaccuracy in the model description of the estuarine circulation prior to the verification survey cause the discrepancy between the field data and the model predictions typified by the salinity verification of Fig. 47. To remedy this discrepancy, additional verification could be conducted against field data collected during several different circulation conditions. In this manner, dispersion would be more accurately quantified. Alternately, a two-dimensional model capable of simulating the vertical structure of the river could be employed.

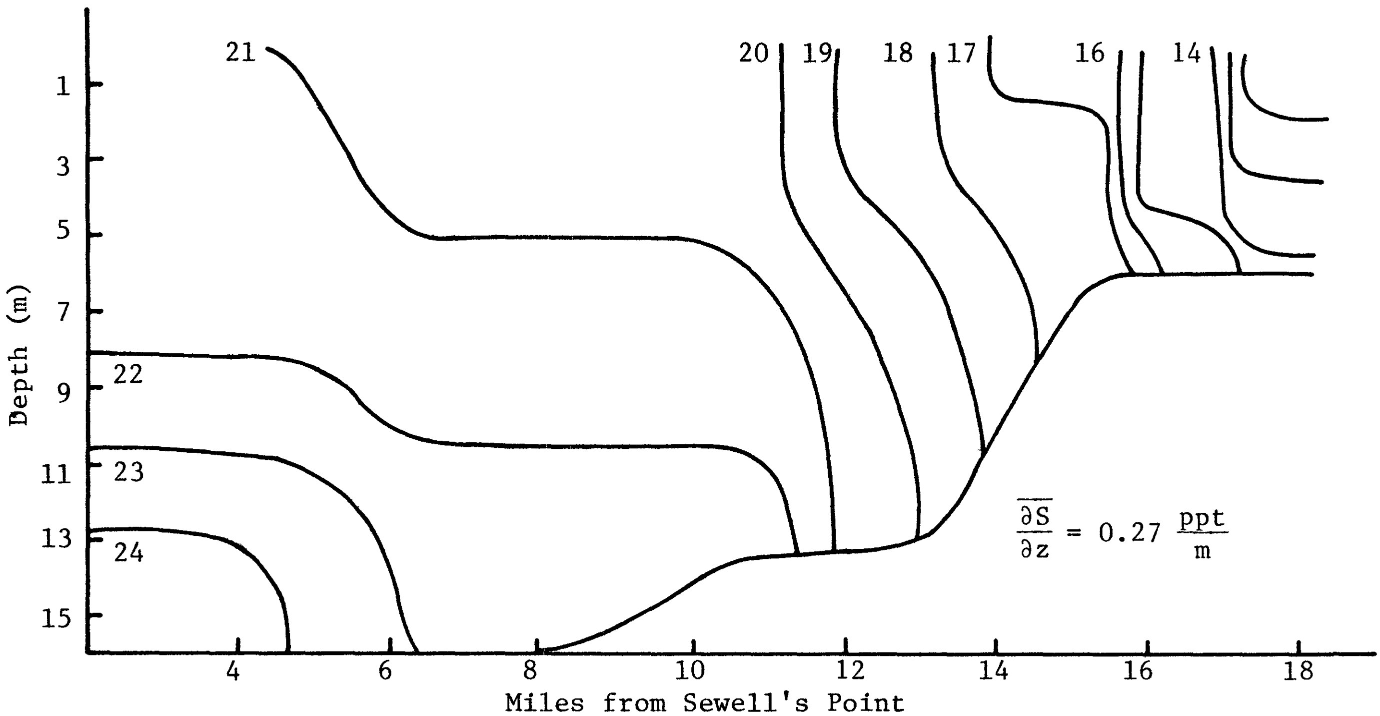

Figure 57. Elizabeth River salinity, low slack water, Aug. 7-9, 1976.

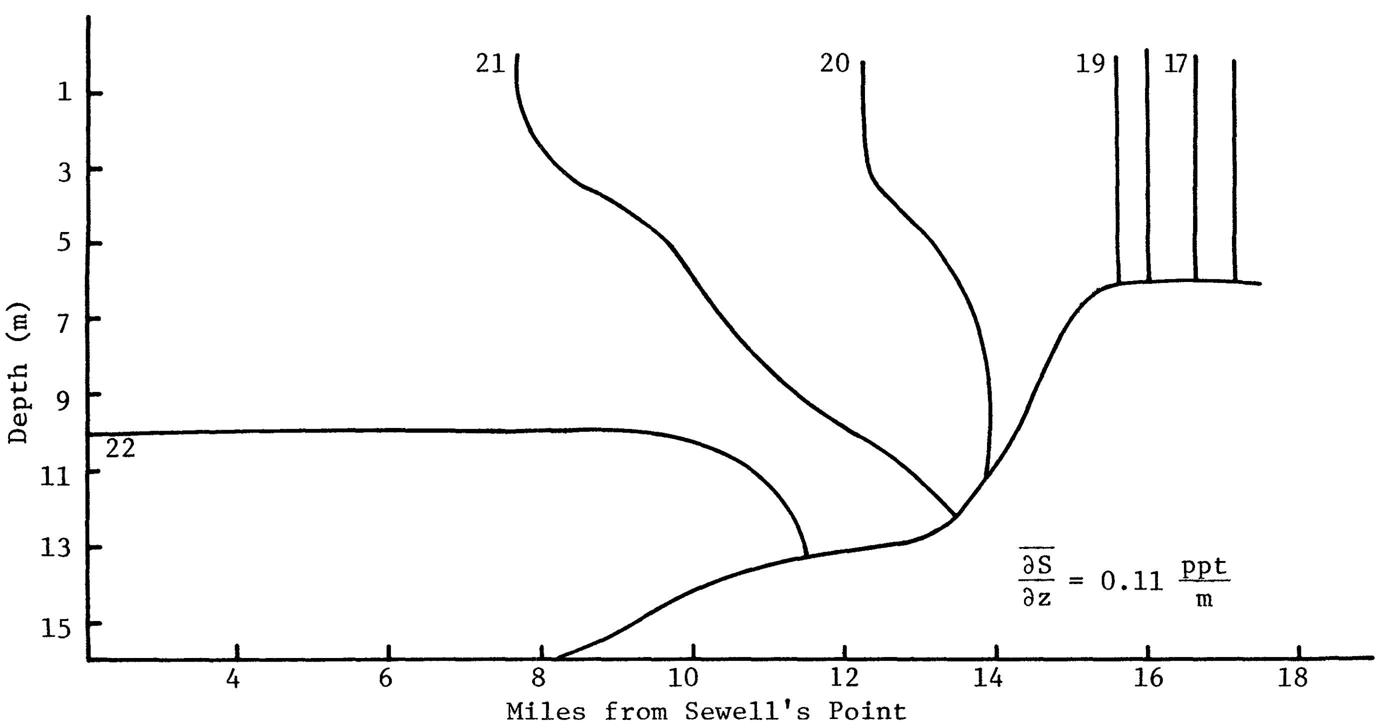

Figure 58. Elizabeth River salinity, low slack water, Aug. 23, 1976.

V. SENSITIVITY ANALYSIS

Sensitivity analysis is the process by which the effect on the model predictions of variations in calibration and input parameters is ascertained. By determining the relative effect on output of a specific parameter change, the modeller can determine which parameters require careful attention in their evaluation and which require less rigorous approximation. Sensitivity analysis also allows the modeller to judge the effect of his assumptions and to weigh the confidence placed in the model's results.

Sensitivity analysis is useful not only in model evaluation, however. It is also a tool by which the influence of various factors such as pollutant inputs or water temperature on the prototype may be discerned and it may be used as a device for evaluating the effect of alternative management schemes before they are implemented.

The sensitivity analysis presented herein is directed primarily towards variations in dissolved oxygen and CBOD. Dissolved oxygen is a prime indicator of the health of a water body and minimum D.O. concentrations in public waterways are protected by law. Thus dissolved oxygen predictions are among the most important results of this study. D.O. is also a central constituent of the ecosystem model. The importance of this constituent from both the regulator's and modeler's viewpoint make it an ideal object for sensitivity analysis.

CBOD is one of the most commonly analyzed pollutant parameters. It also has a major effect on the dissolved oxygen budget of a water body. For these reasons, it is utilized herein as a typical indicator of pollutants in the Elizabeth and of the effect on pollutant concentration of the parameters subjected to sensitivity analysis.

The parameters which are varied were selected due to their known influence on D.O. or because their evaluation involved a large degree of uncertainty. Parameters in the former category include CBOD decay rate, point source inputs, nonpoint source inputs, benthic oxygen demand and photosynthetic production. The latter category includes the organic nitrogen hydrolysis parameter (KN12), the ammonia nitrification parameter (KN23), and the reaeration parameter (ε).

Sensitivity analysis was accomplished by holding all parameters constant at their calibration levels except the parameter to be varied which was increased and/or decreased by an arbitrary amount. The results of the analyses are as follows.

A. Sensitivity to CBOD Decay Rate

The CBOD decay rate, k_1, was varied throughout the Elizabeth River System by $\pm$ 25%. The effects of this variation on CBOD and D.O. in the Southern Branch and Main Stem are shown in Figs. 59 and 60. Generally, a 25% change

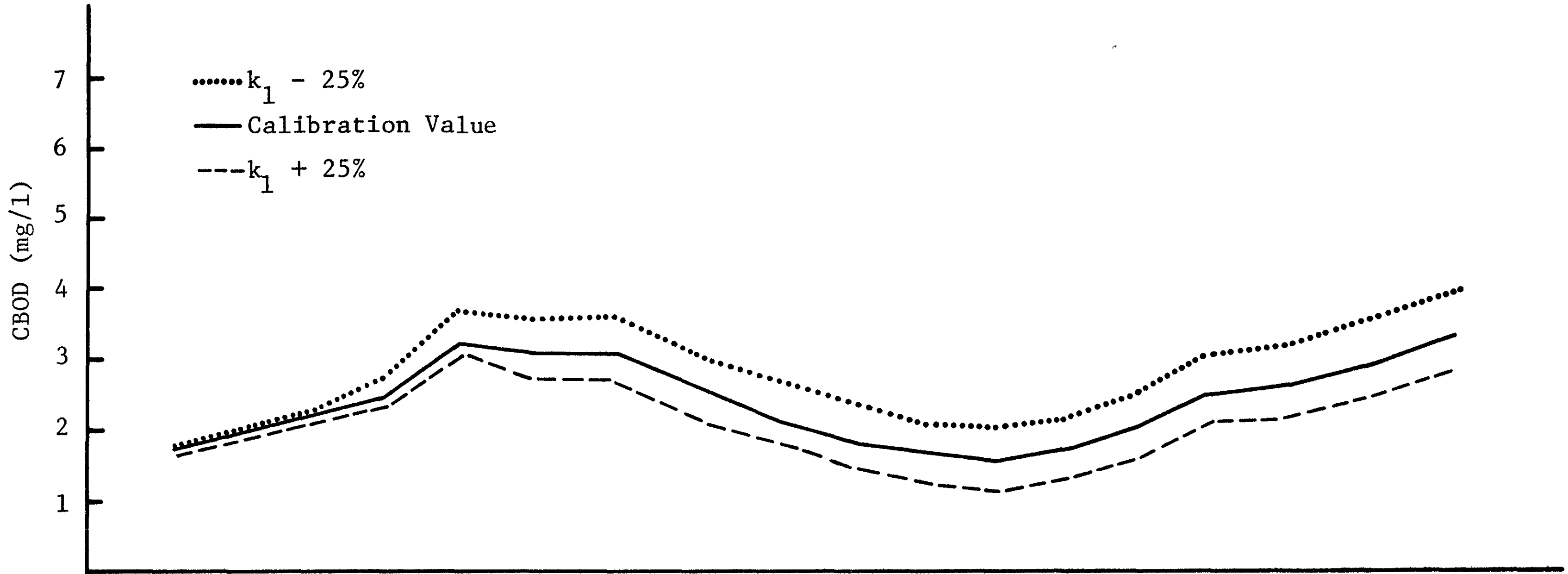

Figure 59. Sensitivity of CBOD concentration to Decay Rate.

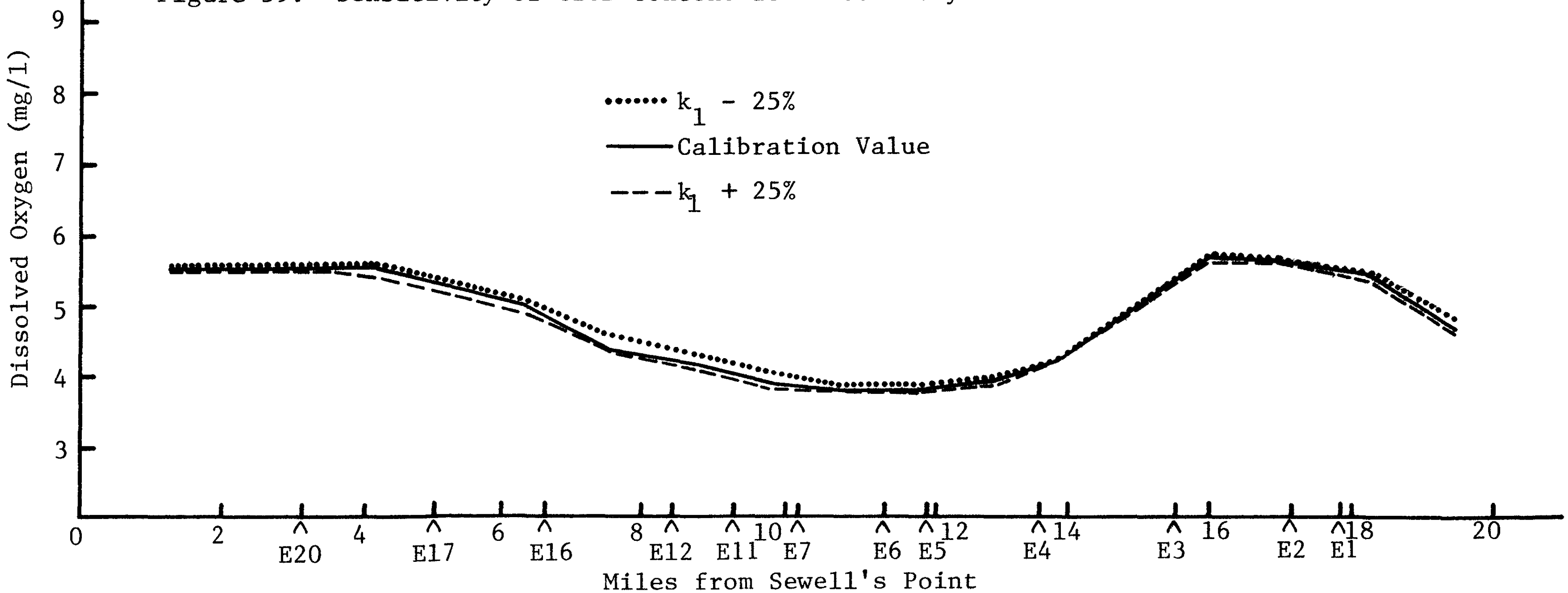

Figure 60. Sensitivity of dissolved oxygen to CBOD decay rate.

in the decay rate produced in a change in CBOD concentration of approximately 0.5 mg/ℓ. The effect of this change in the D.O. concentration was minimal, however, due to reaeration which increases in response to the deficit produced by any additional exertion of CBOD.

B. Sensitivity to Point Source Inputs

Point source inputs such as waste treatment plants are perhaps the most commonly considered pollutant sources. The effect in Elizabeth River water quality of these inputs was tested by first doubling and then eliminating the point sources. The results are shown in Figs. 61 and 62. Except near the upstream boundaries, CBOD concentrations varied by approximately 1-3 mg/ℓ and a maximum change of 1 mg/ℓ D.O. was noted at the D.O. minimum.

C. Non-Point Source Inputs

The Elizabeth River system receives significant quantities of non-point source inputs of stormwater and pollutants. These inputs may improve water quality by flushing the river system or may degrade water quality due to the quantity of pollutants introduced.

The effects of these inputs were evaluated by eliminating all non-point sources and running the model at two temperatures: 25^{o}C and 30^{o}C. The first value is the temperature of the river during the calibration period; the second is the temperature which might result during a

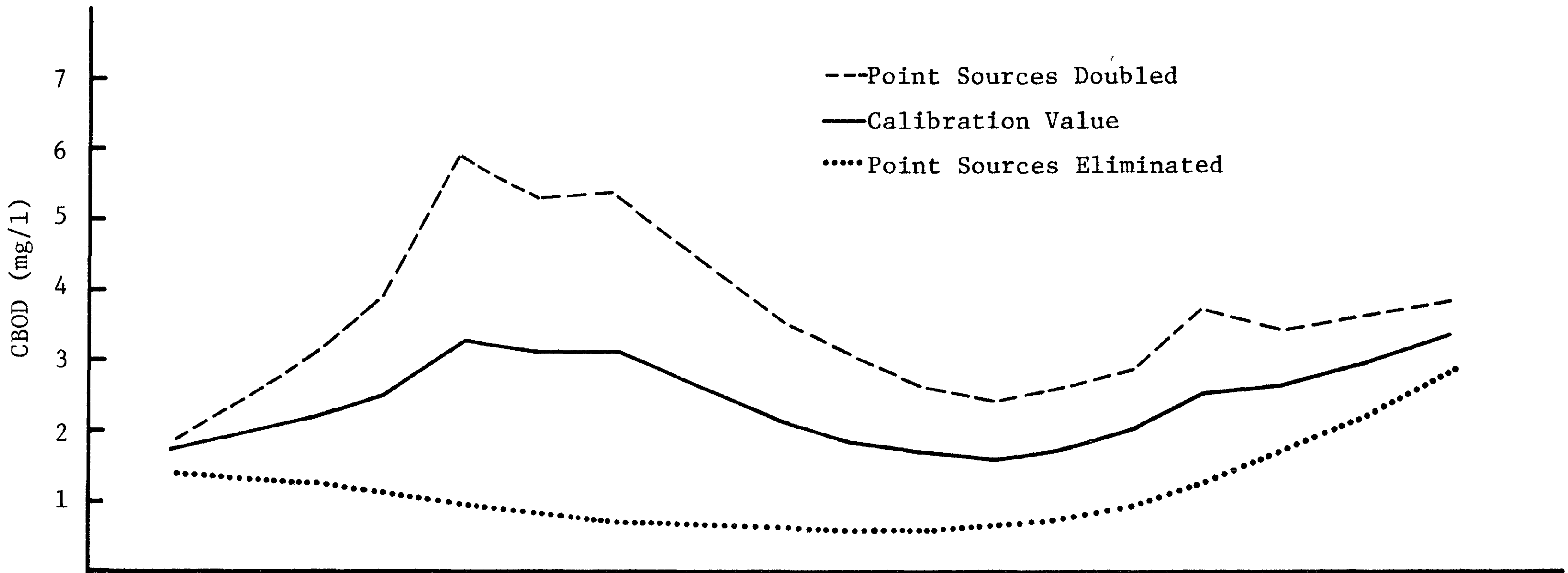

Figure 61. Sensitivity of CBOD concentration to point sources.

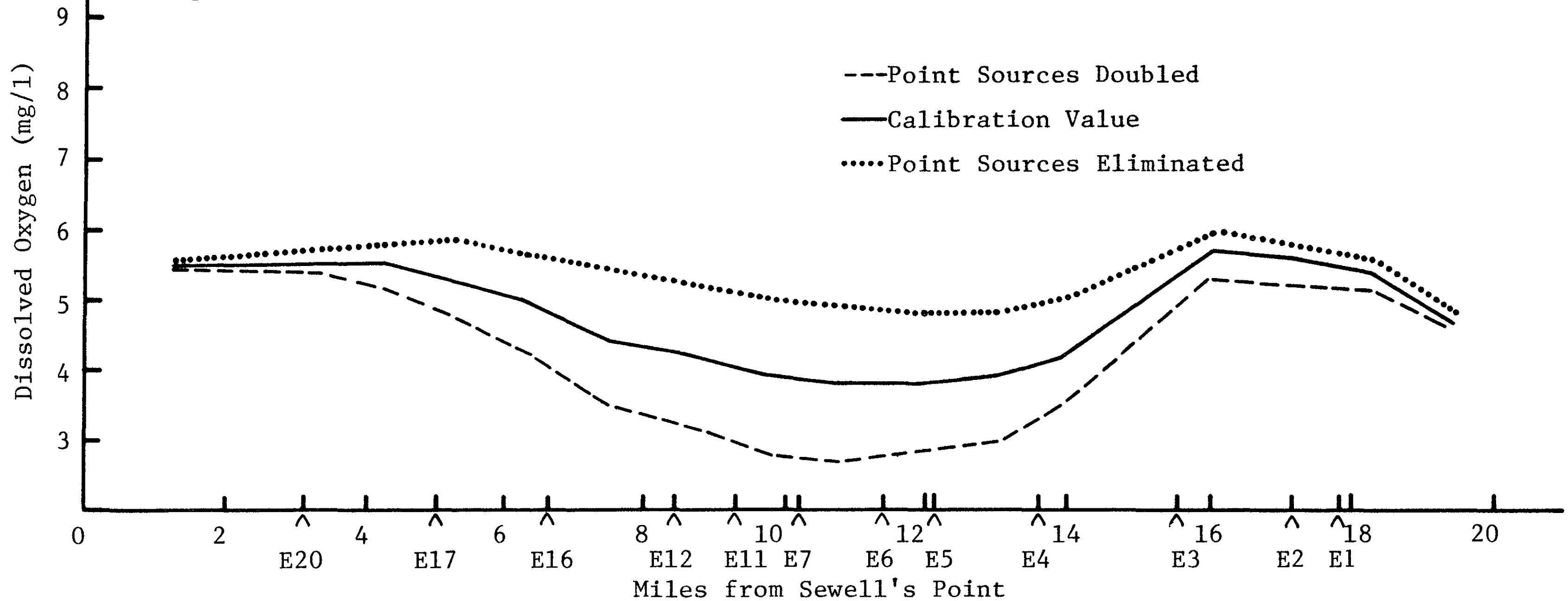

Figure 62. Sensitivity of dissolved oxygen concentration to point sources.

long, worst-case, dry and hot period. The results are shown in Figs. 63 and 64. Except in the upper reaches of the Southern Branch, CBOD is reduced by 0.5 mg/ℓ or less with the elimination of non-point sources. D.O. is improved by less than 0.25 mg/ℓ.

At the estimated temperature of 30°C which might result during a dry period, the change in D.O. is more significant. Decreases of 0.5 mg/ℓ or more from the calibration values are noted near the sag and in the Southern Branch. Since the change in CBOD concentration due to the elimination of non-point sources and due to the temperature change is minimal, the increased D.O. deficit is assigned to a temperature-induced increase in benthic demand. In the extreme upstream reaches of the Southern Branch, chlorophyll concentrations are reduced (not shown) due to the lack of non-point nutrient inputs. The resulting decline of photosynthetic production also contributes to the reduced D.O. in the upstream segments, as does the reduced D.O. saturation concentration at higher temperatures.

These conclusions regarding the effects of non-point sources must be regarded as tentative. A different set of input parameters might result in different and perhaps contradictory effects. In addition, the response of the river system immediately following the non-point

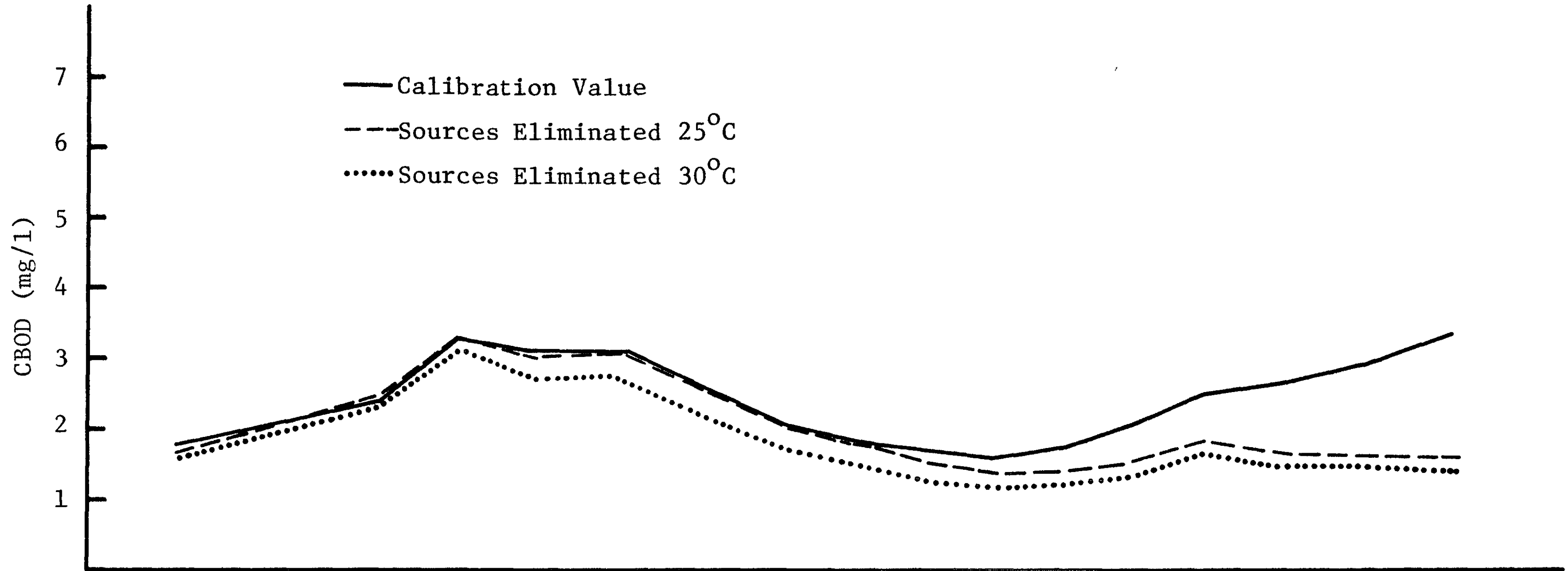

Figure 63. Sensitivity of CBOD concentration to non-point source inputs.

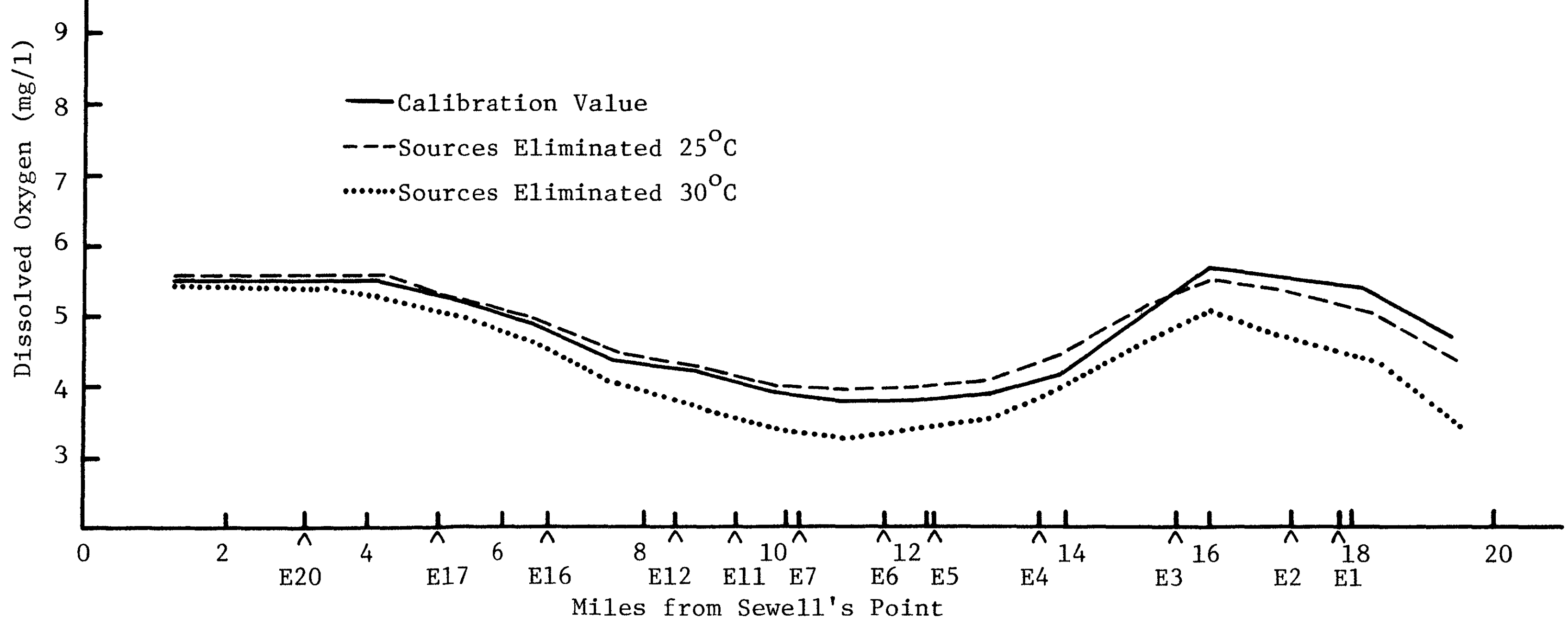

Figure 64. Sensitivity of dissolved oxygen concentration to non-point source inputs.

inputs is not evaluated. Finally, as mentioned previously, the effect of freshwater inputs on dispersive transport cannot be accurately ascertained with a one-dimensional model.

D. Benthic Oxygen Demand

Significant levels of benthic oxygen demand have been measured in the Elizabeth River. The effect of this demand on water quality was evaluated by eliminating benthic demand from the model. The results are shown in Fig. 65. It is seen that except near the mouth of the river, benthic demand reduces the D.O. concentration by 1-2 mg/ℓ and has a more significant effect on the deficit than either point source or non-point source inputs.

E. Photosynthetic Production

The portion of the dissolved oxygen budget attributable to photosynthetic production by phytoplankton was evaluated by reducing the chlorophyll maximum growth rate, k_{gr}, by 90 percent. This had the effect of reducing predicted chlorophyll concentrations to practically zero. The resulting D.O. profile is shown in Fig. 66. The effect on the D.O. budget is minimal except in the upper reaches of the Southern Branch where elevated Chl. 'a' levels were observed. There, photosynthetic production adds 1-2 mg/ℓ to the local D.O. concentration.

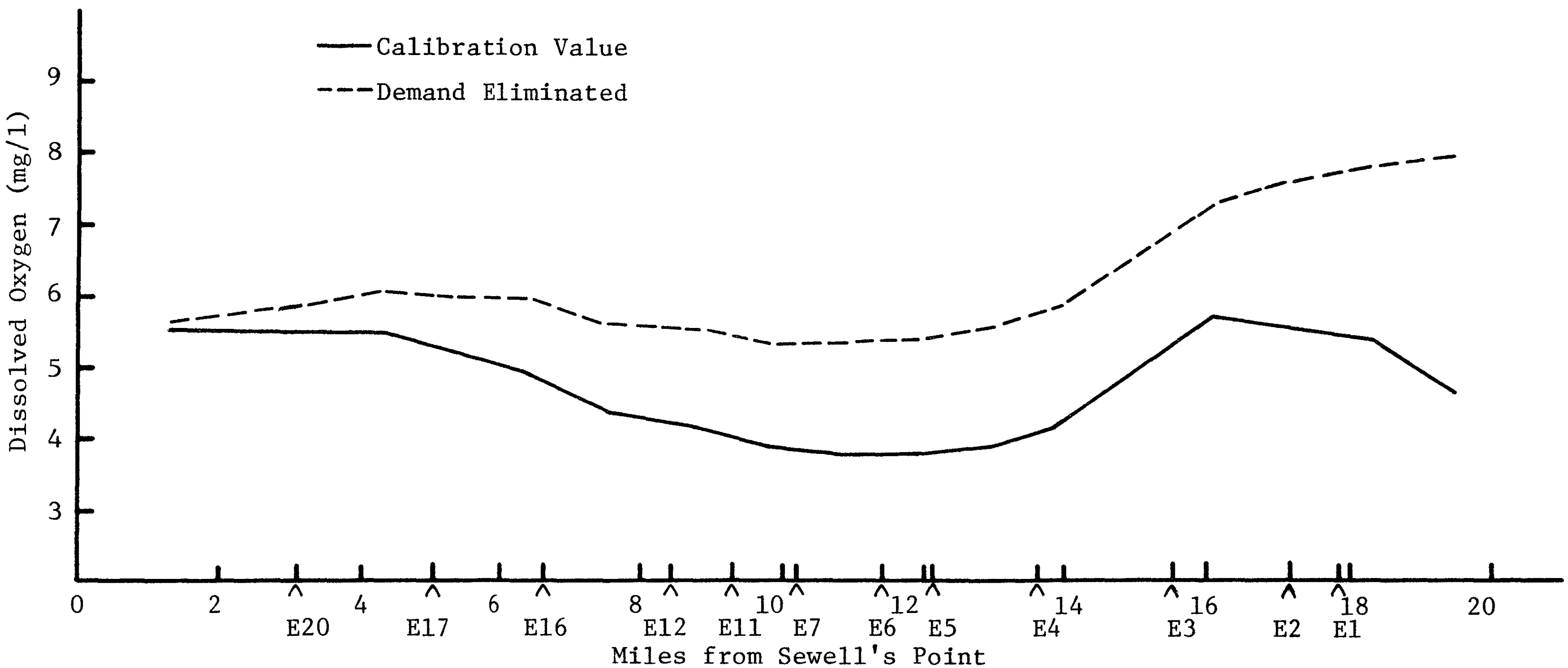

Figure 65. Sensitivity of dissolved oxygen concentration to benthal oxygen demand.

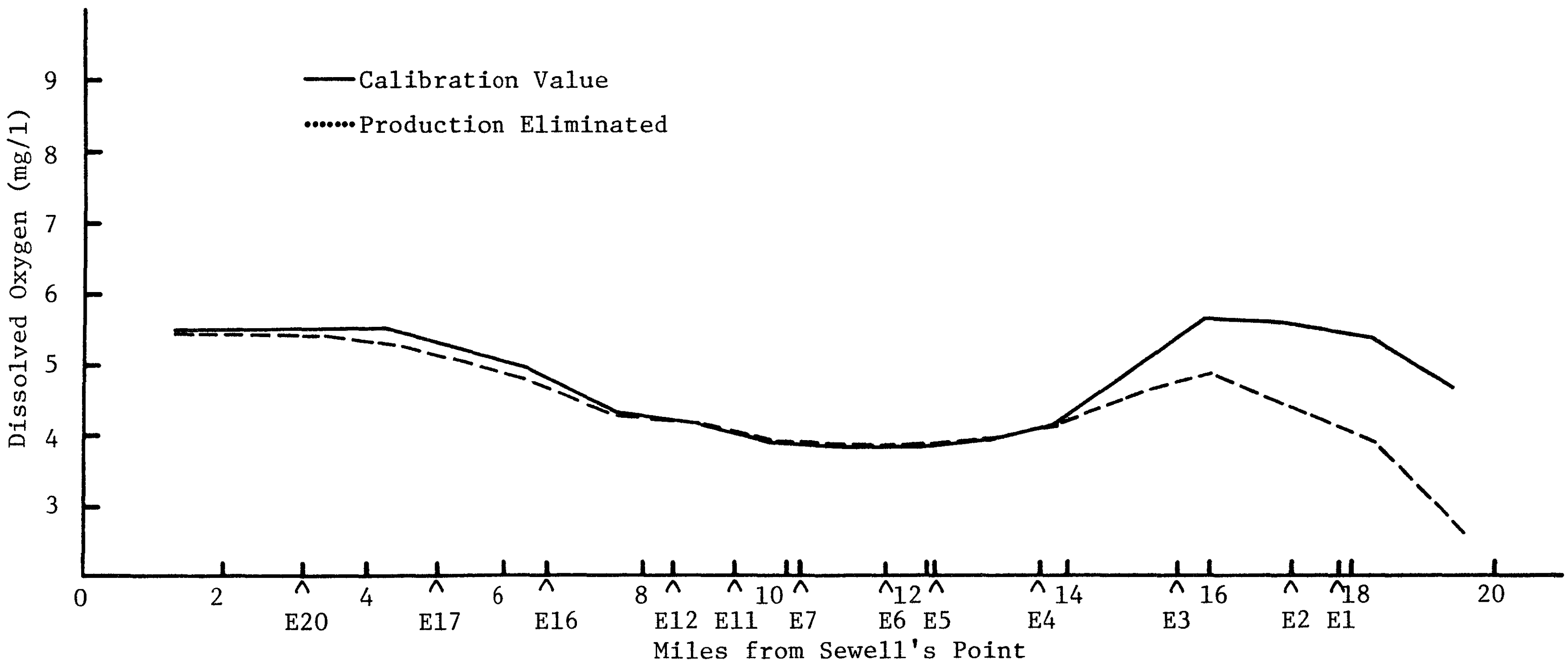

Figure 66. Sensitivity of dissolved oxygen to photosynthetic production.

F. Effect of Hydrolysis and Nitrification Parameters

The parameters KN12 and KN23 could not be determined by the calibration process due to suspected deficiencies in the field data. Instead, values of KN12 and KN23 were assumed based on values used in models of similar water bodies. The model sensitivity to this assumption is illustrated in Figs. 67-69.

Fig. 67 shows the sensitivity of organic nitrogen to a ± 25% change in the hydrolysis parameter, KN12. Except near the downstream boundary, a 25% change in KN12 produces a change of 0.5-1.0 mg/ℓ organic nitrogen.

Simultaneously with KN12, the nitrification parameter, KN23, was varied by + 25 percent. The effect on the ammonia concentration is shown in Fig. 68. Except near the downstream boundary, a 25% change in KN12 and KN23 produces a maximum change of 0.03 mg/ℓ in ammonia nitrogen.

Predictions of organic nitrogen and ammonia are of concern primarily because the nitrification of ammonia to nitrate consumes dissolved oxygen from the water column. (The supply of ammonia is partially replenished by hydrolysis of organic nitrogen). The nitrification reaction may be represented:

$$NH_4^+ + 2O_2 \rightarrow NO_3^- + 2H^+ + H_2O \qquad (25)$$

It can be seen that nitrification of 1 gm of nitrogen as ammonia consumes approximately 4.5 gms of oxygen. Thus an accurate representation of ammonia is needed in the model so

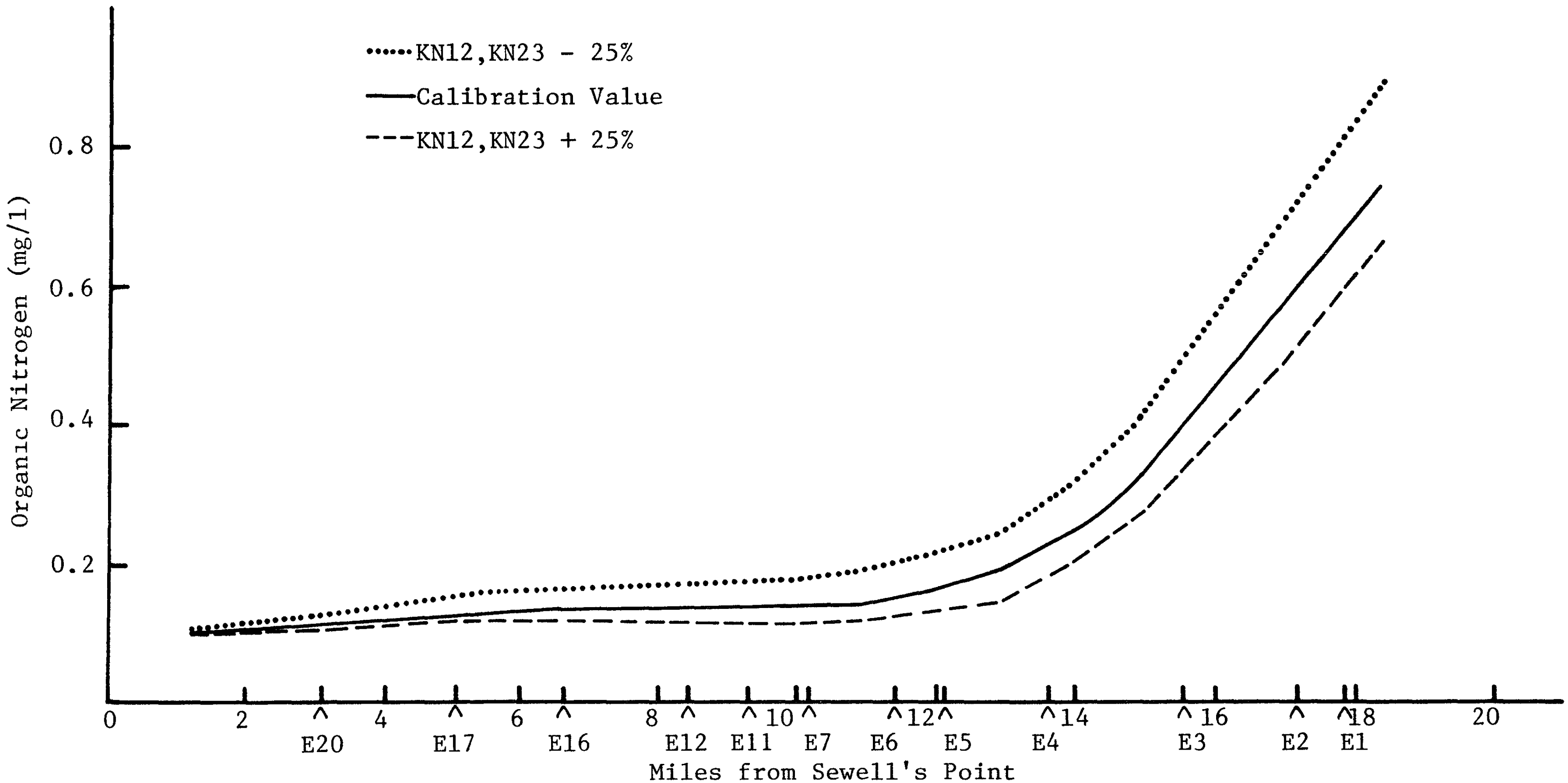

Figure 67. Sensitivity of organic nitrogen to rate parameters.

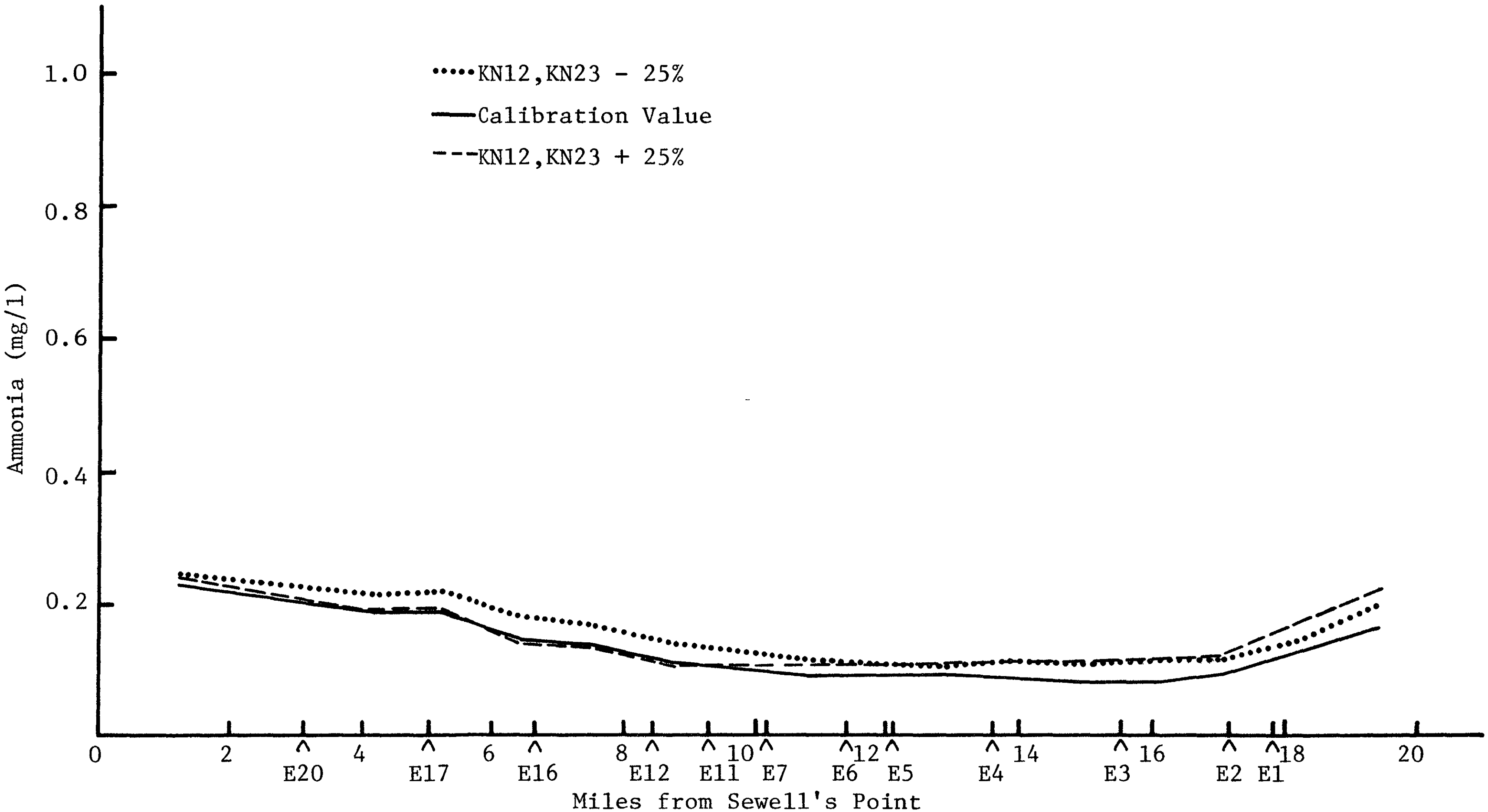

Figure 68. Sensitivity of ammonia concentration to rate parameters.

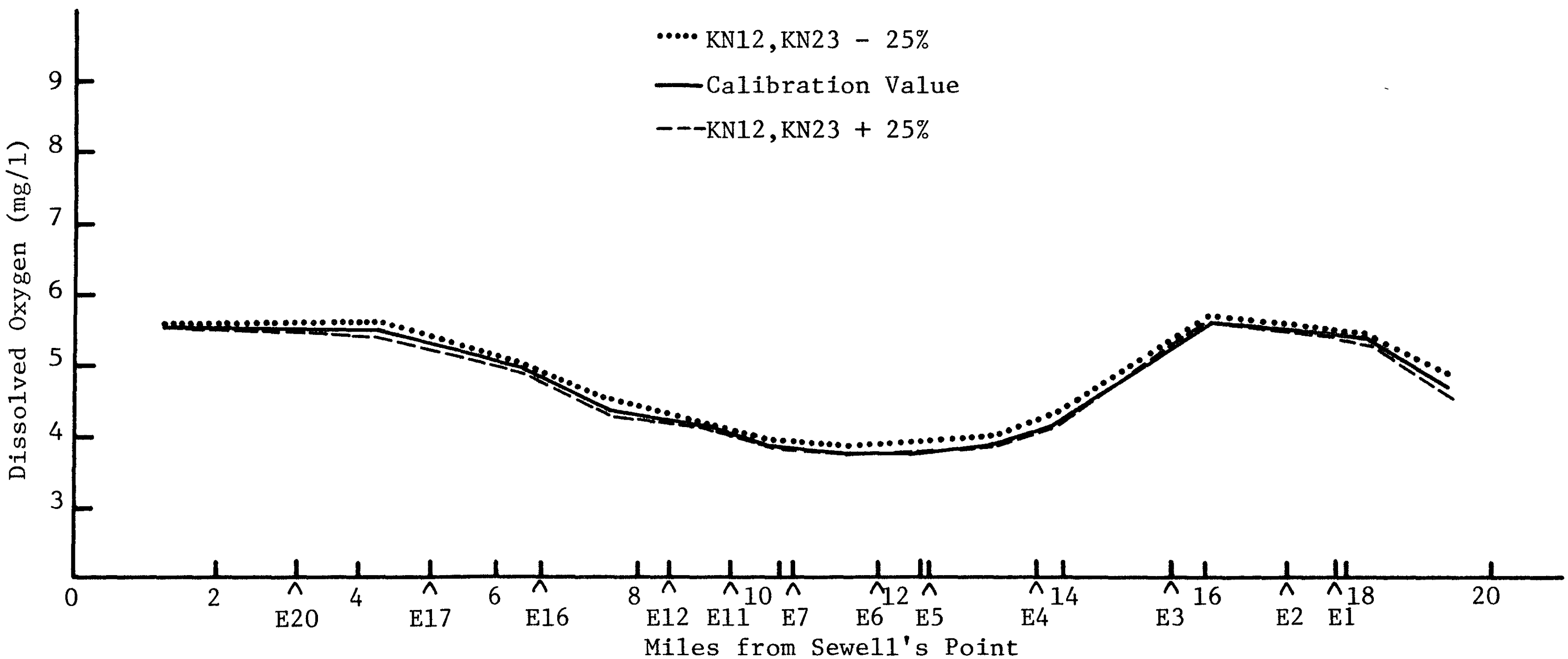

Figure 69. Sensitivity of dissolved oxygen concentration to nitrification rate parameters.

the effect of this nitrogenous demand on the dissolved oxygen concentration can be properly evaluated.

While an accurate ammonia calibration is not possible, the sensitivity of the predicted dissolved oxygen concentration to the ammonia concentration resulting from the assumed nitrification parameter can be evaluated. This sensitivity is illustrated in Fig. 69 which compares the calibration value of dissolved oxygen with the predicted values based on a variation in KN23 of $\pm$ 25 percent. The resulting change in the D.O. prediction is minimal and the assumed values of KN12 and KN23 are deemed satisfactory.

G. Sensitivity to the Reaeration Parameter

Reaeration is increased in the model over the conventional O'Connor-Dobbins formula (Eq. (8)) by an arbitrary factor ε determined through model calibration. The sensitivity of the model to this factor is illustrated in Fig. 70 which shows the variation of predicted dissolved oxygen resulting from a $\pm$ 25% variation in ε. It can be seen that the predictions are very sensitive to ε and that the values selected in the calibration procedure give the best agreement between the field data and the model prediction.

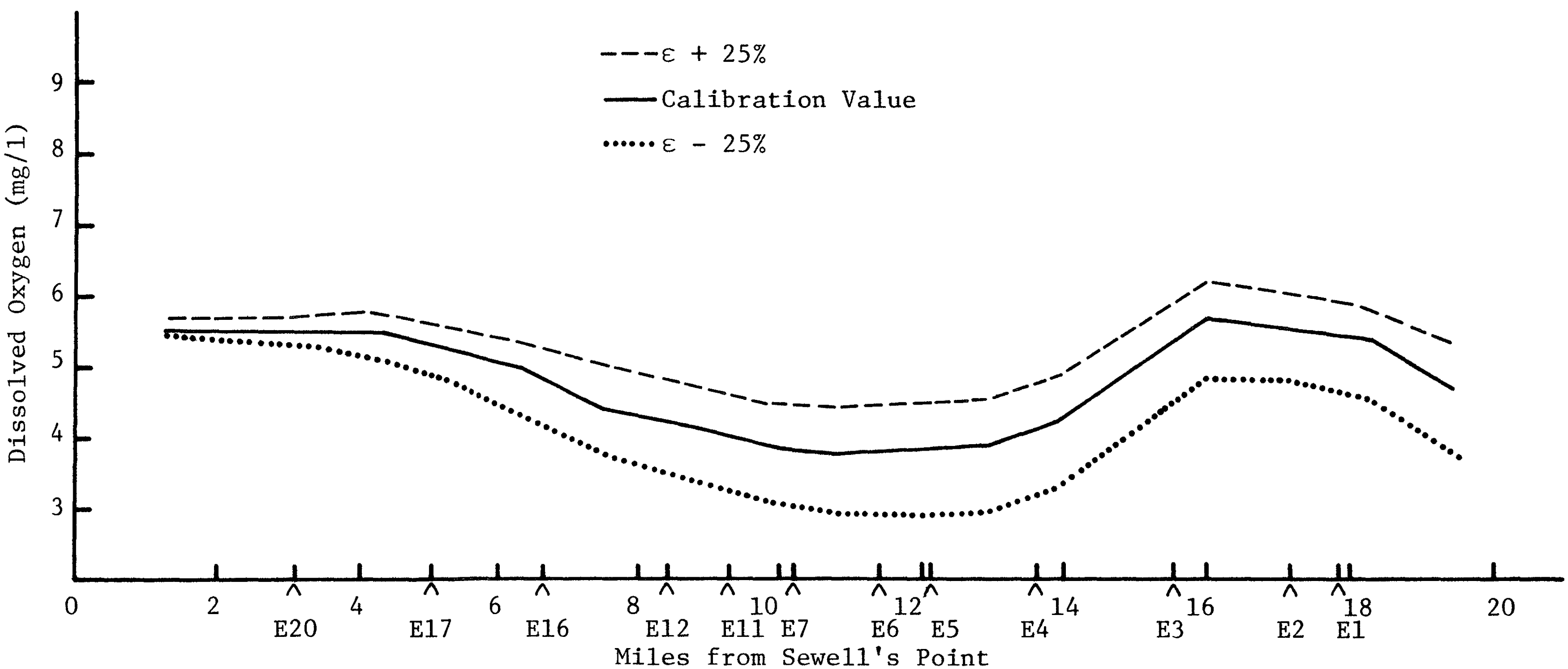

Figure 70. Sensitivity of dissolved oxygen concentration to reaeration correction.

REFERENCES

ASCE. 1961. "Effect of Water Temperature on Stream Reaeration", Comm. on San. Eng. Res., J. San. Eng. Div. of ASCE, Vol. 87, SAG.

Carritt, D. E. and E. J. Green. 1967. "New Tables for Oxygen Saturation in Seawater", J. of Mar. Res., Vol. 25, #2.

DiToro, D. M., D. J. O'Connor and R. V. Thomann. 1971. "A Dynamic Model of the Phytoplankton Population in the Sacremento-San Joaquin Delta". Adventures in Chemistry Series, No. 106, American Chemical Society, pp. 131-180.

Harleman, D. R. F. 1971. "One-Dimensional Models", In Estuarine Modelling: An Assessment, Tracor Incorporated, Water Pollution Control Research Series 16070 DZV, Environmental Protection Agency.

Holley, E. R., D. R. F. Harleman and H. B. Fischer. 1970. "Dispersion in an Homogenous Estuary", Proc. ASCE, Vol. 96 (HY8).

Hyer, P. V., A. Y. Kuo and B. J. Neilson. 1977. "Water Quality Models of Back and Poquoson Rivers, Virginia", Special Scientific Report No. 144, Virginia Institute of Marine Science, Gloucester Point, VA.

Neilson, B. J. 1975. "A Water Quality Study of the Elizabeth River: The Effects of the Army Base and Lambert Point STP Effluents", Special Scientific Report No. 75, Virginia Institute of Marine Science, Gloucester Point, VA.

O'Connor, D. J. and W. E. Dobbins. 1958. "Mechanism of Reaeration in Natural Streams", Trans. Am. Soc. of Civil Eng., Vol. 123.

Riley, G. A. 1956. "Oceanography of Long Island Sound 1952-1954. II. Physical Oceanography", Bull. Bingham Oceanog. Coll. No. 15, pp. 15-46.

Sverdrup, H. U., M. W. Johnson, and R. H. Fleming. 1970. The Oceans, Prentice Hall, Inc., Englewood Cliffs, N. J., p. 82.

Taylor, G. I. 1954. "The Dispersion of Matter in Turbulent Flow Through a Pipe", Proc. Royal Society of London, Ser. A, Vol. 223.

Thatcher, M. L., and D. R. F. Harleman. 1972. "A Mathematical Model for Salinity Intrusion in Estuaries", Report 144, Ralph M. Parsons Laboratory for Water Resources and Hydrodynamics, Massachusetts Institute of Technology, Cambridge, MA.

Thomann, R. V. 1972. Systems Analysis and Water Quality Management, Environmental Science Services Division, Environmental Research and Applications, Inc., New York, N.Y.

VIRGINIA INSTITUTE OF MARINE SCIENCE